MECHANISMS OF TRPV1-MEDIATED LUNG CELL DEATH

by

Karen Christine Thomas

A dissertation submitted to the faculty of
The University of Utah
in partial fulfillment of the requirements for the degree of

Doctor of Philosophy

Department of Pharmacology and Toxicology

The University of Utah

December 2010

The University of Utah Graduate School

STATEMENT OF DISSERTATION APPROVAL

The dissertation of **Karen Christine Thomas**

has been approved by the following supervisory committee members:

Christopher A. Reilly	, Chair	**August 25, 2010** Date Approved
Garold S. Yost	, Member	**August 25, 2010** Date Approved
Philip J. Moos	, Member	**August 25, 2010** Date Approved
John G. Lamb	, Member	**August 25, 2010** Date Approved
Randal O. Dull	, Member	**August 25, 2010** Date Approved

and by **William Crowley**, Chair of the Department of **Pharmacology and Toxicology**

and by Charles A. Wight, Dean of The Graduate School.

ABSTRACT

Capsaicin is the pungent compound in chili peppers. Capsaicin causes dose-dependent respiratory and cardiovascular failure by all routes. The capsaicin receptor, TRPV1, is a ligand-gated calcium channel. TRPV1 is expressed in sensory neurons and various non-neuronal cells in the lung, including epithelial cells of the conducting airways and alveoli. In human lung bronchial epithelial and alveolar cells, plasma membrane and endoplasmic reticulum (ER) populations of TRPV1 differentially influence cytokine gene expression and cell death via changes in cytosolic calcium concentrations, but a precise mechanism for TRPV1-mediated cytotoxicity was previously undefined. This project investigated how prototypical and endogenous TRPV1 agonists damage lung cells. Structure activity relationships between cell death and capsaicinoids with varied potency, and the role of TRPV1 in lung injury due to unfettered systemic inflammation were studied. *In vitro* assays for cell viability and calcium flux, quantitative analysis of gene expression patterns, and mutagenesis of regulatory gene products demonstrated that TRPV1 activation caused extensive ER calcium efflux, ER stress, and cell death. A series of capsaicinoid analogues were developed to determine the specificity of TRPV1 activation and ER stress as a common mechanism of toxicity in various human lung cell types. Structural modifications to the vanilloid ring drastically reduced the ability of capsaicinoids to activate TRPV1 and, accordingly, both ER stress and cytotoxicity were attenuated. Molecular modeling of

analogue-TRPV1 binding corroborated these results and highlighted key structural features of capsaicin required for TRPV1 activation and cytotoxicity. Endogenous TRPV1 agonists have recently been implicated as pneumotoxicants during systemic inflammation. Treatment of mice i.p. with lipopolysaccharides (LPS) promoted systemic inflammation and lung injury. TRPV1 knockout mice and mice co-treated with the TRPV1 antagonist LJO-328 were protected from lung injury and evidence of an ER stress response was diminished. The endovanilloid anandamide induced ER stress and lung cell death *in vitro*, but these effects were not blocked by TRPV1 antagonist co-treatment, suggesting that other endovanilloids may cause ER stress and lung injury in mice. The results of this project provide a concerted mechanism of TRPV1-mediated lung epithelial cell death and illustrate a potential role of TRPV1 and endovanilloids in lung injury.

TABLE OF CONTENTS

LIST OF TABLES

LIST OF FIGURES

LIST OF ABBREVIATIONS

4αPDD…….....….4α-12,13-didecanoate

ANOVA.....analysis of variance

ARDS.....acute respiratory distress syndrome

ASIC…….....……acid-sensing ion channels

ATF6…….....… activating transcription factor 6

BAL.....bronchial alveolar lavage

BEAS-2B…….....…… immortalized human bronchial epithelial cell line

BiP/GRP78.....glucose-regulated protein 78kDa

CCND1…….....….cyclin D1

CCNG2.....cyclin G2

CGRP….....…….calcitonin gene related peptide

C.I. ..... confidence interval

DAG…….....…….diacylglycerol

DEP…….....……..diesel exhaust PM

DTT.....dithiothreitol

DU 145…….....……...human prostate carcinoma cell line

EET…….....…….. epoxyeicosatrienoic acid

EIF2α..... eukaryotic translation initiation factor 2, subunit 1 alpha, 35kDa

eIF2αK3……...……eukaryotic translation initiation factor 2α kinase 3

EGFP.....enhanced green fluorescent protein

eNOS……..……. endothelial nitric oxide synthase

ER…….....……..endoplasmic reticulum

EtBr.....ethidium bromide

FAAH…….....…..fatty acid amide hydrolase

FVC…….....….forced vital capacity

FEV_1…….....……..forced expiratory volume

GADD153…….....…….growth arrest and DNA damage-inducible protein 153

GFP.....green fluorescent protein

G-PCR…….....…….G-protein coupled receptor

GRP78…….....……..glucose-regulated protein 78kDa

H_2S…….....….. hydrogen sulfide

HEK.....human embryonic kidney

HETE.....hydroxyeicosatetraenoic acid

HODE…….....……hydroxyoctadecadienoic acid

HpETE…….....……. hydroperoxyeicosatetraenoic acid

HMVEC-L.....human microvascular endothelial cells – lung

IL..... interleukin

i.p.....intraperitoneal

IRE1α/β…….....….inositol requiring enzyme-1 α/β

Kfc…….....…….lung filtration coefficient

LDH.....lactate dehydrogenase

LPS…….....…….lipopolysaccharides

LTB_4.....leukotriene B_4

MLSN…….....……..Melastatin

mRNA…….....……messenger RNA

NHBE.....normal human bronchial epithelial cell line

NMMAPS…….....……. National Mortality and Morbidity Air Pollution Study

NO-cGMP……..…….. nitric oxide-cyclic guanosine monophosphate

PARP…….....poly-ADP ribose polymerase

PCR.....polymerase chain reaction

PC-3…….....…….human prostate cancer adenocarcinoma cell line

PERK.....dsRNA-activated protein kinase-like ER kinase

PIP…….....……peak inspiratory pressure

PLC…….....….phospholipase-C

PM…….....……..particulate matter

PPTA…….....……..preprotachykinin-A

RLMVEC.…….....….rat lung microvascular endothelial cell line

RNA…….....…….…..ribonucleic acid

RPAEC…….....….....……rat pulmonary artery endothelial cell line

RT.....reverse transcriptase

SERCA……..…….sarco/endoplasmic reticulum Ca^{2+}ATPase

SOC…….....……store-operated calcium

TRP……..... Transient Receptor Potential

TRPA…….....……Transient Receptor Potential Ankyrin

TRPC…….…….Transient Receptor Potential Canonical

TRPM…….....Transient Receptor Potential Melastatin

TRPML…….....……Transient Receptor Potential Mucolipin

TRPN…….....……..Transient Receptor Potential NOMPC

TRPP…….....…….Transient Receptor Potential Polycystin

TRPV….....……..Transient Receptor Potential Vanilloid

TRPV1-OE.....TRPV1-overexpressing BEAS-2B cells

TRPY…….....…Transient Receptor Potential Yeast

VILI…….....……ventilator-induced lung injury

XBP-1…….....…..x-box binding protein 1

CHAPTER 1

INTRODUCTION

The ability to sense and dynamically interact with the ever-changing environment requires an advanced sensory system. For all organisms, even the most rudimentary senses of touch, taste, sight, smell, and sound are vital. Understanding of the mechanisms underlying sensory perception has steadily increased, yet much remains to be discovered about specific receptors that differentially detect sensory stimuli. Investigation continues as to the physiological importance of receptor-mediated events in different cell types, the potential role for neuronal receptors to act as nontraditional 'sensors' of environmental variables in non-neuronal cells, and how receptor protein responses (e.g., ion flux) are coupled with subcellular signaling pathways and higher systemic functions.

Evolution drives the development and refinement of complex systems to sense and to compensate for noxious, irritating, and potentially harmful stimuli. Progressive development of the sensory system allows humans and other organisms to differentiate between pleasant and detrimental experiences. Consider the warmth of sunshine versus the painful burn of a flame, the gentle cooling sensations from a sea breeze versus icy arctic winds, and the ability to sense pleasant food aromas versus a potentially lethal gas exposure. The ability to perceive 'negative' sensory experiences affords protection because the nervous system gathers sensory input and coordinates appropriate responses to minimize harm. Several members of the Transient Receptor Potential (TRP) family of

ion channels have been identified as critical sensors of harmful environmental conditions. Select TRP channels in neurons elicit reflex responses and avoidance (nocifensive) behavior, activate the innate immune system to increase host defenses against injury, and initiate compensatory repair processes to mitigate injury and promote a return to homeostasis. Promotion of homeostasis is also associated with activation of TRP channels in non-neuronal cells.

This review will briefly describe salient traits of different TRP channels, with emphasis on TRP channels expressed in the respiratory tract, followed by a discussion of select TRPs as mediators of normal and pathological processes in the lung. Four areas of research will be highlighted: 1) basic characteristics of TRP channels; 2) endogenous agonists of TRPV1 (endovanilloids) and the role of TRPV1 as a mediator of lung injury due to severe systemic inflammation; 3) the role of TRP channels, particularly TRPC1, TRPC4 and TRPV4, in regulating vascular endothelial barrier integrity with respect to changes in vascular pressure, airway distention, and systemic inflammatory conditions; and 4) the potential role of TRP channels as sensors for inhaled ambient particulate pollutants and mediators of pulmonary inflammation and injury associated with these ubiquitous environmental toxicants.

1.1 TRP Family of Ion Channels

The TRP family of ion channels is comprised of 28 gene products in humans, divided into six different subfamilies: TRPA (ankyrin), TRPC (canonical), TRPM (melastatin), TRPML (mucolipin), TRPP (polycystin), and TRPV (vanilloid) (*1-5*). Two nonmammalian subfamilies, TRPN (*C. elegans*, zebrafish and *Drosophila*) and TRPY

(yeast) also exist, but will not be covered in this review. TRP subfamilies are grouped based on similarities in genetic/amino acid sequence and associated structure and function (*6*). Several comprehensive reviews of TRP channels have been recently published, with additional information that is not included in the scope of this review (*2-5, 7, 8*).

All TRP channels have six trans-membrane domains, a pore-loop region between trans-membrane domains 5 and 6, and are generally permeable to cations. TRP channels are expressed in all tissues and cell types in mammals, and generally function as environmental sensors and signal integrators to help organisms dynamically sense and appropriately respond to their environments. TRP channels function as tetramers, where four channel subunits assemble to form a central pore comprised of the pore-loop regions of the four subunits. Additionally, some TRP channels reportedly form heterotetramers composed of different members of the same (and possibly other) subfamilies to produce functionally distinct complexes. For example, TRPC1 and TRPC3 form heterotetramers with functions that may be distinct from the function of the channel alone, although this is still an area of much research and debate (*9*). Heterotetramer formation further expands the potential capabilities of these channels as selective sensors of diverse conditions and specific mediators of distinct compensatory processes.

Although they are structurally similar, there are many differences between TRP channels. Individual TRP channels are highly diverse in their intracellular N- and C-terminal domains, where significant regulation of TRP channel function occurs via protein-protein interactions and posttranslational modifications. TRP channels also vary in relative subcellular location, expression level in different cell and tissue types, and in

mRNA processing and translated protein composition. TRP channels have distinct agonist and antagonist selectivity, relative cation permeability, modes of action, and sensory and cellular functions.

TRP channels were first identified in *Drosophila* for their role in retinal signal transduction (*10*). Although differences exist between organisms, cell types, and organ systems, TRP channels are highly conserved across species and channel homologs tend to function in similar ways. TRP channels contribute to sensory functions including vision (*Drosophila* TRP), the detection of warm, cool, and cold temperatures (TRPV1-4, TRPA1 and TRPM8), taste (TRPM5 and others activated by spice components), osmolarity and membrane tension (TRPM3, TRPV4), and hearing (TRPV4) (*1-3, 5, 11-15*).

1.1.1 TRPA Subfamily

TRP ankyrin channel 1 (TRPA1) is the only known mammalian TRPA channel and was first characterized in 2003 as a calcium-permeable, cold-sensing channel (*16*). This subfamily of channels is named "ankyrin" because it has many (~14-17) ankyrin repeats in the N-terminal region, depending on the species (*16, 17*). In humans and rodents, TRPA1 expression is documented in a variety of cell and tissue types, including the hair cells of the ear, peripheral sensory nerves, and about 20-35% of sensory neurons that innervate the respiratory tract (*4, 17*). In the ear, TRPA1 mechanotransduction processes may contribute to auditory signal transduction through tethering of the channel, via the ankyrin repeat domain to cytoskeletal components, to generate a "gating spring" that promotes channel opening (*18*). In sensory neurons of the respiratory tract, TRPA1 is mainly coexpressed in TRPV1- and tachykinin expressing C-fibers (*19*). Rodent TRPA1

is strongly activated through covalent modification of residues C415, C422, C622 and K208 (*20, 21*). Many electrophilic and oxidizing chemicals activate TRPA1 to trigger cough and abrupt changes in breathing pattern (*17*). Prototype agonists of TRPA1 include sulfur mustards, crotonaldehyde, acrolein, cinnamaldehyde, 4-hydroxynonenal and 4-oxononenal, isocyanates and isothiocyanates (e.g., allylisothiocyanate), hypochlorous acid and hydrogen peroxide, and even cytochrome P450-derived electrophilic metabolites of naphthalene (*1, 3-5, 17, 19, 21-25*). Additional evidence indicates TRPA1 also senses cold, and is activated by noxious cold temperatures less than about 19°C. However, the function of TRPA1 in temperature sensation is an area of much debate (*4, 26*). Finally, it should be emphasized that species-specific differences exist in relative potency of these agonists, and to date not all of these agents have been shown to activate human TRPA1.

1.1.2 TRPC Subfamily

TRPC1 and 3 were the first mammalian homologs of *Drosophila trp* to be identified (1995). This TRP family is called 'canonical' (*27*). TRPC1-7 share >30% amino acid homology with each other and also with the *Drosophila* TRPCs (*1*). TRPC channels form both homo- and heterotetramers (e.g. TRPC1/C4, TRPC4/C5), which has considerably complicated deorphanization and characterization of the individual channels (*9, 28*). TRPC channels are primarily activated by calcium store depletion, and in some cases, stretch (*1, 3, 4*). TRPC channels are associated with G-protein coupled receptors (G-PCR), such as rhodopsin in *Drosophila*. Activation of the G-PCR signal transduction cascade involves phospholipase-C (PLC), diacylglycerol (DAG) and depletion of calcium stores that, through a poorly defined mechanism for these receptors, activates TRPC channels (*29*). In mammals, TRPCs are variably expressed throughout the body. All

human TRPC channel isoforms are expressed in the lung and have a variety of functions including mechanosensation, regulation of airway vascular tone, mineral uptake and balance, and neuronal growth (*1, 3, 4*). TRPC1 and TRPC4 will be discussed at greater lengths for their role in maintaining vascular permeability in the lung in section IIIb.

1.1.3 TRPM Subfamily

Eight members of the TRPM subfamily have been identified. TRPM1 was initially identified in melanoma cells where expression correlated inversely with the metastatic potential, giving rise to the channel's original name, melastatin (MLSN) (*30*). All genetically related channels were subsequently termed "melastatin" even though their functional properties vary widely. TRPM2 is poorly characterized, but is expressed in immune cells and vascular endothelial cells of the lung and is activated by hydrogen peroxide and intracellular ADP ribose produced by poly ADP ribose polymerase (PARP) during oxidative stress (*29*). TRPM3 is constitutively active and regulates calcium and manganese ion distributions/ion currents across cell membranes, including in vascular endothelial cells. Hypotonic cell swelling can enhance these ion currents (*1, 4, 29*). TRPM4 and TRPM5 are voltage-modulated and can be activated through G-PCRs that are coupled to PLC dependent endoplasmic reticulum (ER) calcium release, but are not calcium store dependent. (*29*) TRPM4 and TRPM5 are permeable to monovalent cations, but unlike all other TRP channels, are impermeable to calcium ions (*4*). TRPM5 appears to be required for taste because it is present in taste receptor cells, and knockout mice (TRPM5-/-) have reduced sweet, bitter and umami responses as measured *in vivo* by gustatory nerve recording, initial lick responses, and two-bottle preference tests (*15*).

TRPM8 is one of only two TRP channels activated by cool temperatures. TRPM8 is activated by decreasing temperatures <23 – 28°C and is also activated by "cooling agents" such as menthol, icilin, citronellol, and a number of other compounds used in the food, cosmetic, and dental industries where "fresh mint" or similar sensations are desired (*31-33*). TRPM8 is highly expressed in some small diameter unmyelinated sensory neurons of the peripheral nervous system and respiratory tract, in certain prostate cancer cell lines (e.g., PC-3, but not DU 145), and as a functional N-terminal truncated variant in human bronchial epithelial cells, where translation of the protein begins at either M758 or M801 (*32-36*). This variant differs from the full length TRPM8 gene product in its sensitivity to prototype agonists that require the high-affinity menthol binding residue Y745, or icilin binding sites, located at residues N799, D802, and G805 (*34, 37, 38*). The variant retains responsiveness to cooling, but is not activated by icilin, and is activated by only high concentrations of menthol (*34*). TRPM8 likely plays a role in cold hypersensitivity, cold allodynia in patients with nerve injuries, and has been proposed to possibly play a role in airway hypersensitivity associated with exercising in cold and dry air via changes in immunomodulatory cytokine expression and inflammation (*34, 39, 40*).

1.1.4 TRPML Subfamily

TRPML1 was identified as a causal mutation for mucolipidosis IV, a severe neurodegenerative lysosomal storage disorder (*41*). TRPML2 and TRPML3 are not yet well characterized but are the subject of much research (*1, 3, 4*). Both TRPML2 and TRPML3 have lysosomal targeting signals and reside in the lysosomal membrane (*1*), but TRPML channel expression in the respiratory tract is unknown and will not be discussed further in this review.

1.1.5 TRPP Subfamily

TRPP2 is disrupted in some forms of autosomal dominant polycystic disease, which lead to the discovery of this channel (*29, 42*). TRPP channels are expressed in a variety of species from worms to mammals, and are thought to be an ancient family of channels (*1*). TRPP1 and 2 appear to function in ciliary movement while TRPP3 may have a role in acid detection and sour taste perception (*3*). TRPP1 and 2 channels show functional importance primarily in the kidney, while TRPP3 has been detected in some lung cancers, and TRPP5 is expressed in the testis (*4*). Very little is known about these channels with respect to respiratory physiology or toxicology so they will not be discussed further.

1.1.6 TRPV Subfamily

In 1997, TRPV1 was cloned and identified as the previously elusive target receptor for capsaicin, the pungent compound responsible for the sensation of spicy heat from chili peppers (*43*). TRPV1 was called "vanilloid receptor 1" because the prototype agonist capsaicin and other natural products that activate this receptor with high selectivity contained (or at least mimicked) the vanilloid (4-hydroxy-3-methoxybenzylamine) pharmacophore (*43*). TRPV1 was also identified as a major sensor for warm to hot temperatures > 42^{o}C, acidity (pH<6.3), and more recently organic acids such as lactate (*43-46*). Since the discovery of TRPV1, many TRPV1 agonists have been reported, ranging from endogenous lipids such as anandamide, leukotriene B_4, and 12(S)-hydroperoxyeicosatetraenoic acid (12(S)-HpETE) to very simple molecules such as hydrogen sulfide (H_2S) and the cannabinoid Δ^9-tetrahydrocannabinol (*47-49*).

Resiniferatoxin, a compound isolated from *Euphorbia Resinifera Berg*, is an ultra-potent TRPV1 agonist (*50*).

Structurally, TRPV1 has the 6 transmembrane domain structure seen in all TRP channels. It is thought that transmembrane domains 3 and 4 form a paddle structure that shifts to open and allow for vanilloid binding (*51*). Jordt *et al.* described the importance of residue Y511 in determining vanilloid sensitivity across species in 2002 (*52*). Further research demonstrated that activation of TRPV1 by capsaicin and other vanilloid agonists occurs through specific binding interactions with residues Y511, S512, L547, W549, and T550 (*51-54*). A different site comprised of glutamic acid residues adjacent to the pore-loop domain is responsible for pH activation and acid potentiation of the channel (*44*). Heat sensitivity (noxious temperatures $\geq$ 43 °C) is apparently mediated through the C-terminus of the protein, but the precise residues responsible have not yet been determined (*55*). Although the responses to capsaicin, protons, and heat are integrally related, the capsaicin binding site appears to be separate from heat or proton activation domains of TRPV1.

Many TRPV1 antagonists have been investigated for various applications, including therapeutic use for pain treatment. Capsazepine was the first TRPV1 antagonist and was designed to be structurally similar to capsaicin (*56*). Capsazepine has been used as a TRPV1 antagonist in many different types of experiments, but its relative lack of specificity for TRPV1 has led to many false conclusions regarding TRPV1 activation. Another more selective antagonist, 5-iodo-resiniferatoxin, is an iodinated form of resiniferatoxin (*50, 57*). Additional potent and selective TRPV1 antagonists are being

developed clinically to alleviate neurogenic pain, although some of them cause significant hyperthermia precluding them from clinical use (*58-60*).

In addition to TRPV1, other TRPV channels have been discovered based on responsiveness to temperature changes and natural products found in spices that characteristically induce sensations of temperature change. TRPV2 activation is highly species dependent, and rat TRPV2 is sensitive to noxious heat > 53^{o}C and some cannabinoids including Δ^{9}-tetrahydrocannabinol, cannabinol, and cannabidiol (*61-63*). TRPV3 senses carvacrol (oregano), thymol (thyme), eugenol (clove) and temperatures >30^{o}C (*64, 65*). TRPV4 is a sensor for phorbol esters such as 4α-12,13-didecanoate (4αPDD) (rodent only), changes in osmolarity/membrane stretch, and temperatures >24^{o}C-34^{o}C (*66*). Like TRPV1, these channels are being actively investigated for a variety of different functions and therapeutic potential. A role for TRPV4 in lung vascular function will be discussed later in this review. TRPV5 and 6 are constitutively active, are inhibited by intracellular calcium, and have been implicated in vitamin D-dependent calcium uptake in the kidney and intestine, respectively (*67*).

In the lung, TRPV1-4 are highly expressed in sensory nerves and non-neuronal cells including nasal, tracheal, bronchial, and bronchiolar epithelial cells, type 1 and 2 pneumocytes, resident macrophages, smooth muscle cells, and pulmonary vascular cells (*4, 14, 68*). The specific roles of these channels as sensors of lung toxicants will be discussed in detail in the sections that follow.

1.2 TRP Channels as Mediators of Pulmonary Injury

1.2.1 TRPV1, Neurogenic and Non-Neurogenic Inflammation, Epithelial Cell Death, and Lung Injury

In the respiratory tract, TRPV1 is expressed at high levels by unmyelinated C-fiber neurons, in the somata of sensory ganglia, and in a small population of thin myelinated Aδ-fibers (*12, 14, 68*). Neuronal TRPV1 activation results in action potentials, which are interpreted as pain and burning sensations. Additionally, the cough reflex is triggered, breathing becomes rapid and shallow, and substance P, calcitonin gene related peptide (CGRP), and neurokinin A are released from the nerve termini (*12, 17*). These tachykinins are key mediators of neurogenic inflammation and are involved in modulating cell signaling pathways that increase vascular permeability leading to plasma extravasation, neutrophil chemotaxis and transmigration into the lung, macrophage activation, and pulmonary edema (*69-72*).

TRPV1 is also expressed in a variety of non-neuronal cells of the respiratory tract, including tracheal, bronchial and bronchiolar epithelial, alveolar type I and II, airway smooth muscle and pulmonary microvascular endothelial cells (*73-77*). In cultured human lung bronchial epithelial and adenocarcinoma cells, two distinct populations of TRPV1 are expressed. Differential activation of each population is also coupled to distinct responses (*75, 77, 78*). Activation of the population of TRPV1 expressed at the cell surface promotes cellular calcium entry and is coupled with increases in the transcription and ultimate secretion of several key immunomodulatory Th1-type cytokines and chemokines including IL-6, IL-8, and TNFα (*74, 75, 78*). Conversely, activation of the main sub-population of TRPV1 that resides on the ER leads to calcium

efflux from the ER and calcium accumulation in the cytosol (*77*). This calcium accumulation is coupled with accumulation of unfolded proteins, ER stress and ultimately cell death.

The ER is the major site of protein folding in cells, particularly for secreted and membrane embedded proteins. ER stress occurs when there is an accumulation of misfolded or partially folded proteins in the ER. ER stress is often initiated when the cell undergoes an insult, such as glucose or amino acid deprivation, which decreases protein production efficiency. In the case of cell permeable TRPV1 agonists, ER calcium depletion leads to ER stress because lower calcium concentrations in the ER destabilize partially folded protein intermediates, causing increased sequestration of specific ER chaperone proteins (*79, 80*). Protein folding efficiency in the ER is monitored and, in part, regulated by chaperones including calreticulin, calnexin, and heat shock proteins, most notably glucose-regulated protein 78kDa (GRP78 a.k.a BiP or HSPA5) (*80, 81*).

GRP78 is critical for "sensing" protein processing through binding to regulatory domains of three proximal transducers of ER stress: activating transcription factor 6 (ATF6), inositol requiring enzyme 1 α/β (IRE1α/β), and eukaryotic translation initiation factor 2α kinase 3(eIF2αK3 a.k.a PERK). When unfolded proteins accumulate, GRP78 dissociates from these proximal sensors to initiate the ER stress response, a highly orchestrated process intended to restore cellular homeostasis through coordinated up and downregulation of specific genes. The release of GRP78 from ATF6 leads to ATF6 cleavage and the production of an active transcription factor primarily associated with up-regulation of membrane synthesis machinery to expand the ER, and induction of chaperones to increase the protein folding capacity of the ER. IRE1α/β activation also

acts in this manner via the production of x-box binding protein 1 (XBP-1) transcription factor (*79, 80, 82, 83*). GRP78 dissociation from PERK activates PERK to phosphorylate eIF2α, leading to translational attenuation, rapid degradation of select non-essential mRNAs (messenger ribonucleic acid), cell cycle arrest due to a loss of cyclin D1 (CCND1) translation and mRNA degradation, and the induction of genes such as growth arrest and DNA damage-inducible protein 153 (GADD153, a.k.a. CHOP and DDIT3) that both establish a negative feedback on the ER stress pathways via transcription factor activity and promote apoptosis, presumably serving as a protective event to eliminate irreparably compromised cells (*79, 80, 82-84*).

Various prototypical agonists activate TRPV1 in human lung bronchial epithelial cells, leading to ER stress and cell death via activation of the PERK pathway (*77*). GADD153 induction leads to cell cycle arrest at the G_1/S transition and the cells eventually die (*85*). Specifically, TRPV1 activation caused ER calcium release, eIF2α phosphorylation, GADD153 induction, and cell death. TRPV1-mediated cell death was preventable with inhibition of ER calcium release using cell-permeable TRPV1 antagonists (e.g., LJO-328), prevention of eIF2α dephosphorylation by salubrinal, (*86*) and over-expression dominant negative forms of either eIF2α (eIF2α-S52A) or GADD153 (GADD153-L134A/L141A) (*77*). These studies provided evidence that acute epithelial cell damage observed following airway exposure to capsaicin (*76*) occurs via ER stress. Of significance, Endo *et al.* has shown that GADD153 induction occurs in lungs of mice treated with lipopolysaccharides (LPS) following i.p. administration (*87*). Additionally, LPS induced lung injury was attenuated in GADD153-/- mice indicating an important role for ER stress in LPS induced lung injury (*87, 88*).

TRPV1 has also been shown to detect a variety of endogenous compounds commonly produced during systemic inflammation. The studies by Endo *et al.* discussed immediately above provide a plausible link between systemic inflammation and lung injury involving ER stress (*87, 88*). However, the role of endogenous TRPV1 agonists as intermediate mediators of these outcomes was not explored. As previously mentioned, TRPV1 has many exogenous and endogenous agonists. Endogenous agonists of TRPV1, or endovanilloids, play a role in inflammatory responses and are generated at concentrations that can activate TRPV1 in local tissue environments after inflammatory insults (*89*). Endovanilloids include anandamide, *n*-arachidonyldopamine, H_2S, leukotriene B_4, 12(S)-HpETE, and a variety of other substances typically derived from arachidonic acid (*47-49*). Several studies have also shown LPS treatments *in vitro* and *in vivo* lead to increases in physiological concentrations of endovanilloids including anandamide and H_2S (*47, 70, 90-97*). Another new class of endogenous TRPV1 agonists are oxidized linoelic acid metabolites, 9-hydroxyoctadecadienoic (HODE), 13-HODE, and 13-oxoHODE, which mediate hyperalgesia, allodynia and contribute to heat sensitivity (*98, 99*).

Anandamide was first identified as an endogenous cannabinoid receptor agonist, and was later shown to act at TRPV1 in addition to cannabinoid receptors 1 and 2 (*49, 100, 101*). Anandamide is essentially synthesized 'on demand' in the central nervous system and at sites of peripheral tissue injury, including the lung, in concentrations sufficient to active TRPV1 (*68, 102, 103*). It is difficult to define the exact physiological role of anandamide because it acts differentially through cannabinoid receptors and TRPV1 receptors, its concentration is modulated by fatty acid amide hydrolases 1 and 2

(FAAH), and some effects may be concentration and duration of exposure dependent (*89, 104, 105*). In guinea pigs, TRPV1 activation by aerosolized anandamide induces cough, and in isolated guinea pig bronchi, anandamide treatment causes bronchoconstriction (*105, 106*). Additional studies indicate that intraluminal administration of *Clostridium difficile* toxin A stimulates the production of anandamide, which then acts through TRPV1 to cause significant ileal inflammation (*107*). The hypothesis that TRPV1 activation by endovanilloids during inflammation exacerbates injury is supported by evidence that anandamide is upregulated during endotoxemic events, and inflammatory mediators potentiate anandamide effects at TRPV1 (*89, 94, 95, 108, 109*). Systemic inflammation and infection often lead to cardiovascular collapse, and anandamide has been proposed as a mediator of endotoxin induced hypotension because it potentiates vasodilation in LPS treated animals and is measurable in septic conditions (*94, 108, 109*).

In animal models, LPS treatment causes marked, and often unbalanced, systemic inflammation via the activation of Toll-like receptor 4 on macrophages (*110-116*). LPS induced inflammation is characterized by hyperthermia (calor), vascular leakage, hypotension, erythema/reddening of the site (rubor), and hyperalgesia (dolor), progressive loss of organ functions, and lung injury generally characterized by neutrophilia and pulmonary edema.

LPS treatment, as well as other models of severe infection and lung injury, including cecal ligation and puncture, also cause increases in the production of, and systemic/circulating concentrations of, H_2S (*48, 90, 91, 117-121*). H_2S is a purported TRPV1 agonist, and was also shown to activate TRPA1 in rat bladder and mouse and

human TRPA1 expressed in CHO cells (*48, 122*). TRPV1 antagonist cotreatment, or capsaicin sensitive efferent neuron depletion via long term, high dose capsaicin (sub-cutaneous) pretreatment, have been shown to attenuate lung injury after treatment with H_2S donors, LPS treatment, and cecal ligation and puncture (*70, 90, 118*). These beneficial effects were attributed to decreased release of substance P, CGRP, and neurokinins by TRPV1 expressing sensory neurons. Accordingly, protective effects were observed in capsazepine and *n*-propargylglycine (an inhibitor of H_2S synthesis) cotreated animals and preprotachykinin A (PPTA-/-) deficient mice (*91, 96, 97, 118, 123, 124*). Preprotachykinin A codes for substance P and neurokinin A, which are both expressed by capsaicin sensitive neurons in the lung and are potent mediators of neurogenic inflammation (*125*). These experiments illustrated that H_2S and TRPV1 contribute to lung injury via TRPV1, and possibly TRPA1, activation and indicate a broader role for TRPV1 and endovanilloids as a mediators of both inflammation and lung injury due to systemic inflammation, such as sepsis.

To date, studies of additional endovanilloids that may contribute to lung injury as a result of systemic inflammation, independent of infection/simulated infection, including burn injury or severe trauma have not been performed. However, literature does indicate that some endovanilloids are produced under these conditions and that lung injury is due to substance P production (*126-128*).

The role of TRPV1 in airway inflammation and lung injury is not simply mediated through neurogenic inflammation. Inflammatory mediators and changes in cellular microenvironment both in the lung and at other sites of injury can activate TRPV1. Stimulation of TRPV1 in non-neuronal cells causes rapid increases in key

immunomodulatory cytokines that regulate innate immune responses, including the release of IL-8 to promote neutrophil chemotaxis and TNFα and IL-6 to activate macrophages and to stimulate downstream events required to balance the immune response. Of significance, TRPV1 activation in the lung is not an all-or-none event leading to neurogenic inflammation and injury. It has been shown that activation of TRPV1 also promotes the release of somatostatin from sensory neurons, which acts to mitigate the severity of inflammation and lung injury (*129, 130*).

Overall, the role of TRPV1 and other TRP channels, including TRPA1 and TRPV4, in lung injury is slowly becoming clearer. TRPV1 is a promising therapeutic target for treatment and prevention of inflammatory lung injury.

1.2.2 TRP Channels in Lung Vasculature: Key Players in Endothelial Barrier Function, Mechanotransduction, and Lung Injury

TRP channels are also rapidly emerging as principle regulators of lung vascular endothelial cell function, specifically in the areas of inflammation, mechanotransduction, and inflammatory and hypertensive lung injury. Select TRP channels perform important roles in modulating lung vascular barrier function in a segment specific manner. It is quickly becoming apparent that coordinated calcium fluxes, second messengers, and other unidentified signals coalesce to produce an integrated lung endothelial barrier response to locally produced (i.e. in the lung) and systemically circulating cytokines, neurally generated signals, and changes in pulmonary vascular pressure and airway distension. The pivotal roles of select TRP channels in regulating vascular permeability and the importance of this event in lung injury proposes a role for certain TRP channels

as mediators of lung injury resulting from pathological conditions including hypertension, sepsis, and ventilator induced lung injury (VILI).

It has been appreciated for almost two decades that changes in intracellular calcium are a primary event leading to altered vascular endothelial barrier function (*131*). Calcium-induced changes in junctional patency occur through processes that are linked to the endothelial cell contractile apparatus (*132, 133*) and the production of other intracellular mediators such as nitric oxide and reactive oxygen species which both have known effects on TRP channels including TRPV1, TRPV4, TRPA1, and possibly TRPM2 (*17, 19, 134-137*). The role of ER calcium release versus calcium influx from extracellular sources in endothelial activation and changes in barrier function was debated for many years, but it is now clear that these two calcium fluxes are linked and represent a coordinated response that is TRP channel mediated and directly linked to changes in barrier function under a diverse range of pathological conditions (*138*).

A sentinel observation on the role of endothelial calcium perturbations on barrier regulation was that calcium influx from external sources, and not ER release, was the signal for alterations in permeability (*139*). Thus arose the concept that ER calcium depletion was the trigger for calcium influx, leading to the term store operated calcium (SOC) entry. This concept ultimately defined the general mechanism(s) that linked calcium fluxes with barrier dysfunction (*140*).

The TRP family of cation conducting channels has become the central focus of SOC entry and calcium mediated barrier dysfunction. TRPC1 and TRPC4 appear to be the major participants in lung endothelial calcium fluxes that are germane to permeability regulation based on the following observations. The use of antisense RNA to reduce

TRPC1 expression in cultured pulmonary artery endothelial cells (*141*) effectively reduced SOC currents (I_{SOC}), and endothelial cells derived from TRPC4 knockout animals showed no evidence of an inducible I_{SOC}. There is also substantial evidence to suggest TRPC1 and TRPC4 interact, perhaps by heteromultimerization or via co-localization (*138*) to coordinate calcium flux in response to challenges.

Studies comparing the relationship between calcium responses and barrier function in macrovascular (rat pulmonary artery endothelial cells, RPAEC) versus rat lung microvascular endothelial cells (RLMVEC) have also been key in elucidating the roles of TRPC channels in permeability regulation. Marked differences were observed between these two cell types. RLMVEC formed tighter, more restrictive, junctions to macromolecules and did not demonstrate increased permeability in response to increases in intracellular calcium (*142*). However, RLMVEC exhibited lower thapsigargin induced flux (i.e., lower intracellular calcium store content) compared to RPAEC, higher SOC entry in response to stimuli, and a reduced permeability response to increased $[Ca^{++}]_i$. Collectively, these observations suggested an uncoupling of calcium from permeability in RLMVEC. RLMVEC cells exhibit lower TRPC1 and TRPC4 expression, further indicating a role of these TRPs in control of vascular integrity and fluid flux across this barrier. Down regulation of TRPC1 and TRPC4 has recently been reported in a rat model of heart failure and was associated with reduced thapsigargin induced permeability, suggesting a clinically relevant direct correlation of TRPC channel expression during a pathological process that usually results in pulmonary edema (*143*).

The functional differences in macrovascular versus microvascular endothelial cell properties have subsequently been extended to *in vivo* studies, where the anatomical

correlates, extra-alveolar vs. alveolar vessel permeability, was examined as a function of site specific stimulation with either thapsigargin or 4αPDD. Thapsigargin is known to increase permeability of extra-alveolar vessels through depletion of ER calcium stores via sarco/endoplasmic reticulum Ca^{2+}ATPase (SERCA) inhibition, while 4αPDD appears to preferentially activate TRPC4 (*144*) and increases alveolar capillary permeability. This differential activation of TRPC channels in different vascular segments produced distinctly different patterns of fluid accumulation; thapsigargin caused fluid cuffing around large vessels while 4αPDD increased alveolar flooding (*145*) suggesting regional differences in TRPC channel expression, as indicated by previous *in vitro* studies. The mechanical properties of the lung were also differentially altered by the site-specific leakage induced by thapsigargin and 4αPDD; dynamic compliance was reduced by the presence of extra-alveolar cuffing, but not by alveolar flooding. Thus, vascular specific TRP channel expression in the lung and the cellular response to calcium via TRP channels influences the permeability response to injury, and the subsequent mechanical sequela that may be involved in lung injury and/or lung diseases.

Rodent TRPV4 is also activated by 4αPDD in vascular cells. Recent studies have shown that TRPV4 activation also causes alveolar-specific injury and contributes to alveolar flooding as previously suggested for TRPC4 (*144, 145*). In fact, TRPV4 may be the primary mediator of alveolar flooding caused by 4αPDD, based on studies using more selective agonists and inhibitors of cytochrome 450 enzymes that attenuate the formation of the endogenous TRPV4 agonists 5,6-epoxyeicosatrienoic acid (EET), 8,9-EET and 14,15-EET (*146, 147*). Vriens *et al*. showed that sulfaphenozale inhibition of cytochrome P450 2C enzymes lessened arachidonic acid stimulated TRPV4 currents by inhibiting

EET formation (*147*). Consider also the effects of GSK1016790A, a potent TRPV4 agonist that upon administration causes immediate loss of vascular integrity and massive pulmonary edema characterized by alveolar flooding (*148*). Similarly, activation of TRPV4 with 5,6- or 14,15-EET increased the whole lung filtration coefficient (Kfc) in a dose and calcium dependent manner. The increases in Kfc were blocked by the cell surface (impermeable) calcium channel blocker ruthenium red, but not by thapsigargin induced ER calcium depletion (*146*). When 4αPDD was tested in TRPV4 knockout mice, there was no change in Kfc but electron microscopy confirmed cellular pathology and demonstrated widened intercellular gaps that were confined to the alveolar capillaries. This supports the notion that the lung vascular barrier is regulated by distinct expression patterns of TRP channels, namely TRPC1, TRPC4 and TRPV4, and associated site specific influences on calcium permeability (*146*).

TRPV4 has also been shown to participate in VILI. Mice ventilated with high peak inspiratory pressure (PIP, 35 cm H_2O) demonstrated a 2.2-fold increase in Kfc that could be blocked by ruthenium red, methanandamide (a cannabinoid receptor antagonist; mainly blocks CB1) and miconazole (a cytochrome P450 epoxygenase inhibitor). When TRPV4 knockout mice were ventilated with identical high PIP there was no measurable increase in Kfc. In parallel experiments, PIP induced calcium entry into endothelial cells was measured using Fura-2. High PIP induced calcium was absent in TRPV4 deficient mice and in wild type mice, but only when cotreated with ruthenium red (*149*). Collectively, these results suggest a role for TRPV4 in acute lung injury and VILI. These results also suggest that endogenous TRPV4 agonists, which may be produced during

sepsis and other inflammatory conditions, promote lung injury. To date, however, this paradigm has not been investigated.

The topic of lung vascular mechanotransduction also has become an important mechanism for the development of pulmonary edema, particularly during states such as congestive heart failure and VILI when pulmonary capillary pressure is increased. Bhattacharya and colleagues demonstrated that elevated pulmonary capillary pressure increased endothelial cell calcium content (*150*), mitochondrial reactive oxygen species production, P-selectin expression (*151*) and leukocyte margination (*152*); events that link mechanotransduction with inflammatory responses that contribute to lung injury. Kuebler *et al.* (*153*) reported that pressure induced increases in cellular calcium activated endothelial nitric oxide synthase (eNOS) leading to an increase in nitric oxide, a known mediator of endothelial permeability responses and recently identified modulator of select TRP channels (*137*). High airway pressures could induce similar changes in lung capillary endothelial nitric oxide, suggesting that alveolar signals may cause alterations in the vascular barrier in response to airway forces. This process is potentially mediated via activation of TRP channels on epithelial cells and sensory nerves, which subsequently release factors that affect endothelial cells (e.g., tachykinins, cytokines, or arachidonic acid metabolites). Jian *et al.* (*154*) showed that the lung capillary response to high vascular pressure involved cytochrome P450 epoxygenase dependent activation of TRPV4, presumably involving 5,6- or 14,15-EET, leading to increased Kfc and vascular leakage. Increases in lung capillary pressure to 30 cm H_2O resulted in a significant increase in Kfc, which was significantly reduced in TRPV4 knockout mice. Using lower capillary pressures (15 cm H_2O) Yin *et al.* (*155*) suggested that high vascular pressure

activated a negative feedback loop involving nitric oxide cyclic guanosine monophosphate (NO-cGMP) that inhibited TRPV4 and attenuated further increases in endothelial permeability. The lower vascular pressures (15 cm H_2O) and the use of statically inflated lungs by Yin *et al.*, as opposed to cyclically ventilated lungs, may contribute to the different responses highlighting the summation of airway and vascular forces into an integrated response controlled to a significant degree by TRP channel function.

How mechanosensitive ion channels like TRPC1, TRPC4 and TRPV4 are activated by physical forces remains largely unknown. Direct interaction of stretch activated channels with elements of the cytoskeleton, akin to the hypotheses for TRPA1 in auditory function, has received the most attention (*156*). Several excellent reviews on TRP channels and mechanotransduction are available (*157, 158*) that discuss the TRP family structure function relationship. In endothelial cells, the ER is in close apposition to the plasma membrane (*159, 160*) and, therefore, likely to be in close proximity to sub-membranous cytoskeleton elements including spectrin, protein 4.1 and actin. Antibodies directed against the spectrin-4.1 protein complex abolished thapsigargin activated I_{SOC}, suggesting a role for structural proteins in regulating channel function (*140*). TRPC, TRPA, TRPV and TRPN channels all possess multiple conserved ankyrin binding domains that may link the channel with other structural proteins including actin. There is a paucity of information, however, to conclude that channel cytoskeletal interaction accounts solely for channel regulation. Other factors such as modification of TRP channels by nitrosylation (e.g., TRPV1), other forms of post-translational modification, or the synthesis of endogenous TRP channel agonists may also regulate TRP channel

function and responses to mechanical stimuli. Accordingly, the combined actions of mechanical stress and secondary biochemical activation may better model the time-dependency and pharmacological inhibition of TRP-mediated responses.

1.3 Air Pollution, Particulate Pollutants, TRP Channels, and Lung Injury

Respiratory irritants and toxicants including industrial chemicals, geological dusts, combustion-derived particulates, smoke components, and other respirable substances pose a severe threat to human health (*161-172*). Epidemiological studies have associated air pollution with adverse health effects ranging from school absences to increased rates of cardiovascular- and cardiopulmonary-related hospitalizations and deaths, motivating scientists to elucidate how pollution components cause deleterious effects on multiple levels.

Inhalation exposure to environmental pollutants is associated with pulmonary inflammation, airway epithelial and respiratory cell damage, respiratory dysfunction, increased susceptibility to infection, and the exacerbation of chronic respiratory diseases including asthma and COPD. In the National Mortality and Morbidity Air Pollution Study (NMMAPS) of the 90 largest U.S. cities, a 0.21% ± 0.06 and 0.31% ± 0.09 increase in daily total and cardiopulmonary mortality was observed for each 10 $\mu g/m^3$ increase in particulate matter (PM) $\leq$10 mm median-mass aerodynamic diameter (PM_{10}) measured over a 24-hour period (*173*). In asthmatic children, PM_{10} exposure is associated with a lower forced vital capacity (FVC), forced expiratory volume (FEV_1), and maximal midexpiratory flow (*174*). Fetal growth and development are impaired by

maternal exposure to PM (*175*), and increased infant mortality due to respiratory illness is also associated with PM exposure (*176*). Infants, children, and the elderly are more sensitive to PM-induced respiratory complications, although mechanisms for these differences in sensitivity remain undefined.

Consequences of human exposure to PM (including homogenous particle preparations made for medical or industrial purposes) depend upon the source of PM, specific chemical and physical properties, and dose, including the route of exposure. Arguably, the most critical route of human exposure to environmental PM and pollutant gases is inhalation since the respiratory tract is sensitive to injury, is a direct route to deliver agents to systemic circulation, and is a vital organ. Suspended environmental particles are generally separated by size (μm) into coarse ($PM_{10-2.5}$), fine ($PM_{2.5}$) and ultrafine ($PM_{0.1}$) fractions (*177*). All fractions of PM are capable of entering the respiratory tract, but the deposition of inhaled PM in the respiratory tract is size-dependent. Larger particles and aggregated submicron particles primarily deposit in the nose and upper respiratory tract, mainly the tracheobronchial region, while small particles (~$PM_{2.5}$) show greater deposition in middle and lower airways**.** Ultrafine or nanosized particles ($PM_{0.1}$) are short lived because of a tendency to coalesce, but due to deposition in alveolar regions and a unique ability to enter the general circulation, $PM_{0.1}$ are potentially more toxic to distant organs, again depending upon their composition and associated chemical and physical properties. In other words, the size, shape, and deposition properties of inhaled PM are key, but are not the only factors that determine their disposition in the lung.

Inflammation, lung cell damage, and respiratory distress often occur in animals and humans exposed to high concentrations of PM. Although different particles exhibit different potencies, respiratory tract responses to PM are strikingly uniform from particle to particle, despite the immense heterogeneity in PM composition and inherent differences in cells that are exposed to different components or forms of PM. For a single lung cell type, many of the same signaling cascades are activated (e.g., mitogen activated and extracellular regulated kinases, NF-κB and antioxidant responses) and similar changes in gene expression profiles (e.g., IL-6, IL-8, TNFα and others) are observed even when vastly different PM types are used. The converse is also often true for a single PM sample applied to different cell types. However, exceptions exist, and it is generally accepted that differences in the expression of yet undefined cellular determinants are the basis of differential reactivity to PM.

Accumulating evidence indicates that a limited subset of gene products may ultimately determine how the lung responds to PM. Responses of different cells to different forms of PM are likely the result of which gene products are expressed, in what cellular location they are expressed, and to which pathways they are coupled. However, the precise gene products that detect PM and ultimately initiate responses have not been fully established making it difficult to formulate comprehensive models of toxicity. Early evidence that lung cell responses to PM may be mediated by specific gene products of the TRP family emanate from studies showing that many cellular responses to PM can be mimicked by treating cells or animals with synthetic homogenous PM (*178-181*), pure chemical agents such as the TRPV1 agonist capsaicin (*73, 76, 181-183*), and the TRPA1 agonists acrolein and crotonaldehyde (*184-187*). These TRPA1 agonists can be found in

certain forms of PM, oxidants (*22, 188, 189*), and acid aerosols (*22*) that elicit responses similar to PM. Additionally, studies showing that pretreatment of animals with capsaicin to delete pulmonary sensory nerves that express TRPV1 and that the TRPV1 antagonist capsazepine attenuates responses to PM suggests that these TRP channels may be important mediators of PM toxicity.

Currently, only a few examples exist where a specific receptor or "PM sensor" is responsible for the majority of the cellular responses to certain forms of PM or select components of PM. First is the toll-like receptor 4 for LPS, a common, but not ubiquitous component of environmental dusts. The lipid A moiety of LPS binds to CD14 and toll-like receptor 4 on pulmonary macrophages (*190, 191*) resulting in the activation of mitogen activated kinases (MAPK), which promotes NF-kB dependent transcription of a variety of proinflammatory genes. Additional examples include the epidermal growth factor receptor (EGFR, ErbB1) and the macrophage scavenger receptor MARCO (*192-197*) for silica. However, while these three receptors appear to be important determinants of responses to select forms of PM in the lung, they do not represent a unifying mechanism explaining the effects of different PM and antagonists on different lung cell types, or even composite responses of the intact lung. Additional gene products must also have the capacity to differentially detect select forms of PM and initiate responses that contribute to the overall effects in the lung.

There are several hypotheses explaining how PM toxicity is manifested in the lung. Studies have correlated cellular responses with PM size, shape, redox active transition metal ($Cu^{+/2+}$ and $Fe^{2+/3+}$) content and leachability, and even the presence or absence of adsorbed, but often unidentified organics. However, these correlations have

been disproven in large studies of PM and different cell types suggesting that they are specific for a limited set of PM and cell types.

An evolving hypothesis focuses on TRPV1. In several studies, TRPV1 was found to be a key molecular determinant and mediator of the inflammatory and cytotoxic effects of PM (*179, 181-183, 198-200*). Epithelial cells lining the nasal passages and major airways are arguably the first cells to encounter inhaled PM due to both their location and abundance. Thus, these cells are likely early responders to irritating airborne stimuli, such as PM (*74*). Additionally, sensory neurons that terminate immediately below the epithelial cell layers of the respiratory tract are critical mediators of behavioral, reflex and molecular responses to many toxicants adsorbed to PM and also likely initially respond to PM or its components.

As discussed previously, neurogenic inflammation involves the activation of various sensory receptors including TRPV1 and TRPA1. Evidence linking sensory nerves and TRPV1 to PM responses includes the following: TRPV1 postive C-fiber depletion in animals by capsaicin pretreatment reduces plasma extravasation evoked by pollutants in airways (*200*) and attenuates many neuronally mediated responses (e.g., cough, apnea, cardiac arrhythmia and oxidative stress, and inflammation) elicited by PM (*201, 202*) and other components of air pollution (*96, 125, 203*). Accordingly, capsazepine, a moderately selective TRPV1 antagonist, has also been shown to prevent several responses to PM and other known components of air pollution (*201*). However, capsaicin pretreatment can also exacerbate lung injury after exposure to some PM, including diesel exhaust PM (DEP) suggesting TRPV1 positive sensory nerves may also fetter the immune response, potentially via somatostatin as shown for LPS. Alternate

pathways must also contribute to PM-induced lung injury, including the activation of additional receptors, TRPV1 deficient sensory nerves, and other cell types.

The ability of nonneuronal lung cells to initiate proinflammatory responses to PM has been known for some time, but the involvement of a specific "PM sensor" was first shown in seminal studies by Agopyan *et al.* (*73, 178, 179*) and Veronesi *et al.* (*181-183, 198*) TRPV1 and acid sensing (ASIC) ion channels expressed by immortalized (BEAS-2B) and primary (NHBE and SAEC) airway epithelial cells were activated by PM that carried a net-negative surface charge (i.e., a negative *zeta* potential) and activation was coupled with elicited cytokine/chemokine (i.e., IL-6, IL-8, and TNFα) production and apoptosis (*73, 178, 181-183, 198*). Furthermore, TRPV1 activation was enhanced by sensory neuropeptides (i.e., CGRP and substance P), suggesting that complementary interactions between sensory neurons and epithelial cells occur in the intact lung. These results were significant for several reasons: they identified specific gene products that detect PM, established plausible mechanisms of action at the molecular level, and demonstrated that lung epithelial cells also contribute to the deleterious effects of PM in the intact lung since the expression of TRPV1 in lung epithelial cells is not eliminated by capsaicin pretreatment. As such, the ability of TRPV1 to be activated by PM in airway epithelial cells is likely a contributory factor to composite responses to PM.

To date, the activation of other TRP channels by particulate pollutants has not been evaluated. Correlations between biological activity of particulate materials, inhibition by antioxidants, transition metal content, oxidant potential, organic carbon content, acidity, and their ability to produce lipid aldehydes strongly suggest that TRPA1 may be an additional mediator of particulate pollutant toxicities in the lung.

Interestingly, multiple components of ambient particulate materials (e.g., acrolein and crotonaldehyde) are potent agonists of TRPA1 (*19, 22, 187, 204, 205*), and not TRPV1, suggesting that the origin and composition of ambient particles will impact the ability of TRPV1 and/or TRPA1 to ultimately sense PM and initiate deleterious processes such as neurogenic or epithelial cell-derived inflammation and damage.

Understanding the pathways by which PM elicits adverse effects in the lung is complicated by the heterogeneous composition of pollutants as well as the diverse responses observed after exposure. However, by identifying target receptors for different PM or components of PM, such as TRPV1, TLR-4, etc, the construction of a more defined mechanism associating PM and adverse health effects will be feasible. Thus, TRP channels are promising new targets for understanding the adverse health effects of PM.

1.4 Summary

TRP channels are central to respiratory physiology: as pulmonary sensors of potentially deleterious stimuli; as regulators of reflex responses such as cough, changes in breathing pattern; as initiators of innate immune responses; and for maintenance of vascular barrier function. TRP channels are now recognized as critical for the maintenance of normal pulmonary physiology and as key mediators of pulmonary injury elicited by both endogenous and exogenous stimuli. The TRP channel field is exciting and rapidly advancing, and will continue to enhance our understanding of sensory physiology, and the mechanisms through which these channels regulate normal and abnormal respiratory conditions. TRPV1 antagonists will continue to be developed for pain treatment and it is likely that the availability of such probes will continue to advance

the field of TRP channels in respiratory physiology. Additional research is expected to elucidate how endovanilloids, TRPV1, and other endogenous agents and TRP channels contribute to lung injury during systemic inflammation and through direct channel activation by agonists. Understanding of TRP channels in respiratory disease may lead to novel treatment modalities for complicated and often lethal disease states such as acute respiratory distress syndrome (ARDS), asthma, COPD, or chronic lung disease associated with mechanical ventilation. Finally, identification of select TRP channels as sensors for respiratory irritants and air pollutants such as PM will help establish more precise cause/effect relationships for environmental lung diseases, improving our ability to link the morbidity and mortality associated with high pollution events with distinct cellular responses and susceptibility factors.

Additional chapters in this dissertation will focus on the pharmacology and physiology of TRPV1 in the lung epithelium. Research showing how TRPV1 induces ER stress and lung cell death will be presented in Chapter 2. Chapter 3 will discuss the structure activity relationship between capsaicinoid analogues and TRPV1, highlighting structural features of capsaicin and nonivamide that are essential for TRPV1 activity. Chapter 4 will examine TRPV1 as a mediator of lung injury in mice after LPS treatment, with evidence that TRPV1 blockade can attenuate lung injury in a model of inflammatory lung injury.

1.5 Footnotes

A sincere thank you to Dr. Randal O. Dull and Dr. Cassandra Deering-Rice for contributing the text for sections 2.B. and 2.C. and for sharing their expertise.

1.6 References

1. Venkatachalam, K., and Montell, C. (2007) TRP channels, *Annu Rev Biochem 76*, 387-417.

2. Vriens, J., Appendino, G., and Nilius, B. (2009) Pharmacology of vanilloid transient receptor potential cation channels, *Mol Pharmacol 75*, 1262-1279.

3. Nilius, B., Owsianik, G., Voets, T., and Peters, J. A. (2007) Transient receptor potential cation channels in disease, *Physiol Rev 87*, 165-217.

4. Pedersen, S. F., Owsianik, G., and Nilius, B. (2005) TRP channels: an overview, *Cell Calcium 38*, 233-252.

5. Voets, T., Talavera, K., Owsianik, G., and Nilius, B. (2005) Sensing with TRP channels, *Nat Chem Biol 1*, 85-92.

6. Montell, C., Birnbaumer, L., Flockerzi, V., Bindels, R. J., Bruford, E. A., Caterina, M. J., Clapham, D. E., Harteneck, C., Heller, S., Julius, D., Kojima, I., Mori, Y., Penner, R., Prawitt, D., Scharenberg, A. M., Schultz, G., Shimizu, N., and Zhu, M. X. (2002) A unified nomenclature for the superfamily of TRP cation channels, *Mol Cell 9*, 229-231.

7. Venkatachalam, K., Montell, C., Bessac, B. F., Jordt, S. E., Cioffi, D. L., Lowe, K., Alvarez, D. F., Barry, C., Stevens, T., Colburn, R. W., Lubin, M. L., Stone, D. J., Jr., Wang, Y., Lawrence, D., D'Andrea, M. R., Brandt, M. R., Liu, Y., Flores, C. M., Qin, N., Foulkes, T., Wood, J. N., Groneberg, D. A., Quarcoo, D., Frossard, N., Fischer, A., Khairatkar-Joshi, N., Szallasi, A., Yoshida, T., Inoue, R., Morii, T., Takahashi, N., Yamamoto, S., Hara, Y., Tominaga, M., Shimizu, S., Sato, Y., and Mori, Y. (2007) TRP channels. *Annu Rev Biochem 76*, 387-417.

8. Wu, L. J., Sweet, T. B., and Clapham, D. E. International Union of Basic and Clinical Pharmacology. LXXVI. Current progress in the mammalian TRP ion channel family, *Pharmacol Rev 62*, 381-404.

9. Hofmann, T., Schaefer, M., Schultz, G., and Gudermann, T. (2002) Subunit composition of mammalian transient receptor potential channels in living cells, *Proc Natl Acad Sci U S A 99*, 7461-7466.

10. Montell, C., and Rubin, G. M. (1989) Molecular characterization of the Drosophila trp locus: a putative integral membrane protein required for phototransduction, *Neuron 2*, 1313-1323.

11. Minke, B. (1982) Light-induced reduction in excitation efficiency in the trp mutant of Drosophila, *J Gen Physiol 79*, 361-385.

12. Szallasi, A., Cortright, D. N., Blum, C. A., and Eid, S. R. (2007) The vanilloid receptor TRPV1: 10 years from channel cloning to antagonist proof-of-concept, *Nat Rev Drug Discov 6*, 357-372.

13. Tabuchi, K., Suzuki, M., Mizuno, A., and Hara, A. (2005) Hearing impairment in TRPV4 knockout mice, *Neurosci Lett 382*, 304-308.

14. Mandadi, S., and Roufogalis, B. D. (2008) ThermoTRP Channels in Nociceptors: Taking a Lead from Capsaicin Receptor TRPV1, *Curr Neuropharmacol 6*, 21-38.

15. Damak, S., Rong, M., Yasumatsu, K., Kokrashvili, Z., Perez, C. A., Shigemura, N., Yoshida, R., Mosinger, B., Jr., Glendinning, J. I., Ninomiya, Y., and Margolskee, R. F. (2006) Trpm5 null mice respond to bitter, sweet, and umami compounds, *Chem Senses 31*, 253-264.

16. Story, G. M., Peier, A. M., Reeve, A. J., Eid, S. R., Mosbacher, J., Hricik, T. R., Earley, T. J., Hergarden, A. C., Andersson, D. A., Hwang, S. W., McIntyre, P., Jegla, T., Bevan, S., and Patapoutian, A. (2003) ANKTM1, a TRP-like channel expressed in nociceptive neurons, is activated by cold temperatures, *Cell 112*, 819-829.

17. Bessac, B. F., and Jordt, S. E. (2008) Breathtaking TRP channels: TRPA1 and TRPV1 in airway chemosensation and reflex\ control, *Physiology (Bethesda) 23*, 360-370.

18. Sotomayor, M., Corey, D. P., and Schulten, K. (2005) In search of the hair-cell gating spring elastic properties of ankyrin and cadherin repeats, *Structure 13*, 669-682.

19. Andrè, E., Campi, B., Materazzi, S., Trevisani, M., Amadesi, S., Massi, D., Creminon, C., Vaksman, N., Nassini, R., Civelli, M., Baraldi, P. G., Poole, D. P., Bunnett, N. W., Geppetti, P., and Patacchini, R. (2008) Cigarette smoke-induced neurogenic inflammation is mediated by α,β-unsaturated aldehydes and the TRPA1 receptor in rodents, *The Journal of Clinical Investigation 118*, 2574-2582.

20. Hinman, A., Chuang, H. H., Bautista, D. M., and Julius, D. (2006) TRP channel activation by reversible covalent modification, *Proc Natl Acad Sci U S A 103*, 19564-19568.

21. Macpherson, L. J., Dubin, A. E., Evans, M. J., Marr, F., Schultz, P. G., Cravatt, B. F., and Patapoutian, A. (2007) Noxious compounds activate TRPA1 ion channels through covalent modification of cysteines, *Nature 445*, 541-545.

22. Bessac, B. F., Sivula, M., von Hehn, C. A., Escalera, J., Cohn, L., and Jordt, S. E. (2008) TRPA1 is a major oxidant sensor in murine airway sensory neurons, *J Clin Invest 118*, 1899-1910.

23. Brooks, S. M. (2008) Irritant-induced chronic cough: irritant-induced TRPpathy, *Lung 186 Suppl 1*, S88-93.

24. Lanosa, M. J., Willis, D. N., Jordt, S., and Morris, J. B. Role of metabolic activation and the TRPA1 receptor in the sensory irritation response to styrene and naphthalene, *Toxicol Sci 115*, 589-595.

25. Jordt, S. E., Bautista, D. M., Chuang, H. H., McKemy, D. D., Zygmunt, P. M., Hogestatt, E. D., Meng, I. D., and Julius, D. (2004) Mustard oils and cannabinoids excite sensory nerve fibres through the TRP channel ANKTM1, *Nature 427*, 260-265.

26. Karashima, Y., Talavera, K., Everaerts, W., Janssens, A., Kwan, K. Y., Vennekens, R., Nilius, B., and Voets, T. (2009) TRPA1 acts as a cold sensor in vitro and in vivo, *Proc Natl Acad Sci U S A 106*, 1273-1278.

27. Wes, P. D., Chevesich, J., Jeromin, A., Rosenberg, C., Stetten, G., and Montell, C. (1995) TRPC1, a human homolog of a Drosophila store-operated channel, *Proc Natl Acad Sci U S A 92*, 9652-9656.

28. Strubing, C., Krapivinsky, G., Krapivinsky, L., and Clapham, D. E. (2003) Formation of novel TRPC channels by complex subunit interactions in embryonic brain, *J Biol Chem 278*, 39014-39019.

29. Clapham, D. E. (2003) TRP channels as cellular sensors, *Nature 426*, 517-524.

30. Duncan, L. M., Deeds, J., Hunter, J., Shao, J., Holmgren, L. M., Woolf, E. A., Tepper, R. I., and Shyjan, A. W. (1998) Down-regulation of the novel gene melastatin correlates with potential for melanoma metastasis, *Cancer Res 58*, 1515-1520.

31. McKemy, D. D. (2005) How cold is it? TRPM8 and TRPA1 in the molecular logic of cold sensation, *Mol Pain 1*, 16.

32. McKemy, D. D., Neuhausser, W. M., and Julius, D. (2002) Identification of a cold receptor reveals a general role for TRP channels in thermosensation, *Nature 416*, 52-58.

33. Peier, A. M., Moqrich, A., Hergarden, A. C., Reeve, A. J., Andersson, D. A., Story, G. M., Earley, T. J., Dragoni, I., McIntyre, P., Bevan, S., and Patapoutian, A. (2002) A TRP channel that senses cold stimuli and menthol, *Cell 108*, 705-715.

34. Sabnis, A. S., Shadid, M., Yost, G. S., and Reilly, C. A. (2008) Human lung epithelial cells express a functional cold-sensing TRPM8 variant, *Am J Respir Cell Mol Biol 39*, 466-474.

35. Thebault, S., Lemonnier, L., Bidaux, G., Flourakis, M., Bavencoffe, A., Gordienko, D., Roudbaraki, M., Delcourt, P., Panchin, Y., Shuba, Y., Skryma, R., and Prevarskaya, N. (2005) Novel role of cold/menthol-sensitive transient receptor potential melastatine family member 8 (TRPM8) in the activation of store-operated channels in LNCaP human prostate cancer epithelial cells, *J Biol Chem 280*, 39423-39435.

36. Tsavaler, L., Shapero, M. H., Morkowski, S., and Laus, R. (2001) Trp-p8, a novel prostate-specific gene, is up-regulated in prostate cancer and other malignancies and shares high homology with transient receptor potential calcium channel proteins, *Cancer Res 61*, 3760-3769.

37. Bandell, M., Dubin, A. E., Petrus, M. J., Orth, A., Mathur, J., Hwang, S. W., and Patapoutian, A. (2006) High-throughput random mutagenesis screen reveals TRPM8 residues specifically required for activation by menthol, *Nat Neurosci 9*, 493-500.

38. Chuang, H. H., Neuhausser, W. M., and Julius, D. (2004) The super-cooling agent icilin reveals a mechanism of coincidence detection by a temperature-sensitive TRP channel, *Neuron 43*, 859-869.

39. Chung, M. K., and Caterina, M. J. (2007) TRP channel knockout mice lose their cool, *Neuron 54*, 345-347.

40. Sabnis, A. S., Reilly, C. A., Veranth, J. M., and Yost, G. S. (2008) Increased transcription of cytokine genes in human lung epithelial cells through activation of a TRPM8 variant by cold temperatures, *Am J Physiol Lung Cell Mol Physiol 295*, L194-200.

41. Bargal, R., Avidan, N., Ben-Asher, E., Olender, Z., Zeigler, M., Frumkin, A., Raas-Rothschild, A., Glusman, G., Lancet, D., and Bach, G. (2000) Identification of the gene causing mucolipidosis type IV, *Nat Genet 26*, 118-123.

42. Wu, G., Mochizuki, T., Le, T. C., Cai, Y., Hayashi, T., Reynolds, D. M., and Somlo, S. (1997) Molecular cloning, cDNA sequence analysis, and chromosomal localization of mouse Pkd2, *Genomics 45*, 220-223.

43. Caterina, M. J., Schumacher, M. A., Tominaga, M., Rosen, T. A., Levine, J. D., and Julius, D. (1997) The capsaicin receptor: a heat-activated ion channel in the pain pathway, Nature 389, 816-824.

44. Jordt, S. E., Tominaga, M., and Julius, D. (2000) Acid potentiation of the capsaicin receptor determined by a key extracellular site, *Proc Natl Acad Sci U S A 97*, 8134-8139.

45. Light, A. R., Hughen, R. W., Zhang, J., Rainier, J., Liu, Z., and Lee, J. (2008) Dorsal root ganglion neurons innervating skeletal muscle respond to physiological combinations of protons, ATP, and lactate mediated by ASIC, P2X, and TRPV1, *J Neurophysiol 100*, 1184-1201.

46. Tominaga, M., Caterina, M. J., Malmberg, A. B., Rosen, T. A., Gilbert, H., Skinner, K., Raumann, B. E., Basbaum, A. I., and Julius, D. (1998) The cloned capsaicin receptor integrates multiple pain-producing stimuli, *Neuron 21*, 531-543.

47. Hwang, S. W., Cho, H., Kwak, J., Lee, S. Y., Kang, C. J., Jung, J., Cho, S., Min, K. H., Suh, Y. G., Kim, D., and Oh, U. (2000) Direct activation of capsaicin receptors by products of lipoxygenases: endogenous capsaicin-like substances, *Proc Natl Acad Sci U S A 97*, 6155-6160.

48. Trevisani, M., Patacchini, R., Nicoletti, P., Gatti, R., Gazzieri, D., Lissi, N., Zagli, G., Creminon, C., Geppetti, P., and Harrison, S. (2005) Hydrogen sulfide causes vanilloid receptor 1-mediated neurogenic inflammation in the airways, *Br J Pharmacol 145*, 1123-1131.

49. Zygmunt, P. M., Petersson, J., Andersson, D. A., Chuang, H., Sorgard, M., Di Marzo, V., Julius, D., and Hogestatt, E. D. (1999) Vanilloid receptors on sensory nerves mediate the vasodilator action of anandamide, *Nature 400*, 452-457.

50. Szallasi, A., and Blumberg, P. M. (1989) Resiniferatoxin, a phorbol-related diterpene, acts as an ultrapotent analog of capsaicin, the irritant constituent in red pepper, *Neuroscience 30*, 515-520.

51. Johnson, D. M., Garrett, E. M., Rutter, R., Bonnert, T. P., Gao, Y. D., Middleton, R. E., and Sutton, K. G. (2006) Functional mapping of the transient receptor potential vanilloid 1 intracellular binding site, *Mol Pharmacol 70*, 1005-1012.

52. Jordt, S. E., and Julius, D. (2002) Molecular basis for species-specific sensitivity to "hot" chili peppers, *Cell 108*, 421-430.

53. Gavva, N. R., Klionsky, L., Qu, Y., Shi, L., Tamir, R., Edenson, S., Zhang, T. J., Viswanadhan, V. N., Toth, A., Pearce, L. V., Vanderah, T. W., Porreca, F., Blumberg, P. M., Lile, J., Sun, Y., Wild, K., Louis, J. C., and Treanor, J. J. (2004) Molecular determinants of vanilloid sensitivity in TRPV1, *J Biol Chem 279*, 20283-20295.

54. Sutton, K. G., Garrett, E. M., Rutter, A. R., Bonnert, T. P., Jarolimek, W., and Seabrook, G. R. (2005) Functional characterisation of the S512Y mutant vanilloid human TRPV1 receptor, *Br J Pharmacol 146*, 702-711.

55. Brauchi, S., Orta, G., Salazar, M., Rosenmann, E., and Latorre, R. (2006) A hot-sensing cold receptor: C-terminal domain determines thermosensation in transient receptor potential channels, *J Neurosci 26*, 4835-4840.

56. Walpole, C. S., Bevan, S., Bovermann, G., Boelsterli, J. J., Breckenridge, R., Davies, J. W., Hughes, G. A., James, I., Oberer, L., Winter, J., and et al. (1994) The discovery of capsazepine, the first competitive antagonist of the sensory neuron excitants capsaicin and resiniferatoxin, *J Med Chem 37*, 1942-1954.

57. Wahl, P., Foged, C., Tullin, S., and Thomsen, C. (2001) Iodo-resiniferatoxin, a new potent vanilloid receptor antagonist, *Mol Pharmacol 59*, 9-15.

58. Khairatkar-Joshi, N., and Szallasi, A. (2009) TRPV1 antagonists: the challenges for therapeutic targeting, *Trends Mol Med 15*, 14-22.

59. Romanovsky, A. A., Almeida, M. C., Garami, A., Steiner, A. A., Norman, M. H., Morrison, S. F., Nakamura, K., Burmeister, J. J., and Nucci, T. B. (2009) The transient receptor potential vanilloid-1 channel in thermoregulation: a thermosensor it is not, *Pharmacol Rev 61*, 228-261.

60. Westaway, S. M. (2007) The potential of transient receptor potential vanilloid type 1 channel modulators for the treatment of pain, *J Med Chem 50*, 2589-2596.

61. Caterina, M. J., Rosen, T. A., Tominaga, M., Brake, A. J., and Julius, D. (1999) A capsaicin-receptor homologue with a high threshold for noxious heat, *Nature 398*, 436-441.

62. Neeper, M. P., Liu, Y., Hutchinson, T. L., Wang, Y., Flores, C. M., and Qin, N. (2007) Activation properties of heterologously expressed mammalian TRPV2: evidence for species dependence, *J Biol Chem 282*, 15894-15902.

63. Qin, N., Neeper, M. P., Liu, Y., Hutchinson, T. L., Lubin, M. L., and Flores, C. M. (2008) TRPV2 is activated by cannabidiol and mediates CGRP release in cultured rat dorsal root ganglion neurons, *J Neurosci 28*, 6231-6238.

64. Smith, G. D., Gunthorpe, M. J., Kelsell, R. E., Hayes, P. D., Reilly, P., Facer, P., Wright, J. E., Jerman, J. C., Walhin, J. P., Ooi, L., Egerton, J., Charles, K. J., Smart, D., Randall, A. D., Anand, P., and Davis, J. B. (2002) TRPV3 is a temperature-sensitive vanilloid receptor-like protein, *Nature 418*, 186-190.

65. Xu, H., Delling, M., Jun, J. C., and Clapham, D. E. (2006) Oregano, thyme and clove-derived flavors and skin sensitizers activate specific TRP channels, *Nat Neurosci 9*, 628-635.

66. Nilius, B., Vriens, J., Prenen, J., Droogmans, G., and Voets, T. (2004) TRPV4 calcium entry channel: a paradigm for gating diversity, *Am J Physiol Cell Physiol 286*, C195-205.

67. van de Graaf, S. F., Hoenderop, J. G., and Bindels, R. J. (2006) Regulation of TRPV5 and TRPV6 by associated proteins, *Am J Physiol Renal Physiol 290*, F1295-1302.

68. Jia, Y., and Lee, L. Y. (2007) Role of TRPV receptors in respiratory diseases, *Biochim Biophys Acta 1772*, 915-927.

69. Baluk, P., Thurston, G., Murphy, T. J., Bunnett, N. W., and McDonald, D. M. (1999) Neurogenic plasma leakage in mouse airways, *Br J Pharmacol 126*, 522-528.

70. Elekes, K., Helyes, Z., Nemeth, J., Sandor, K., Pozsgai, G., Kereskai, L., Borzsei, R., Pinter, E., Szabo, A., and Szolcsanyi, J. (2007) Role of capsaicin-sensitive afferents and sensory neuropeptides in endotoxin-induced airway inflammation and consequent bronchial hyperreactivity in the mouse, *Regul Pept 141*, 44-54.

71. Jancso, N., Jancso-Gabor, A., and Szolcsanyi, J. (1967) Direct evidence for neurogenic inflammation and its prevention by denervation and by pretreatment with capsaicin, *Br J Pharmacol Chemother 31*, 138-151.

72. Jia, Y., McLeod, R. L., and Hey, J. A. (2005) TRPV1 receptor: a target for the treatment of pain, cough, airway disease and urinary incontinence, *Drug News Perspect 18*, 165-171.

73. Agopyan, N., Head, J., Yu, S., and Simon, S. A. (2004) TRPV1 receptors mediate particulate matter-induced apoptosis, *Am J Physiol Lung Cell Mol Physiol 286*, L563-572.

74. Veronesi, B., Carter, J. D., Devlin, R. B., Simon, S. A., and Oortgiesen, M. (1999) Neuropeptides and capsaicin stimulate the release of inflammatory cytokines in a human bronchial epithelial cell line, *Neuropeptides 33*, 447-456.

75. Reilly, C. A., Johansen, M. E., Lanza, D. L., Lee, J., Lim, J. O., and Yost, G. S. (2005) Calcium-dependent and independent mechanisms of capsaicin receptor (TRPV1)-mediated cytokine production and cell death in human bronchial epithelial cells, *J Biochem Mol Toxicol 19*, 266-275.

76. Reilly, C. A., Taylor, J. L., Lanza, D. L., Carr, B. A., Crouch, D. J., and Yost, G. S. (2003) Capsaicinoids cause inflammation and epithelial cell death through activation of vanilloid receptors, *Toxicol Sci 73*, 170-181.

77. Thomas, K. C., Sabnis, A. S., Johansen, M. E., Lanza, D. L., Moos, P. J., Yost, G. S., and Reilly, C. A. (2007) Transient receptor potential vanilloid 1 agonists cause endoplasmic reticulum stress and cell death in human lung cells, *J Pharmacol Exp Ther 321*, 830-838.

78. Johansen, M. E., Reilly, C. A., and Yost, G. S. (2006) TRPV1 antagonists elevate cell surface populations of receptor protein and exacerbate TRPV1-mediated toxicities in human lung epithelial cells, *Toxicol Sci 89*, 278-286.

79. Bernales, S., Papa, F. R., and Walter, P. (2006) Intracellular signaling by the unfolded protein response, *Annu Rev Cell Dev Biol 22*, 487-508.

80. Schroder, M., and Kaufman, R. J. (2005) The mammalian unfolded protein response, *Annu Rev Biochem 74*, 739-789.

81. Kozutsumi, Y., Segal, M., Normington, K., Gething, M. J., and Sambrook, J. (1988) The presence of malfolded proteins in the endoplasmic reticulum signals the induction of glucose-regulated proteins, *Nature 332*, 462-464.

82. Lin, J. H., Li, H., Zhang, Y., Ron, D., and Walter, P. (2009) Divergent effects of PERK and IRE1 signaling on cell viability, *PLoS One 4*, e4170.

83. Ron, D., and Walter, P. (2007) Signal integration in the endoplasmic reticulum unfolded protein response, *Nat Rev Mol Cell Biol 8*, 519-529.

84. Harding, H. P., Zhang, Y., and Ron, D. (1999) Protein translation and folding are coupled by an endoplasmic-reticulum-resident kinase, *Nature 397*, 271-274.

85. Barone, M. V., Crozat, A., Tabaee, A., Philipson, L., and Ron, D. (1994) CHOP (GADD153) and its oncogenic variant, TLS-CHOP, have opposing effects on the induction of G1/S arrest, *Genes Dev 8*, 453-464.

86. Boyce, M., Bryant, K. F., Jousse, C., Long, K., Harding, H. P., Scheuner, D., Kaufman, R. J., Ma, D., Coen, D. M., Ron, D., and Yuan, J. (2005) A selective inhibitor of eIF2alpha dephosphorylation protects cells from ER stress, *Science 307*, 935-939.

87. Endo, M., Oyadomari, S., Suga, M., Mori, M., and Gotoh, T. (2005) The ER stress pathway involving CHOP is activated in the lungs of LPS-treated mice, *J Biochem 138*, 501-507.

88. Endo, M., Mori, M., Akira, S., and Gotoh, T. (2006) C/EBP homologous protein (CHOP) is crucial for the induction of caspase-11 and the pathogenesis of lipopolysaccharide-induced inflammation, *J Immunol 176*, 6245-6253.

89. Van Der Stelt, M., and Di Marzo, V. (2004) Endovanilloids. Putative endogenous ligands of transient receptor potential vanilloid 1 channels, *Eur J Biochem 271*, 1827-1834.

90. Ang, S. F., Moochhala, S. M., and Bhatia, M. (2010) Hydrogen sulfide promotes transient receptor potential vanilloid 1-mediated neurogenic inflammation in polymicrobial sepsis, *Crit Care Med 38*, 619-628.

91. Li, L., Bhatia, M., Zhu, Y. Z., Zhu, Y. C., Ramnath, R. D., Wang, Z. J., Anuar, F. B., Whiteman, M., Salto-Tellez, M., and Moore, P. K. (2005) Hydrogen sulfide is a novel mediator of lipopolysaccharide-induced inflammation in the mouse, *Faseb J 19*, 1196-1198.

92. Liu, J., Batkai, S., Pacher, P., Harvey-White, J., Wagner, J. A., Cravatt, B. F., Gao, B., and Kunos, G. (2003) Lipopolysaccharide induces anandamide synthesis in macrophages via CD14/MAPK/phosphoinositide 3-kinase/NF-kappaB independently of platelet-activating factor, *J Biol Chem 278*, 45034-45039.

93. Maccarrone, M., De Petrocellis, L., Bari, M., Fezza, F., Salvati, S., Di Marzo, V., and Finazzi-Agro, A. (2001) Lipopolysaccharide downregulates fatty acid amide hydrolase expression and increases anandamide levels in human peripheral lymphocytes, *Arch Biochem Biophys 393*, 321-328.

94. Orliac, M. L., Peroni, R., Celuch, S. M., and Adler-Graschinsky, E. (2003) Potentiation of anandamide effects in mesenteric beds isolated from endotoxemic rats, *J Pharmacol Exp Ther 304*, 179-184.

95. Singh Tahim, A., Santha, P., and Nagy, I. (2005) Inflammatory mediators convert anandamide into a potent activator of the vanilloid type 1 transient receptor potential receptor in nociceptive primary sensory neurons, *Neuroscience 136*, 539-548.

96. Zhang, H., Hegde, A., Ng, S. W., Adhikari, S., Moochhala, S. M., and Bhatia, M. (2007) Hydrogen sulfide up-regulates substance P in polymicrobial sepsis-associated lung injury, *J Immunol 179*, 4153-4160.

97. Zhang, H., Zhi, L., Moore, P. K., and Bhatia, M. (2006) Role of hydrogen sulfide in cecal ligation and puncture-induced sepsis in the mouse, *Am J Physiol Lung Cell Mol Physiol 290*, L1193-1201.

98. Patwardhan, A. M., Akopian, A. N., Ruparel, N. B., Diogenes, A., Weintraub, S. T., Uhlson, C., Murphy, R. C., and Hargreaves, K. M. (2010) Heat generates oxidized linoleic acid metabolites that activate TRPV1 and produce pain in rodents, *J Clin Invest 120*, 1617-1626.

99. Patwardhan, A. M., Scotland, P. E., Akopian, A. N., and Hargreaves, K. M. (2009) Activation of TRPV1 in the spinal cord by oxidized linoleic acid metabolites contributes to inflammatory hyperalgesia, *Proc Natl Acad Sci U S A 106*, 18820-18824.

100. Devane, W. A., Hanus, L., Breuer, A., Pertwee, R. G., Stevenson, L. A., Griffin, G., Gibson, D., Mandelbaum, A., Etinger, A., and Mechoulam, R. (1992) Isolation and structure of a brain constituent that binds to the cannabinoid receptor, *Science 258*, 1946-1949.

101. Smart, D., Gunthorpe, M. J., Jerman, J. C., Nasir, S., Gray, J., Muir, A. I., Chambers, J. K., Randall, A. D., and Davis, J. B. (2000) The endogenous lipid anandamide is a full agonist at the human vanilloid receptor (hVR1), *Br J Pharmacol 129*, 227-230.

102. Calignano, A., Katona, I., Desarnaud, F., Giuffrida, A., La Rana, G., Mackie, K., Freund, T. F., and Piomelli, D. (2000) Bidirectional control of airway responsiveness by endogenous cannabinoids, *Nature 408*, 96-101.

103. Di Marzo, V., Fontana, A., Cadas, H., Schinelli, S., Cimino, G., Schwartz, J. C., and Piomelli, D. (1994) Formation and inactivation of endogenous cannabinoid anandamide in central neurons, *Nature 372*, 686-691.

104. Andersson, D. A., Adner, M., Hogestatt, E. D., and Zygmunt, P. M. (2002) Mechanisms underlying tissue selectivity of anandamide and other vanilloid receptor agonists, *Mol Pharmacol 62*, 705-713.

105. Jia, Y., McLeod, R. L., Wang, X., Parra, L. E., Egan, R. W., and Hey, J. A. (2002) Anandamide induces cough in conscious guinea-pigs through VR1 receptors, *British journal of pharmacology 137*, 831-836.

106. Kollarik, M., and Undem, B. J. (2004) Activation of bronchopulmonary vagal afferent nerves with bradykinin, acid and vanilloid receptor agonists in wild-type and TRPV1-/- mice, *J Physiol 555*, 115-123.

107. McVey, D. C., Schmid, P. C., Schmid, H. H., and Vigna, S. R. (2003) Endocannabinoids induce ileitis in rats via the capsaicin receptor (VR1), *J Pharmacol Exp Ther 304*, 713-722.

108. Orliac, M. L., Peroni, R. N., Abramoff, T., Neuman, I., Podesta, E. J., and Adler-Graschinsky, E. (2007) Increases in vanilloid TRPV1 receptor protein and CGRP content during endotoxemia in rats, *Eur J Pharmacol 566*, 145-152.

109. Starowicz, K., Nigam, S., and Di Marzo, V. (2007) Biochemistry and pharmacology of endovanilloids, *Pharmacol Ther 114*, 13-33.

110. Fenton, M. J., and Golenbock, D. T. (1998) LPS-binding proteins and receptors, *J Leukoc Biol 64*, 25-32.

111. Hotchkiss, R. S., and Karl, I. E. (2003) The pathophysiology and treatment of sepsis, *N Engl J Med 348*, 138-150.

112. Jeyaseelan, S., Chu, H. W., Young, S. K., Freeman, M. W., and Worthen, G. S. (2005) Distinct roles of pattern recognition receptors CD14 and Toll-like receptor 4 in acute lung injury, *Infect Immun 73*, 1754-1763.

113. Moreland, J. G., Fuhrman, R. M., Pruessner, J. A., and Schwartz, D. A. (2002) CD11b and intercellular adhesion molecule-1 are involved in pulmonary neutrophil recruitment in lipopolysaccharide-induced airway disease, *Am J Respir Cell Mol Biol 27*, 474-480.

114. Perera, P. Y., Mayadas, T. N., Takeuchi, O., Akira, S., Zaks-Zilberman, M., Goyert, S. M., and Vogel, S. N. (2001) CD11b/CD18 acts in concert with CD14 and Toll-like receptor (TLR) 4 to elicit full lipopolysaccharide and taxol-inducible gene expression, *J Immunol 166*, 574-581.

115. Pugin, J., Schurer-Maly, C. C., Leturcq, D., Moriarty, A., Ulevitch, R. J., and Tobias, P. S. (1993) Lipopolysaccharide activation of human endothelial and epithelial cells is mediated by lipopolysaccharide-binding protein and soluble CD14, *Proc Natl Acad Sci U S A 90*, 2744-2748.

116. Wright, S. D., Ramos, R. A., Tobias, P. S., Ulevitch, R. J., and Mathison, J. C. (1990) CD14, a receptor for complexes of lipopolysaccharide (LPS) and LPS binding protein, *Science 249*, 1431-1433.

117. Bhatia, M., Wong, F. L., Fu, D., Lau, H. Y., Moochhala, S. M., and Moore, P. K. (2005) Role of hydrogen sulfide in acute pancreatitis and associated lung injury, *Faseb J 19*, 623-625.

118. Bhatia, M., Zhi, L., Zhang, H., Ng, S. W., and Moore, P. K. (2006) Role of substance P in hydrogen sulfide-induced pulmonary inflammation in mice, *Am J Physiol Lung Cell Mol Physiol 291*, L896-904.

119. Collin, M., Anuar, F. B., Murch, O., Bhatia, M., Moore, P. K., and Thiemermann, C. (2005) Inhibition of endogenous hydrogen sulfide formation reduces the organ injury caused by endotoxemia, *Br J Pharmacol 146*, 498-505.

120. Patacchini, R., Santicioli, P., Giuliani, S., and Maggi, C. A. (2005) Pharmacological investigation of hydrogen sulfide (H2S) contractile activity in rat detrusor muscle, *Eur J Pharmacol 509*, 171-177.

121. Zhang, J. Y., Wang, Y., and Prakash, C. (2006) Xenobiotic-metabolizing enzymes in human lung, *Curr Drug Metab 7*, 939-948.

122. Streng, T., Axelsson, H. E., Hedlund, P., Andersson, D. A., Jordt, S. E., Bevan, S., Andersson, K. E., Hogestatt, E. D., and Zygmunt, P. M. (2008) Distribution and function of the hydrogen sulfide-sensitive TRPA1 ion channel in rat urinary bladder, *Eur Urol 53*, 391-399.

123. Hegde, A., Zhang, H., Moochhala, S. M., and Bhatia, M. (2007) Neurokinin-1 receptor antagonist treatment protects mice against lung injury in polymicrobial sepsis, *J Leukoc Biol 82*, 678-685.

124. Ng, S. W., Zhang, H., Hegde, A., and Bhatia, M. (2008) Role of preprotachykinin-A gene products on multiple organ injury in LPS-induced endotoxemia, *J Leukoc Biol 83*, 288-295.

125. Puneet, P., Hegde, A., Ng, S. W., Lau, H. Y., Lu, J., Moochhala, S. M., and Bhatia, M. (2006) Preprotachykinin-A gene products are key mediators of lung injury in polymicrobial sepsis, *J Immunol 176*, 3813-3820.

126. Dib, M., Zsengeller, Z., Mitsialis, A., Lu, B., Craig, S., Gerard, C., and Gerard, N. P. (2009) A paradoxical protective role for the proinflammatory peptide substance P receptor (NK1R) in acute hyperoxic lung injury, *Am J Physiol Lung Cell Mol Physiol 297*, L687-697.

127. Sio, S. W., Moochhala, S., Lu, J., and Bhatia, M. (2009) Early protection from burn-induced acute lung injury by deletion of preprotachykinin-A gene, *Am J Respir Crit Care Med 181*, 36-46.

128. Sio, S. W., Puthia, M. K., Lu, J., Moochhala, S., and Bhatia, M. (2008) The neuropeptide substance P is a critical mediator of burn-induced acute lung injury, *J Immunol 180*, 8333-8341.

129. Helyes, Z., Elekes, K., Nemeth, J., Pozsgai, G., Sandor, K., Kereskai, L., Borzsei, R., Pinter, E., Szabo, A., and Szolcsanyi, J. (2007) Role of transient receptor potential vanilloid 1 receptors in endotoxin-induced airway inflammation in the mouse, *Am J Physiol Lung Cell Mol Physiol 292*, L1173-1181.

130. Tsuji, F., Murai, M., Oki, K., Inoue, H., Sasano, M., Tanaka, H., Inagaki, N., and Aono, H. Effects of SA13353, a Transient Receptor Potential Vanilloid 1 Agonist, on Leukocyte Infiltration in Lipopolysaccharide-Induced Acute Lung Injury and Ovalbumin-Induced Allergic Airway Inflammation, *J Pharmacol Sci 2010*, 30.

131. Adams DJ, R. J., Van Slooten G. (1993) Calcium Signaling in the Vascular Endothelial Cells: Ca+2 Entry and Release, in Ion Fluxes in Pulmonary Vascular COntrol (Weir EK, H. J., Reeves JT, Ed.), Plenum Press, NY, NY.

132. Dudek, S. M., and Garcia, J. G. (2001) Cytoskeletal regulation of pulmonary vascular permeability, *J Appl Physiol 91*, 1487-1500.

133. Garcia, J. G., and Schaphorst, K. L. (1995) Regulation of endothelial cell gap formation and paracellular permeability, *J Investig Med 43*, 117-126.

134. Balligand, J. L., Feron, O., and Dessy, C. (2009) eNOS activation by physical forces: from short-term regulation of contraction to chronic remodeling of cardiovascular tissues, *Physiol Rev 89*, 481-534.

135. Forstermann, U. (2006) Endothelial NO synthase as a source of NO and superoxide, Eur J Clin Pharmacol 62, 5-12.

136. Hara, Y., Wakamori, M., Ishii, M., Maeno, E., Nishida, M., Yoshida, T., Yamada, H., Shimizu, S., Mori, E., Kudoh, J., Shimizu, N., Kurose, H., Okada, Y., Imoto, K., and Mori, Y. (2002) LTRPC2 Ca2+-permeable channel activated by changes in redox status confers susceptibility to cell death, *Mol Cell 9*, 163-173.

137. Yoshida, T., Inoue, R., Morii, T., Takahashi, N., Yamamoto, S., Hara, Y., Tominaga, M., Shimizu, S., Sato, Y., and Mori, Y. (2006) Nitric oxide activates TRP channels by cysteine S-nitrosylation, *Nat Chem Biol 2*, 596-607.

138. Cioffi, D. L., Lowe, K., Alvarez, D. F., Barry, C., and Stevens, T. (2009) TRPing on the lung endothelium: calcium channels that regulate barrier function, *Antioxid Redox Signal 11*, 765-776.

139. Moore, T. M., Chetham, P. M., Kelly, J. J., and Stevens, T. (1998) Signal transduction and regulation of lung endothelial cell permeability. Interaction between calcium and cAMP, *Am J Physiol 275*, L203-222.

140. Wu, S., Cioffi, E. A., Alvarez, D., Sayner, S. L., Chen, H., Cioffi, D. L., King, J., Creighton, J. R., Townsley, M., Goodman, S. R., and Stevens, T. (2005) Essential role of a Ca2+-selective, store-operated current (ISOC) in endothelial cell permeability: determinants of the vascular leak site, *Circ Res 96*, 856-863.

141. Brough, G. H., Wu, S., Cioffi, D., Moore, T. M., Li, M., Dean, N., and Stevens, T. (2001) Contribution of endogenously expressed Trp1 to a Ca2+-selective, store-operated Ca2+ entry pathway, *Faseb J 15*, 1727-1738.

142. Kelly, J. J., Moore, T. M., Babal, P., Diwan, A. H., Stevens, T., and Thompson, W. J. (1998) Pulmonary microvascular and macrovascular endothelial cells: differential regulation of Ca2+ and permeability, *Am J Physiol 274*, L810-819.

143. Hellwig, N., Albrecht, N., Harteneck, C., Schultz, G., and Schaefer, M. (2005) Homo- and heteromeric assembly of TRPV channel subunits, *J Cell Sci 118*, 917-928.

144. Hofer, A. M., Fasolato, C., and Pozzan, T. (1998) Capacitative Ca2+ entry is closely linked to the filling state of internal Ca2+ stores: a study using simultaneous measurements of ICRAC and intraluminal [Ca2+], *J Cell Biol 140*, 325-334.

145. Lowe, K., Alvarez, D., King, J., and Stevens, T. (2007) Phenotypic heterogeneity in lung capillary and extra-alveolar endothelial cells. Increased extra-alveolar endothelial permeability is sufficient to decrease compliance, *J Surg Res 143*, 70-77.

146. Alvarez, D. F., King, J. A., Weber, D., Addison, E., Liedtke, W., and Townsley, M. I. (2006) Transient receptor potential vanilloid 4-mediated disruption of the alveolar septal barrier: a novel mechanism of acute lung injury, *Circ Res 99*, 988-995.

147. Vriens, J., Owsianik, G., Fisslthaler, B., Suzuki, M., Janssens, A., Voets, T., Morisseau, C., Hammock, B. D., Fleming, I., Busse, R., and Nilius, B. (2005) Modulation of the Ca2 permeable cation channel TRPV4 by cytochrome P450 epoxygenases in vascular endothelium, *Circ Res 97*, 908-915.

148. Willette, R. N., Bao, W., Nerurkar, S., Yue, T. L., Doe, C. P., Stankus, G., Turner, G. H., Ju, H., Thomas, H., Fishman, C. E., Sulpizio, A., Behm, D. J., Hoffman, S., Lin, Z., Lozinskaya, I., Casillas, L. N., Lin, M., Trout, R. E., Votta, B. J., Thorneloe, K., Lashinger, E. S., Figueroa, D. J., Marquis, R., and Xu, X. (2008) Systemic activation of the transient receptor potential vanilloid subtype 4 channel causes endothelial failure and circulatory collapse: Part 2, *J Pharmacol Exp Ther 326*, 443-452.

149. Hamanaka, K., Jian, M. Y., Weber, D. S., Alvarez, D. F., Townsley, M. I., Al-Mehdi, A. B., King, J. A., Liedtke, W., and Parker, J. C. (2007) TRPV4 initiates the acute calcium-dependent permeability increase during ventilator-induced lung injury in isolated mouse lungs, *Am J Physiol Lung Cell Mol Physiol 293*, L923-932.

150. Kuebler, W. M., Ying, X., and Bhattacharya, J. (2002) Pressure-induced endothelial Ca(2+) oscillations in lung capillaries, *Am J Physiol Lung Cell Mol Physiol 282*, L917-923.

151. Ichimura, H., Parthasarathi, K., Quadri, S., Issekutz, A. C., and Bhattacharya, J. (2003) Mechano-oxidative coupling by mitochondria induces proinflammatory responses in lung venular capillaries, *J Clin Invest 111*, 691-699.

152. Ichimura, H., Parthasarathi, K., Issekutz, A. C., and Bhattacharya, J. (2005) Pressure-induced leukocyte margination in lung postcapillary venules, *Am J Physiol Lung Cell Mol Physiol 289*, L407-412.

153. Kuebler, W. M., Uhlig, U., Goldmann, T., Schael, G., Kerem, A., Exner, K., Martin, C., Vollmer, E., and Uhlig, S. (2003) Stretch activates nitric oxide production in pulmonary vascular endothelial cells in situ, *Am J Respir Crit Care Med 168*, 1391-1398.

154. Jian, M. Y., King, J. A., Al-Mehdi, A. B., Liedtke, W., and Townsley, M. I. (2008) High vascular pressure-induced lung injury requires P450 epoxygenase-dependent activation of TRPV4, *Am J Respir Cell Mol Biol 38*, 386-392.

155. Yin, J., Hoffmann, J., Kaestle, S. M., Neye, N., Wang, L., Baeurle, J., Liedtke, W., Wu, S., Kuppe, H., Pries, A. R., and Kuebler, W. M. (2008) Negative-feedback loop attenuates hydrostatic lung edema via a cGMP-dependent regulation of transient receptor potential vanilloid 4, *Circ Res 102*, 966-974.

156. Sachs, F. Stretch-activated ion channels: what are they?, *Physiology (Bethesda) 25*, 50-56.

157. Inoue, R., Jian, Z., and Kawarabayashi, Y. (2009) Mechanosensitive TRP channels in cardiovascular pathophysiology, *Pharmacol Ther 123*, 371-385.

158. Yin, J., and Kuebler, W. M. (2010) Mechanotransduction by TRP channels: general concepts and specific role in the vasculature, *Cell Biochem Biophys* 56, 1-18.

159. King, J., Hamil, T., Creighton, J., Wu, S., Bhat, P., McDonald, F., and Stevens, T. (2004) Structural and functional characteristics of lung macro- and microvascular endothelial cell phenotypes, *Microvasc Res 67*, 139-151.

160. Wu, S., Chen, H., Alexeyev, M. F., King, J. A., Moore, T. M., Stevens, T., and Balczon, R. D. (2007) Microtubule motors regulate ISOC activation necessary to increase endothelial cell permeability, *J Biol Chem 282*, 34801-34808.

161. Amdur, M. O. (1989) Helath effects of air pollutants: sulfuric acid, the old and the new., *Environ Health Perspect 81*, 109-113.

162. Churg, A., and Brauer, M. (2000) Ambient Atmospheric Particles in the Airways of Human Lungs, *Ultrastructural Pathology 24*, 353 - 361.

163. Dockery, D. W. (1993) Epidemiologic study design for investigating respiratory health effects of complex air pollution mixtures, *Environ Health Perspect 101 Suppl 4*, 187-191.

164. Dockery, D. W. (2001) Epidemiologic evidence of cardiovascular effects of particulate air pollution, *Environ Health Perspect 109 Suppl 4*, 483-486.

165. Dockery, D. W., Pope, C. A., Xu, X., Spengler, J. D., Ware, J. H., Fay, M. E., Ferris, B. G., and Speizer, F. E. (1993) An Association between Air Pollution and Mortality in Six U.S. Cities, *N Engl J Med 329*, 1753-1759.

166. Kagawa, J. (2002) Health effects of diesel exhaust emissions--a mixture of air pollutants of worldwide concern, *Toxicology 181-182*, 349-353.

167. Lighty, J., Veranth, J., and Sarofim, A. (2000) Combustion aerosols: Factors governing their size and composition and implications to human health, *Journal of the Air & Waste Management Association 50*, 174-227.

168. Mortimer, K. M., Neas, L. M., Dockery, D. W., Redline, S., and Tager, I. B. (2002) The effect of air pollution on inner-city children with asthma, *Eur Respir J 19*, 699-705.

169. Pope III, C. A. (1989) Respiratory disease associated with community air pollution and a steel mill, Utah Valley, *American Journal of Public Health 89*, 623-628.

170. Pope III, C. A. (1998) Epidemiology investigations of health effects of particulate air pollution: strengths and limitations., *Appl Occup Environ Hyg 13*, 356-363.

171. Veronesi, B., and Oortgiesen, M. (2001) Neurogenic Inflammation and Particulate Matter (PM) Air Pollutants, *NeuroToxicology 22*, 795-810.

172. Xu, X. P., Dockery, D. W., and Wang, L. H. (1991) Effects of air pollution on adult pulmonary function., *Arch Environ Health 46*, 198-206.

173. Dominici, F., McDermott, A, Daniels, M, Zeger, SL, Samet, JM. (2005) Revised analyses of the National Morbidity, Mortality, and Air Pollution Study: mortality among residents of 90 cities, *J Toxicol Environ Health A 68*, 1071-1092.

174. Peters, J. M., Avol, E., Gauderman, W. J., Linn, W. S., Navidi, W., London, S. J., Margolis, H., Rappaport, E., Vora, H., Gong, H., Jr., and Thomas, D. C. (1999) A study of twelve Southern California communities with differing levels and types of air pollution. II. Effects on pulmonary function, *Am J Respir Crit Care Med 159*, 768-775.

175. Glinianaia, S. V., Rankin, J., Bell, R., Pless-Mulloli, T., and Howel, D. (2004) Particulate air pollution and fetal health: a systematic review of the epidemiologic evidence, *Epidemiology 15*, 36-45.

176. Bobak, M., and Leon, D. A. (1992) Air pollution and infant mortality in the Czech Republic, 1986-88, *Lancet 340*, 1010-1014.

177. Pope III, C. A. (2000) Epidemiology of fine particulate air pollution and human health: biologic mechanisms and who's at risk?, *EHP 108*, 713-723.

178. Agopyan, N., Bhatti, T., Yu, S., and Simon, S. A. (2003) Vanilloid receptor activation by 2- and 10-[mu]m particles induces responses leading to apoptosis in human airway epithelial cells, *Toxicology and Applied Pharmacology 192*, 21-35.

179. Agopyan, N., Li, L., Yu, S., and Simon, S. A. (2003) Negatively charged 2- and 10-[mu]m particles activate vanilloid receptors, increase cAMP, and induce cytokine release, *Toxicology and Applied Pharmacology 186*, 63-76.

180. Driscoll, K. E. (2000) TNF[alpha] and MIP-2: role in particle-induced inflammation and regulation by oxidative stress, *Toxicology Letters 112-113*, 177-183.

181. Veronesi, B., Wei, G., Zeng, J.-Q., and Oortgiesen, M. (2003) Electrostatic charge activates inflammatory vanilloid (VR1) receptors, *NeuroToxicology 24*, 463-473.

182. Veronesi, B., Oortgiesen, M., Carter, J. D., and Devlin, R. B. (1999) Particulate Matter Initiates Inflammatory Cytokine Release by Activation of Capsaicin and Acid Receptors in a Human Bronchial Epithelial Cell Line, *Toxicology and Applied Pharmacology 154*, 106-115.

183. Veronesi, B., Oortgiesen, M., Roy, J., Carter, J. D., Simon, S. A., and Gavett, S. H. (2000) Vanilloid (Capsaicin) Receptors Influence Inflammatory Sensitivity in Response to Particulate Matter, *Toxicology and Applied Pharmacology 169*, 66-76.

184. Kilburn, K. H., and McKenzie, W. N. (1978) Leukocyte recruitment to airways by aldehyde-carbon combinations that mimic cigarette smoke, *Lab Invest 38*, 134-142.

185. Leikauf, G. D., Leming, L. M., O'Donnell, J. R., and Doupnik, C. A. (1989) Bronchial responsiveness and inflammation in guinea pigs exposed to acrolein, *J Appl Physiol 66*, 171-178.

186. Mio, T., Romberger, D. J., Thompson, A. B., Robbins, R. A., Heires, A., and Rennard, S. I. (1997) Cigarette smoke induces interleukin-8 release from human bronchial epithelial cells, *Am J Respir Crit Care Med 155*, 1770-1776.

187. Simon, S. A., and Liedtke, W. (2008) How irritating: the role of TRPA1 in sensing cigarette smoke and aerogenic oxidants in the airways, *J Clin Invest 118*, 2383-2386.

188. Lay, J. C., Zeman, K. L., Ghio, A. J., and Bennett, W. D. (2001) Effects of inhaled iron oxide particles on alveolar epithelial permeability in normal subjects, *Inhal Toxicol 13*, 1065-1078.

189. Rhoden, C. R., Lawrence, J., Godleski, J. J., and Gonzalez-Flecha, B. (2004) N-acetylcysteine prevents lung inflammation after short-term inhalation exposure to concentrated ambient particles, *Toxicol Sci 79*, 296-303.

190. Becker, S., Fenton, M. J., and Soukup, J. M. (2002) Involvement of microbial components and toll-like receptors 2 and 4 in cytokine responses to air pollution particles, *Am J Respir Cell Mol Biol 27*, 611-618.

191. Schulz, C., Farkas, L., Wolf, K., Kratzel, K., Eissner, G., and Pfeifer, M. (2002) Differences in LPS-induced activation of bronchial epithelial cells (BEAS-2B) and type II-like pneumocytes (A-549), *Scand J Immunol 56*, 294-302.

192. Hamilton, R. F., Thakur, S. A., Mayfair, J. K., and Holian, A. (2006) MARCO Mediates Silica Uptake and Toxicity in Alveolar Macrophages from C57BL/6 Mice, *Journal of Biological Chemistry 281*, 34218-34226.

193. Palecanda, A., and Kobzik, L. (2001) Receptors for unopsonized particles: the role of aveolar macorphage scavenger receptors., *Curr Mol Med 1*, 589-595.

194. Palecanda, A., Paulauskis, J., Al-Mutairi, E., Imrich, A., Qin, G., Suzuki, H., Kodama, T., Tryggvason, K., Koziel, H., and Kobzik, L. (1999) Role of the Scavenger Receptor MARCO in Alveolar Macrophage Binding of Unopsonized Environmental Particles, *J. Exp. Med. 189*, 1497-1506.

195. Thakur, S. A., Beamer, C. A., Migliaccio, C. T., and Holian, A. (2009) Critical Role of MARCO in Crystalline Silica-Induced Pulmonary Inflammation, *Toxicol. Sci. 108*, 462-471.

196. Thakur, S. A., Hamilton, R., Jr., Pikkarainen, T., and Holian, A. (2009) Differential Binding of Inorganic Particles to MARCO, *Toxicol. Sci. 107*, 238-246.

197. Thakur, S. A., Hamilton, R. F., and Holian, A. (2008) Role of Scavenger Receptor A Family in Lung Inflammation from Exposure to Environmental Particles, *Journal of Immunotoxicology 5*, 151-157.

198. Oortgiesen, M., Veronesi, B., Eichenbaum, G., Kiser, P. F., and Simon, S. A. (2000) Residual oil fly ash and charged polymers activate epithelial cells and nociceptive sensory neurons, *Am J Physiol Lung Cell Mol Physiol 278*, L683-695.

199. Veronesi, B., Haar, C. d., Lee, L., and Oortgiesen, M. (2002) The Surface Charge of Visible Particulate Matter Predicts Biological Activation in Human Bronchial Epithelial Cells, *Toxicology and Applied Pharmacology 178*, 144-154.

200. Veronesi, B., Haar, C. d., Roy, J., and Oortgiesen, M. (2002) Particulate matter inflammation and receptor sensitivity are target cell specific, *Inhalation Toxicology 14*, 159-183.

201. Ghelfi, E., Rhoden, C. R., Wellenius, G. A., Lawrence, J., and Gonzalez-Flecha, B. (2008) Cardiac oxidative stress and electrophysiological changes in rats exposed to concentrated ambient particles are mediated by TRP-dependent pulmonary reflexes, *Toxicol Sci 102*, 328-336.

202. Wong, S. S., Sun, N. N., Keith, I., Kweon, C. B., Foster, D. E., Schauer, J. J., and Witten, M. L. (2003) Tachykinin substance P signaling involved in diesel exhaust-induced bronchopulmonary neurogenic inflammation in rats, *Arch Toxicol 77*, 638-650.

203. Bhatia, M., Slavin, J., Cao, Y., Basbaum, A. I., and Neoptolemos, J. P. (2003) Preprotachykinin-A gene deletion protects mice against acute pancreatitis and associated lung injury, *Am J Physiol Gastrointest Liver Physiol 284*, G830-836.

204. Andrè, E., Gatti, R., Trevisani, M., Preti, D., Baraldi, P. G., Patacchini, R., and Geppetti, P. (2009) Transient receptor potential ankyrin receptor 1 is a novel target for pro-tussive agents, *British Journal of Pharmacology 158*, 1621-1628.

205. Birrell, M. A., Belvisi, M. G., Grace, M., Sadofsky, L., Faruqi, S., Hele, D. J., Maher, S. A., Freund-Michel, V., and Morice, A. H. (2009) TRPA1 Agonists Evoke Coughing in Guinea Pig and Human Volunteers, *Am. J. Respir. Crit. Care Med. 180*, 1042-1047.

CHAPTER 2

TRANSIENT RECEPTOR POTENTIAL VANILLOID 1 AGONISTS CAUSE ENDOPLASMIC RETICULUM STRESS AND CELL DEATH IN HUMAN LUNG CELLS

Karen C. Thomas, Ashwini S. Sabnis, Mark E. Johansen, Diane L. Lanza, Philip J. Moos, Garold S. Yost and Christopher A. Reilly,

J Pharmacol Exp Ther June 2007 321:830-838

0022-3565/07/3213-830–838$20.00
THE JOURNAL OF PHARMACOLOGY AND EXPERIMENTAL THERAPEUTICS
JPET 321:830–838, 2007

Vol. 321, No. 3
119412/3205306
Printed in U.S.A.

Transient Receptor Potential Vanilloid 1 Agonists Cause Endoplasmic Reticulum Stress and Cell Death in Human Lung Cells[S]

Karen C. Thomas, Ashwini S. Sabnis, Mark E. Johansen,[1] Diane L. Lanza, Philip J. Moos, Garold S. Yost, and Christopher A. Reilly

Department of Pharmacology and Toxicology, University of Utah, Salt Lake City, Utah

Received January 3, 2007; accepted February 28, 2007

ABSTRACT

Transient receptor potential vanilloid 1 (TRPV1) is a calcium-selective ion channel expressed in human lung cells. We show that activation of the intracellular subpopulation of TRPV1 causes endoplasmic reticulum (ER) stress and cell death in human bronchial epithelial and alveolar cells. TRPV1 agonist (nonivamide) treatment caused calcium release from the ER and altered the transcription of growth arrest- and DNA damage-inducible transcript 3 (GADD153), GADD45α, GRP78/BiP, ATF3, CCND1, and CCNG2) in a manner comparable with prototypical ER stress-inducing agents. The TRPV1 antagonist *N*-(4-*tert*-butylbenzyl)-*N*′-(1-[3-fluoro-4-(methylsulfonylamino)-phenyl]ethyl)thiourea (LJO-328) inhibited mRNA responses and cytotoxicity. EGTA and ruthenium red inhibited cell surface TRPV1 activity, but they did not prevent ER stress gene responses or cytotoxicity. Cytotoxicity paralleled eukaryotic translation initiation factor 2, subunit 1 (EIF2α) phosphorylation and the induction of GADD153 mRNA and protein. Transient overexpression of GADD153 caused cell death independent of agonist treatment, and cells selected for stable overexpression of a GADD153 dominant-negative mutant exhibited reduced sensitivity. Salubrinal, an inhibitor of ER stress-induced cytotoxicity via the EIF2αK3/EIF2α pathway, or stable overexpression of the EIF2α-S52A dominant-negative mutant also inhibited cell death. Treatment of the TRPV1-null human embryonic kidney 293 cell line with TRPV1 agonists did not initiate ER stress responses. Likewise, *n*-benzylnonanamide, an inactive analog of nonivamide, failed to cause ER calcium release, an increase in GADD153 expression, and cytotoxicity. We conclude that activation of ER-bound TRPV1 and stimulation of GADD153 expression via the EIF2αK3/EIF2α pathway represents a common mechanism for cytotoxicity by cell-permeable TRPV1 agonists. These findings are significant within the context of lung inflammatory diseases where elevated concentrations of endogenous TRPV1 agonists are probably produced in sufficient quantities to cause TRPV1 activation and lung cell death.

Lung cell damage causes acute respiratory distress and contributes to the pathogenesis of chronic lung diseases (Knight and Holgate, 2003). Evidence suggests that the transient receptor potential vanilloid type-1 receptor (TRPV1, capsaicin receptor, VR1; Hs. 268606) may be a mediator of lung pathologies caused by xenobiotic toxicants and endogenous agonists as well as a therapeutic target for treating and/or preventing lung disorders (Jia et al., 2005; Szallasi et al., 2006).

TRPV1 is widely expressed in the respiratory tract, including nasal mucosal cells (Seki et al., 2006), C-fiber neurons and airway smooth muscle cells (Mitchell et al., 2005; Watanabe et al., 2005), and alveolar and bronchial epithelial cells (Veronesi et al., 1999; Reilly et al., 2003; Agopyan et al., 2004). TRPV1 is selectively activated by capsaicin, the pri-

This study was supported by National Heart, Lung, and Blood Institute Grant HL069813.
[1] Current affiliation: Jacobs Dugway Team, Life Sciences Testing Facility, Dugway, Utah.Article, publication date, and citation information can be found at http://jpet.aspetjournals.org.
doi:10.1124/jpet.107.119412.
[S] The online version of this article (available at http://jpet.aspetjournals.org) contains supplemental material.

ABBREVIATIONS: TRPV1, transient receptor potential vanilloid 1 (a.k.a. VR1 or the capsaicin receptor); ER, endoplasmic reticulum; LJO-328, *N*-(4-*tert*-butylbenzyl)-*N*′-(1-[3-fluoro-4-(methylsulfonylamino)phenyl]ethyl)thiourea; 5-iodo-RTX, 5-iodo-resiniferatoxin; ATF, activating transcription factor; EIF2α, eukaryotic translation initiation factor 2, subunit 1 (α, 35kDa); GADD153, growth arrest- and DNA damage-inducible transcript 3 (a.k.a. DDIT3 and CHOP); GADD45α, growth arrest and DNA-damage-inducible, α (a.k.a. DDIT1); BiP/GRP78, glucose-regulated protein, 70 kDa (a.k.a. HSPA5); CCND1, cyclin D1; CCNG2, cyclin G_2; EIF2α-P, phosphorylated eukaryotic translation initiation factor 2, subunit 1; DTT, dithiothreitol; PCR, polymerase chain reaction; NHBE, normal human bronchial epithelial; HEK, human embryonic kidney; RT, reverse transcription; ANOVA, analysis of variance; GFP, green fluorescent protein; EtBr, ethidium bromide; EGFP, enhanced green fluorescent protein; SC0030, *N*-(4-*tert*-butylbentyl)-*N*′-[3-fluoro-4-(methylsulfonylamino)benzyl]thiourea.

mary pain-producing chemical in hot peppers, and a variety of exogenous and endogenous respiratory toxicants, including anandamide (Van Der Stelt and Di Marzo, 2004), products of arachidonic acid metabolism by lipoxygenases (Hwang et al., 2000), H_2S (Trevisani et al., 2005), ethanol (Trevisani et al., 2004), acids (Tominaga et al., 1998; Ricciardolo et al., 2004), and particulate pollutants (Veronesi et al., 1999; Agopyan et al., 2004). Capsaicin and other TRPV1 agonists are routinely used to study the TRPV1 pharmacology and have proven instrumental in defining the physiological roles of TRPV1 in the lung and other organs. Here, we use capsaicin to elucidate toxicological phenomena associated with TRPV1 activation in lung cells.

Capsaicin is used clinically to induce cough (Morice et al., 2001) and to treat rhinitis (van Rijswijk and Gerth van Wijk, 2006). However, numerous case reports have described adverse respiratory effects and death in humans following exposures to concentrated capsaicinoid aerosols (Heck, 1995; Steffee et al., 1995; Billmire et al., 1996). In animal models, high doses of capsaicin cause acute respiratory and cardiovascular failure, independently of the route of administration (Glinsukon et al., 1980). Inhalation of capsaicinoids by rats causes lung inflammation and widespread damage to tracheal, bronchial, and alveolar cells (Reilly et al., 2003). In vitro studies with human bronchial epithelial cells have demonstrated two principal outcomes associated with TRPV1 activation: proinflammatory cytokine (interleukin-6 and interleukin-8) production and oncotic cell death (Reilly et al., 2003, 2005). Cytokine synthesis and cell death were inhibited by TRPV1 antagonists that prevented calcium release from the endoplasmic reticulum (ER) and included LJO-328, SC0030, and 5-iodo-RTX. Conversely, inhibition of the cell surface population of TRPV1 using EGTA, ruthenium red, and calcium-free media only prevented cytokine responses.

In mammalian cells, depletion of ER calcium initiates a homeostatic stress response program termed ER stress. ER stress is generally initiated by a reduction in protein processing efficiency in the ER, and its roles in human diseases and xenobiotic toxicities have been reviewed (Cribb et al., 2005; Schroder and Kaufman, 2005; Zhang and Kaufman, 2006). ER stress is predominantly regulated by three sensors: activating transcription factor 6 (ATF6; *Hs. 492740*), eukaryotic initiation factor 2α kinase-3 (EIF2αK3 or PERK; *Hs. 591589*), and ER to nucleus signaling 1 and 2 (a.k.a. IRE1α and β; *Hs. 133982* and *Hs. 592041*) (Schroder and Kaufman, 2005). Activation of one or more of these proximal sensors is dependent upon the type of cellular stress. For example, the prototypical ER stress-inducing agent thapsigargin preferentially activates the "translational branch" involving EIF2αK3. Activated EIF2αK3 catalyzes the phosphorylation of cytosolic EIF2α (*Hs. 151777*) (Lu et al., 2004; Boyce et al., 2005). Heterodimerization of EIF2α-P with EIF2β promotes ATF4 translation (*Hs. 496487*) and inhibits the translation of "nonessential" genes (Wek et al., 2006). ATF4 translocates to the nucleus where it modulates the expression of a subset of stress-response genes that include ATF3, GADD153, CCND1, and BiP/GRP78 (see Table 1 for UniGene identifications numbers). Phosphorylation of EIF2α is considered protective (Lu et al., 2004; Boyce et al., 2005), but increased expression of GADD153, as a consequence of EIF2α phosphorylation, causes cell cycle arrest at G_1/S and cell death (Oyadomari and Mori, 2004).

In this study, we tested the hypothesis that activation of the intracellular ER subpopulation of TRPV1 by prototypical and endogenous TRPV1 agonists would disrupt ER calcium homeostasis and activate EIF2αK3-dependent ER stress responses to cause cytotoxicity. The data obtained from this work imply that a common mechanism of cytotoxicity exists for cell-permeable TRPV1 agonists and that conditions that promote TRPV1 activation in vivo (e.g., inflammation, inhalation of polluted air) may promote lung pathologies through TRPV1- and EIF2αK3-dependent procytotoxic ER stress pathways.

Materials and Methods

Chemicals. Structures of the TRPV1 agonists and antagonists used in this study are shown in Fig. 1. Nonivamide (*n*-vanillylnonanamide), sulfinpyrazone, dithiothreitol (DTT), H_2O_2, ruthenium red, EGTA, benzylamine-HCl, and nonanoyl chloride were purchased from Sigma-Aldrich (St. Louis, MO). LJO-328 was generously provided by Dr. Jeewoo Lee (Seoul National University, Seoul, Korea). Thapsigargin and 5-iodo-resiniferatoxin were purchased from Axxora Life Sciences, Inc. (San Diego, CA). Salubrinal (EIF2α-inhibitor) was purchased from Calbiochem (San Diego, CA). PCR primers were purchased from Integrated DNA Technologies (Coralville, IA). *n*-Benzylnonanamide was synthesized by reacting benzylamine-HCl and nonanoyl chloride in 0.1 M NaOH and collecting the precipitate. Product structure was verified by liquid chromatography-tandem mass spectrometry (*m/z* 248) and ^{1}H and ^{13}C NMR. Purity was estimated to be ~98% by high-performance liquid chromatogra-

TABLE 1
Primer sequences used for RT-PCR analysis of selected ER stress-responsive genes

Gene Name, UniGene ID	PCR Product Size (Nucleotides)	Primer Sequence
GADD153, *Hs. 505777*	395	(+) 5′-GACCTGCAAGAGGTCCTGTC-3′ (−) 5′-TCGCCTCTACTTCCCTGGTC-3′
GADD45α, *Hs. 80409*	258	(+) 5′-TCTCGGCTGGAGAGCAGAAG-3′ (−) 5′-CGCGCAGGATGTTGATGTCG-3′
BiP/GRP78, *Hs. 605502*	296	(+) 5′-CGTGGAATGACCCGTCTGTG-3′ (−) 5′-CTGCCGTAGGCTCGTTGATG-3′
CCND1, *Hs. 523852*	480	(+) 5′-AGTGCGAGGAGGAGGTCTTC-3′ (−) 5′-AGCGTGTGAGGCGGTAGTAG-3′
CCNG2, *Hs. 13291*	744	(+) 5′-AGGGCTGAGTTTGATTGAGG-3′ (−) 5′-TAGCTGTTGTGGAGGTTCTG-3′
ATF3, *Hs. 460*	302	(+) 5′-CTCGGAAGTGAGTGCTTCTG-3′ (−) 5′-CCGTCTTCTCCTTCTTCTTG-3′
β-Actin, *Hs. 520640*	183	(+) 5′-GACAACGGCTCCGGCATGTGGCA-3′ (−) 5′-TGAGGATGCCTCTCTTGCTCTG-3′

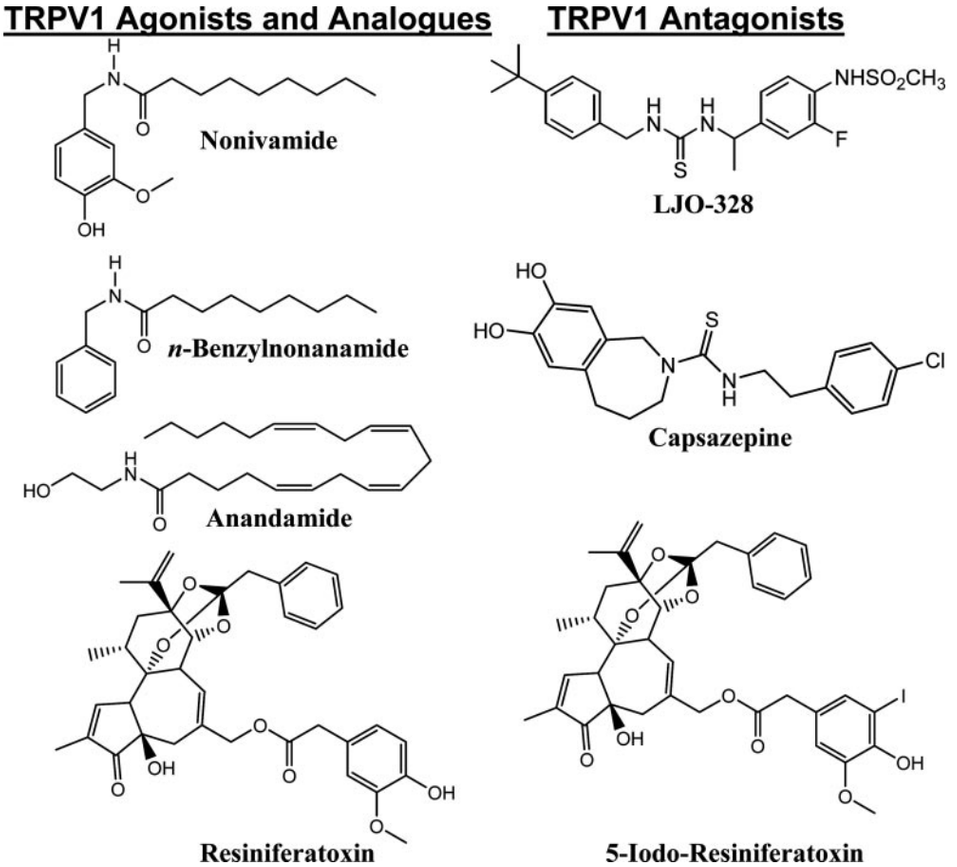

Fig. 1. Chemical structures for the TRPV1 agonists and antagonists used in this study.

phy/UV analysis (230 nm). See supplemental data for chemical analysis data. All other chemicals and reagents were purchased from established suppliers.

Cell Culture. BEAS-2B human bronchial epithelial cells (CRL-9609) were purchased from American Type Culture Collection (Manassas, VA). TRPV1-overexpressing cells were generated as described previously (Reilly et al., 2003). BEAS-2B and TRPV1-overexpressing cells were cultured in LHC-9 media (BioSource International, Camarillo, CA). Normal human bronchial epithelial (NHBE) cells, a primary cell line, were purchased from Cambrex Bio Science Walkersville, Inc. (Walkersville, MD) and cultured in BEGM media. Human embryonic kidney (HEK)-293 human embryonic kidney (CRL-1573) and A549 human lung carcinoma (CCL-185) cells were purchased from American Type Culture Collection and were cultured in Dulbecco's modified Eagle's medium:F-12 containing 10% fetal bovine serum (Hyclone Laboratories, Logan, UT). Culture flasks for BEAS-2B and TRPV1-overexpressing BEAS-2B cells were coated with LHC basal media fortified with 30 μg/ml collagen, 10 μg/ml fibronectin, and 10 μg/ml bovine serum albumin. Cells were maintained between 30 and 90% maximal density and were subcultured every 2 to 4 days.

Fluorometric Calcium Flux Assays. TRPV1-overexpressing cells were used to evaluate calcium flux. Flux in BEAS-2B, A549, and NHBE cells was not detectable. Functional evidence provided here and in previous studies (Reilly et al., 2003, 2005; Johansen et al., 2006) demonstrates that the TRPV1-overexpressing cells model responses of BEAS-2B and other lung cells when treated with diverse TRPV1 agonists, with the exceptions that TRPV1-dependent calcium flux is quantifiable and dose responses for TRPV1 agonists are shifted to lower concentrations. To assay calcium flux, TRPV1-overexpressing cells were subcultured into 96-well culture plates and grown to ~90% maximal density. Cells were loaded with the fluorogenic calcium indicator Fluo-4-acetoxymethyl ester (2.5 μM) (Invitrogen, Carlsbad, CA) for 90 min at room temperature (~22°C) in LHC-9 media containing 200 μM sulfinpyrazone. Cells were washed and incubated for an additional 20 min at room temperature to permit methyl ester hydrolysis and activation of Fluo-4. Changes in cellular fluorescence in response to agonist and antagonist treatments were assessed microscopically on cell populations 1 min after treatments using methods described previously (Reilly et al., 2005; Johansen et al., 2006). ER calcium flux was evaluated by pretreating cells with 2.5 μM thapsigargin for 5 min followed by addition of 2.5 μM nonivamide. Calcium flux due to cell surface TRPV1 activity was assessed by treating cells with nonivamide in calcium-free media containing 50 μM EGTA and 250 μM ruthenium red. Differences in fluorescence responses observed between the treatments and controls were used to assess the relative contribution of ER-bound and cell surface TRPV1 in total calcium flux initiated by agonists. Data are expressed as -fold change in fluorescence intensity.

Cytotoxicity Assays. Cells were subcultured into Multiwell plates and allowed to reach ~90% confluence. The cells were treated for 24 h with various agonists and antagonists prepared in the appropriate culture media without fetal bovine serum. Cell viability was assessed using the Dojindo cell counting kit-8 (Dojindo Laboratories, Gaithersburg, MD), according to the supplier's recommendations. Loss of cell monolayer integrity due to treatment with toxic TRPV1 agonists was confirmed microscopically. Toxicity data are expressed as the percentage of remaining viable cells relative to untreated controls, calculated using the absorbance ratio of the formazan dye product generated from the Dojindo reagent.

RT-PCR Analysis. Cells were subcultured into 25-cm^2 cell culture flasks, grown to a density of ~90%, and treated with TRPV1 agonists and antagonists. Total RNA was extracted from cells using the RNeasy RNA isolation kit (QIAGEN, Valencia, CA), and 2.5 μg of total RNA was transcribed into cDNA using PolyT and Superscript III (Invitrogen). cDNA corresponding to GADD153, GADD45α,

ATF3, CCND1, CCNG2, BiP/GRP78, and β-actin was amplified by PCR from 1 μl of the cDNA synthesis reaction using the primers listed in Table 1 and GoTaq Green PCR Master Mix (Promega, Madison, WI). The PCR program consisted of an initial 2 min incubation at 94°C and 28 cycles of 94°C (30 s), 55°C (30 s), and 72°C (30 s). A final extension period of 10 min at 72°C followed. PCR products were resolved on 1% SB agarose gels, and images were captured using a Gel-Doc imaging system (Bio-Rad, Hercules, CA). Product quantification was achieved by determining the band intensities for each PCR product relative to β-actin, the internal PCR control, using the Gel Doc density analysis tools in the Quantity One software (Bio-Rad). Experiments were reproduced a minimum of three times on different passages of cells.

Cloning of ER Stress Gene cDNA. The full-length cDNA for human GADD153, ATF3, EIF2α, and ATF4 were amplified from BEAS-2B cells using Phusion GC-rich PCR Super Mix (New England Biolabs, Ipswich, MA). The following primers were used: GADD153 (+) 5′-CACCATGGCAGCTGAGTCATTGCCTTTC-3′ and (−) 5′-TGCTTGGTGCAGATTCACCATTC-3′, ATF3 (+) 5′-CACCATGATGCTTCAACACCCAG-3′, and (−) 5′-ATACTGAAGCTGCAGGCACTC-3′, EIF2α (+) 5′-CACCATGCCGGGTCTAAGTTGTAG-3′ and (−) 5′-ATCTTCAGCTTTGGCTTCCATTTC-3′, and ATF4 (+) 5′-CACCATGACCGAAATGAGCTTCCTG-3′ and (−) 5′-GGGGACCCTTTTCTTCCCCCTTG-3′. These primers incorporated a 5′-CACC sequence immediately before the ATG start site to permit directional cloning into the pcDNA3.1-V5/His6 mammalian expression vector (Invitrogen) and eliminated the stop codon to allow for epitope tagging with V5-His6. An expression plasmid for $p58^{IPK}$ (pcDNA1-$p58^{IPK}$) was generously provided by Dr. Michael G. Katze (University of Washington, Seattle, WA). The pMaxGFP expression vector was purchased from Amaxa Biosystems (Gaithersburg, MD). All clones were sequence verified by comparison to the appropriate GenBank sequences. Plasmids used in the transient transfection assays were simultaneously purified using the QIAGEN Plasmid DNA Midi-Prep kit and further purified using the GeneElute HP Plasmid Mini-Prep kit (Sigma-Aldrich).

Site-Directed Mutagenesis. The GADD153-L134A/L141A (Matsumoto et al., 1996) and EIF2α-S52A (Srivastava et al., 1998) dominant-negative mutants were constructed using the QuikChange XL site-directed mutagenesis kit (Stratagene, La Jolla, CA) and the following primers: GADD153-L134A/L141A (+) 5′-GGCACAGGCAGCTGAAGAGAATGAACGGGCCAAGCAGG-3′ and (−) 5′-CCTGCTTGGCCCGTTCATTCTCTTCAGCTGCCTGTGCC-3′ and EIF2αS52A (+) 5′-CTTCTTAGTGAATTAGCCAGAAGGCG-3′ and (−) 5′-GGATACGCCTTCTGGCTAATTCACTA-3′.

Transient Overexpression Assays and Stable Overexpressing Cell Lines. A459 cells respond to TRPV1 agonists similar to BEAS-2B, NHBE, and TRPV1-overexpressing cells, with the exception that they exhibit slightly reduced sensitivity to agonists due to lower levels of TRPV1 expression (Reilly et al., 2003). A549 cells were used as transfection hosts to evaluate the protoxic effects of ER stress-induced gene products in lung cells, because they exhibited reproducibility in transfection efficiency and limited toxicity due to transfection reagents. Transfection efficiency typically reached ~80% using A549 cells versus ~5 to 10% with BEAS-2B cells, or <1% using NHBE cells. This level of transfection was necessary to evaluate the effects of ER stress genes on cell populations. A549 cells were subcultured into 48-well cell culture plates and grown to a density of ~70 to 80%. Cells were washed with Opti-MEM media and transfected for ~18 h using Lipofectamine 2000 (Invitrogen) at a ratio of 3:1 lipid/plasmid DNA. After transfection, cells were washed with Opti-MEM and allowed to grow for an additional 24 h. Cell viability was assessed as described above. All experiments were performed in triplicate and were normalized to control cells transfected with equal quantities of the pMaxGFP plasmid.

Stably overexpressing cell lines were generated by culturing transfected A549 cells in media fortified with 600 μg/ml G-418 (Geneticin; Invitrogen) for ~3 weeks. Resistant foci were isolated and expanded in selective media. Individual clones were screened for overexpression of the target genes by assaying for V5-His6 expression by RT-PCR and subsequently used for cytotoxicity screening.

Western Blotting. BEAS-2B cells were grown to ~90% maximal density in 25-cm^2 flasks. Before treatment cells were cultured in fresh media for 2 h. Cells were treated for 0, 1, 2, 4, and 8 h, rinsed with phosphate-buffered saline, and immediately lysed on ice using 20 mM HEPES, pH 7.5, containing 150 mM NaCl, 1% Triton X-100, 1 mM EDTA, 10 mM sodium pyrophosphate, 100 mM sodium fluoride, 17.5 mM β-glycerophosphate, 1 mM phenylmethylsulfonyl fluoride, 4 mg/ml aprotinin, and 2 mg/ml pepstatin A. The lysates were clarified by centrifugation at ~20,000*g* for 15 min at 4°C, and the concentration of protein was determined using the BCA protein assay (Pierce Chemical, Rockford, IL). Fifty micrograms of soluble protein from each sample then was resolved on a 10% NuPAGE gel (Invitrogen) and subsequently transferred to polyvinylidene difluoride membrane. The blots were probed for EIF2α-P using a rabbit polyclonal IgG fraction specific to EIF2α-pS52 (BioSource, International) according to supplier protocols. GADD153 expression was determined using an anti-GADD153 antibody from Biolegend (San Diego, CA) and the protocol provided by the supplier.

Statistical Analysis. Statistical testing used the paired *t* tests and ANOVA with post hoc testing using Dunnett's test to determine significance. A 95% confidence interval was used as the limit for significance. Specific details on statistical analyses are presented in the figure legends.

Results

Treatment of TRPV1-overexpressing cells with 2.5 μM nonivamide produced marked increases in cytosolic calcium due to release of calcium from ER stores (Fig. 2A). EGTA and ruthenium red cotreatment had little to no effect on calcium flux, but cotreatment with LJO-328 or prior depletion of ER calcium stores with thapsigargin completely prevented calcium flux. *n*-Benzylnonanamide failed to elicit ER calcium release at 2.5 μM (Fig. 2A) or at concentrations up to 25 μM (data not shown). Treatment of TRPV1-overexpressing cells with 1 μM nonivamide caused an approximate 50% loss in cell viability after a 24-h period (Fig. 2B). Cell death corresponded to a loss of monolayer consistency (data not shown) and was inhibited by LJO-328 cotreatment, but not by EGTA and ruthenium red. *n*-Benzylnonanamide did not cause cell death, consistent with a lack of TRPV1 activation.

Analysis of collective genetic responses in TRPV1-overexpressing and BEAS-2B cells exposed to 1 and 100 μM (LC_{50} concentrations) nonivamide, respectively, for 4 h, in the presence or absence of LJO-328, by microarray yielded preliminary insight into cellular processes that constituted the cell death process (see Supplemental Data, explanation of microarray data and microarray data). Increased expression of GADD153, GADD45α, ATF3, CCNG2, and BiP/GRP78 mRNA and a decrease in CCND1 mRNA were observed, and these responses were validated by RT-PCR (Fig. 3A). Cotreatment of cells with the TRPV1 antagonist LJO-328 prevented changes in gene expression, whereas little to no inhibition was observed using EGTA and ruthenium red (Fig. 3A). Treatment of BEAS-2B cells with the prototypical ER stress-inducing agents thapsigargin and DTT produced similar changes in the expression of GADD153, GADD45α, ATF3, CCND1, CCNG3, and BiP/GRP78 (Fig. 3B) mRNA.

BEAS-2B cells treated with 100 and 200 μM nonivamide also exhibited a shift in the relative amount of EIF2α-P and an increase in the expression of GADD153 mRNA and pro-

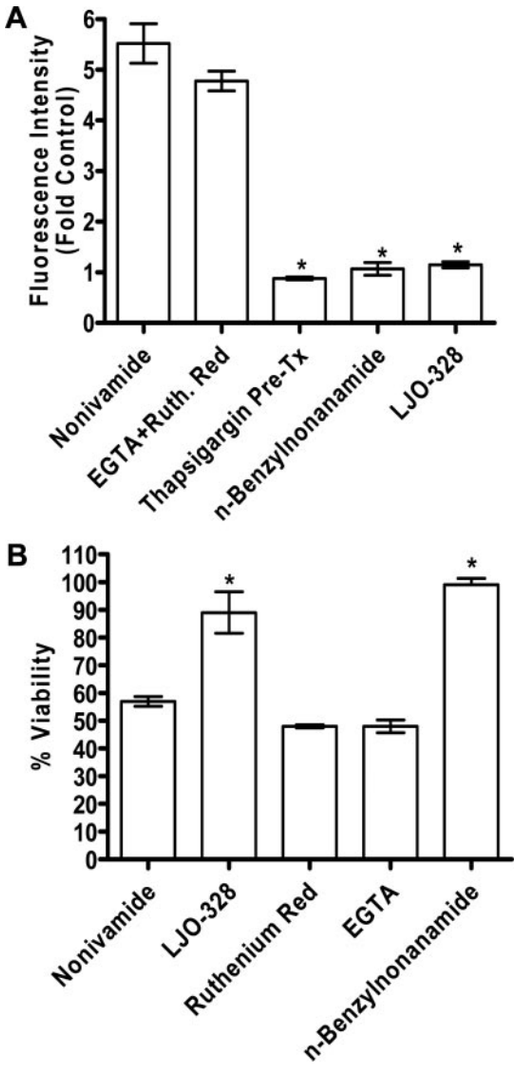

Fig. 2. Relationship between calcium flux (A) and cell death (B) in TRPV1-overexpressing cells. Cells were assayed for calcium flux and cell death, as described under *Materials and Methods*. A, treatments were 2.5 μM nonivamide, nonivamide + EGTA, and ruthenium red (50 + 250 μM), nonivamide following 5-min pretreatment with 2.5 μM thapsigargin, 2.5 μM *n*-benzylnonanamide, and nonivamide + 20 μM LJO-328. Identical treatments were used in B with the exception that ruthenium red and EGTA were used separately. *, $p < 0.025$, paired t test; $n = 3$.

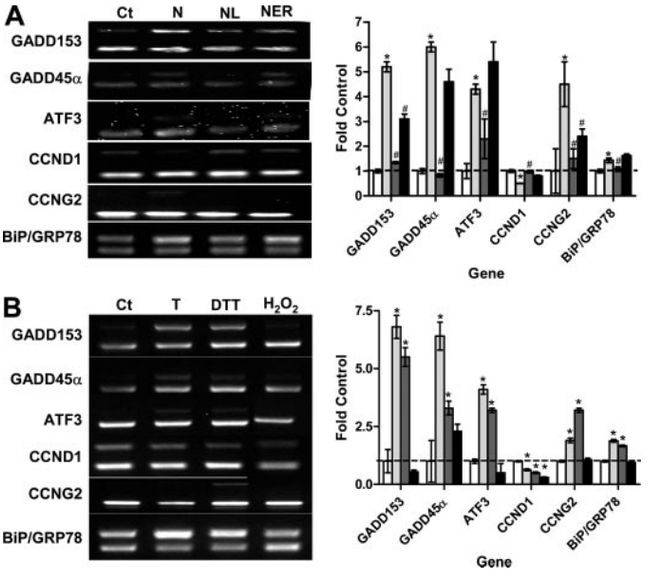

Fig. 3. Modulation of ER stress response gene expression in BEAS-2B cells treated with nonivamide (A) and prototypical ER stress-inducing agents (B). All treatments were performed for 4 h at 37°C in six-well plates using LHC-9 as the vehicle. A, BEAS-2B cells treated with fresh media (Ct), 100 μM nonivamide (N), nonivamide and 30 μM LJO-328 (NL), or nonivamide and EGTA (50 μM) and ruthenium red (250 μM) (NER). Total RNA was extracted for analysis of gene expression, as described under *Materials and Methods*. Images showing changes in the expression of GADD153, GADD45α, ATF3, CCND1, CCNG2, and BiP/GRP78 as well as quantitative results for changes in gene expression (bar graph) are shown. All data are normalized to β-actin, the smaller PCR product shown for each image panel. White bars represent untreated control cells, light gray bars represent cells treated with 100 μM nonivamide for 4 h at 37°C, medium gray bars represent cells treated with nonivamide and 20 μM LJO-328, and black bars represent cells treated with nonivamide and EGTA + ruthenium red (50 + 250 μM). B, BEAS-2B cells were treated with Ct, thapsigargin (2.5 μM), DTT (1 mM), or H_2O_2 (1 mM), processed, and assayed by RT-PCR, as described for A. White bars represent untreated cells, light gray bars represent cells treated with thapsigargin, medium gray bars represent cells treated with DTT, and black bars represent cells treated with H_2O_2. *, significant changes in expression relative to control cells; #, statistically significant changes relative to nonivamide treatment (ANOVA, 95% confidence interval; $n = 3$).

tein (Fig. 4, A–C). EIF2α phosphorylation and GADD153 expression was inhibited by LJO-328, but not by EGTA and ruthenium red (Fig. 4A). The kinetic and dose-dependent features of GADD153 induction and EIF2α-P accumulation paralleled cytotoxicity (Fig. 4, A–C). The highest levels of EIF2α phosphorylation and GADD153 protein were detected at ~8 h with 200 μM nonivamide. For GADD153, increases in mRNA in BEAS-2B cells was maximal at ~4 h and occurred at concentrations >150 μM. Similar responses were observed using the TRPV1-overexpressing cells, but maximal increases in protein and mRNA were observed with a dose of 1 to 2 μM (data not shown).

Transient overexpression of GADD153 in A549 cells produced an approximate 50% loss in cell viability relative to pMaxGFP-transfected control cells in the absence of cytotoxic TRPV1 agonists (Fig. 5A). Transient overexpression of ATF4, which stimulates GADD153 transcription, also produced ~20% cell death. GADD153-L134A/L141A, ATF3, or p58^{IPK} were not cytotoxic. Transient cotransfection of A549 cells with ATF3 and GFP (10:1) yielded a high proportion of viable GFP-expressing cells 48 h after the transfection procedure (Fig. 5B). No ethidium bromide (EtBr)-stained nuclei were observed in these cells, indicating cellular integrity. Conversely, very few cells transfected with GADD153 and GFP (10:1) survived, whereas those that remained attached to the culture dish exhibited intense nuclear staining with EtBr. These data were consistent with a loss of cell viability, cell membrane integrity, and oncotic cell death, as reported previously for BEAS-2B and A549 cells treated with capsaicin (Reilly et al., 2003).

Inhibition of cytotoxicity using dominant-negative forms of EIF2α (EIF2α-S52A) and GADD153 (GADD153-L134A/L141A) was also evaluated (Fig. 6). Figure 6A shows that both the EIF2α-S52A- and GADD153-L134A/L141A-overexpressing A549 cells were less susceptible to cytotoxicity by nonivamide. Likewise, the addition of salubrinal to treatment solutions containing 1 or 100 μM nonivamide inhibited

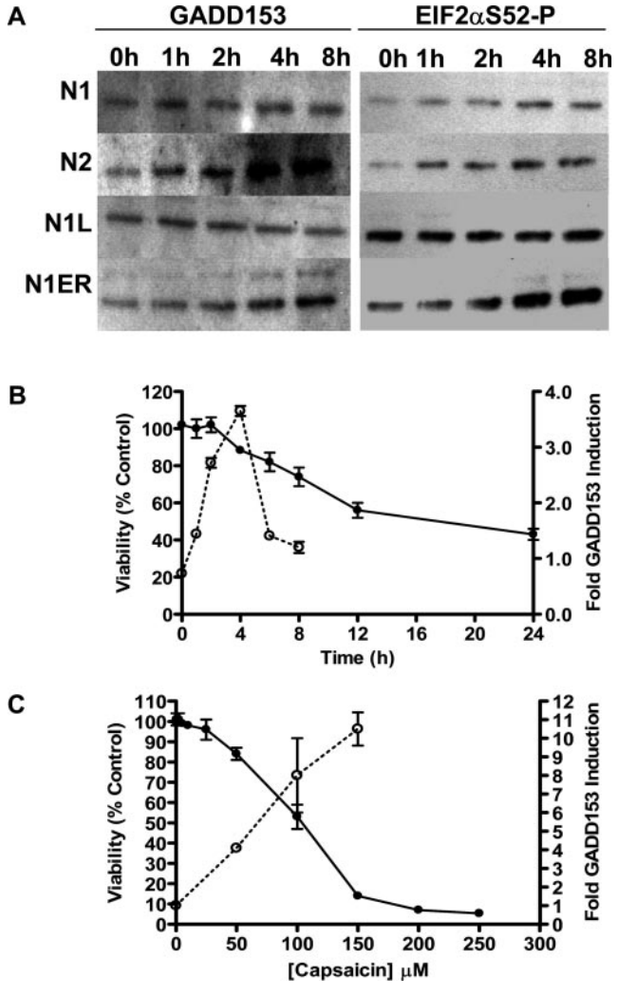

Fig. 4. Concentration- and time-dependent changes in GADD153 expression, EIF2α phosphorylation, and cell viability in BEAS-2B cells. A, Western blot analysis showing the time- and dose-dependent changes in GADD153 expression and EIF2α phosphorylation in BEAS-2B cells treated with 100 μM nonivamide (N1), 200 μM nonivamide (N2), 100 μM nonivamide plus 30 μM LJO-328 (N1L), or 100 μM nonivamide plus 50 μM EGTA and 250 μM ruthenium red (N1ER). B, dose-response relationship between cell death and GADD153 induction. Dose-response cytotoxicity curve for nonivamide in BEAS-2B cells (solid circles, solid line) and induction of GADD153 (open circles, dashed line; right axis). C, time-dependent loss of cell viability and increased expression of GADD153 mRNA. BEAS-2B cells (solid squares, cell viability; open squares, GADD153 expression) were treated with 100 μM nonivamide. All data are relative to control cells treated in an identical manner using media only (n = 3).

cell death in TRPV1-overexpressing and BEAS-2B cells with a maximal effect between 2.5 and 5 μM (Fig. 6B). Salubrinal inhibits EIF2αK3-induced cytotoxicity (Lu et al., 2004; Boyce et al., 2005)

Induction of the proapoptotic/oncotic ER stress-induced gene GADD153 was also compared in TRPV1-overexpressing, BEAS-2B, A549, and NHBE lung cells as well as HEK-293 cells (Table 2). All four lung cell types express TRPV1, but HEK-293 cells do not. Significant (6- to 8-fold) GADD153 mRNA induction was observed following 4-h treatment of BEAS-2B, TRPV1-overexpressing, A549, and NHBE cells with LC_{50} concentrations of nonivamide, resiniferatoxin, and anandamide, but not with n-benzylnonanamide. Interestingly, n-benzylnonanamide inhibited cell death caused by nonivamide in the TRPV1-overexpressing cells at concentration ratios >5:1 (data not shown). Induction of GADD153 transcription was attenuated by LJO-328 in all cells types exhibiting a response as well as by 5-iodo-RTX in the TRPV1-overexpressing line. GADD153 induction was not observed in HEK-293 cells treated with nonivamide or resiniferatoxin.

Discussion

Previous studies of TRPV1 and the effects of its agonists on cultured lung cells and in animal models of airway injury support the hypothesis that TRPV1 is a mediator of lung injury and inflammation (Reilly et al., 2003, 2005; Vargaftig and Singer, 2003; Li et al., 2005; Trevisani et al., 2005; Bhatia et al., 2006; Geppetti et al., 2006). However, precise molecular mechanisms of cell death have not been established.

Quantitation of calcium flux in TRPV1-overexpressing cells demonstrated that 85 to 90% of functional TRPV1 existed in the ER membrane (Fig. 2A). Selective inhibitors of TRPV1 and treatments that reduced the passage of calcium ions from extracellular sources into cells (Fig. 2, A and B) confirmed previous data demonstrating a correlation between ER calcium release and cytotoxicity in TRPV1-overexpressing cells (Reilly et al., 2005). Although calcium flux was not detected in BEAS-2B, NHBE, or A549 cells, results presented here demonstrate that the TRPV1-overexpressing cells model the TRPV1 agonist-induced effects in these cell types.

cDNA microarray analysis (see supplemental data, explanation of microarray data and microarray data) demonstrated that TRPV1 activation was associated with changes in the expression of several prototypical ER stress genes in lung cells. Comparisons between gene expression changes elicited by nonivamide in the presence and absence of LJO-328 and EGTA/ruthenium red (Fig. 3A) and changes elicited by the prototypical ER stress inducing-agents thapsigargin and DTT (Fig. 3B) support our conclusion that TRPV1 activation causes ER stress. Furthermore, ER stress proceeded via pathways similar to those activated by thapsigargin and DTT (Schroder and Kaufman, 2005).

ER stress responses are compensatory responses. Up-regulation of specific gene products through dedicated signaling pathways, coupled with cell cycle arrest and a temporary halt of general transcription and translation, are coordinated processes that have evolved to help cells overcome inefficiencies in protein processing (Schroder and Kaufman, 2005). Alterations in ER processing efficiency occur with nutrient deprivation, viral infection, disruption of cellular redox state, changes in ER folding environment (e.g., alterations in calcium homeostasis, redox state), expression of unstable polymorphic variant proteins, and toxicant exposures (Cribb et al., 2005; Schroder and Kaufman, 2005). If cells cannot compensate for a specific stress, they die.

ER stress-induced cell death has been primarily attributed to the expression of GADD153 following EIF2αK3 activation (Matsumoto et al., 1996; McCullough et al., 2001; Oyadomari and Mori, 2004). GADD153 inhibits cell proliferation by reducing the expression of CCND1, and it causes cell death by sequestering the antiapoptotic Bcl-2 protein and inhibiting nuclear factor-κB and Akt/protein kinase B-mediated cyto-

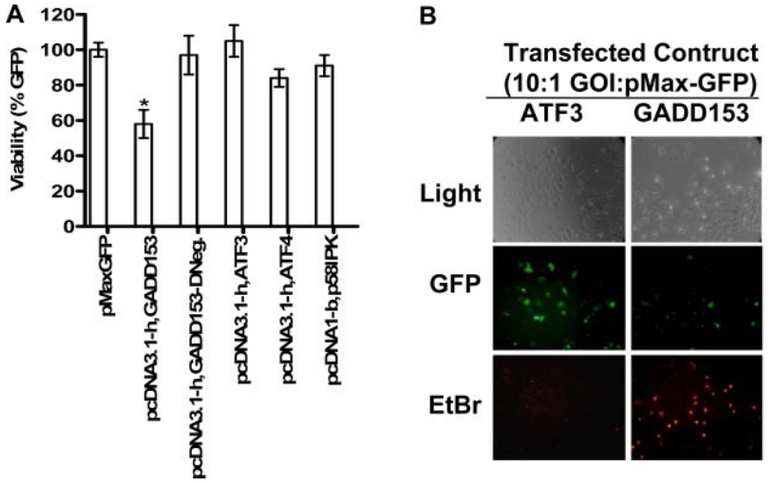

Fig. 5. A, viability of A549 cells transiently transfected with ER stress-induced genes. Cells were subcultured into 48-well plates and transfected for 18 h with mammalian expression plasmids harboring cDNA for EGFP, GADD153, ATF3, ATF4, and p58^{IPK}. After a 24-h recovery period, cell viability was determined. ∗, statistically significant decrease in viability (ANOVA, 95% confidence interval; $n = 3$). B, bright field and fluorescence micrographs of A549 cells cotransfected with ATF3 + EGFP and GADD153 + EGFP (10:1 target gene plasmid:pMax-GFP). Light, bright field image; GFP, fluorescence image using a filter set to image GFP expression; EtBr, fluorescence image using a filter set to visualize propidium iodide- or ethidium bromide-stained cell nuclei. After transfection and a 24-h recovery period, cells were sequentially imaged to assess the survival of GFP-transfected cells and dead/damaged cells (EtBr+) resulting from transfection of either ATF3 (−control) or GADD153. In total, 25 ng of plasmid DNA was used for each transfection. ∗, $p < 0.025$, paired t tests; $n = 3$.

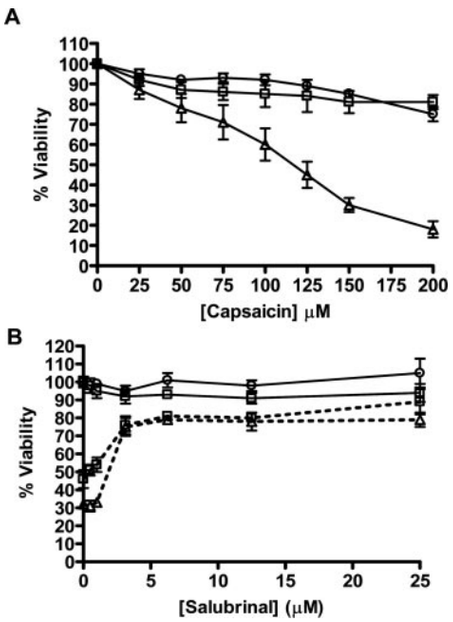

Fig. 6. A, dose-response cytotoxicity curves for A549 (open triangles) and stably overexpressing cell lines harboring the dominant-negative EIF2α-S52A (open squares) and GADD153-L134A/L141A (open circles) genes. B, inhibition of cell death in BEAS-2B and TRPV1-overexpressing cells using salubrinal. Cells were treated with 1 μM nonivamide (TRPV1-overexpressing cells) or 100 μM nonivamide (BEAS-2B cells) in the presence and absence of salubrinal for 24 h at 37°C in LHC-9 media. Circles, TRPV1-overexpressing cells; triangles, BEAS-2B cells treated with nonivamide and increasing concentrations of salubrinal. Data representing changes in viability due to treatment of BEAS-2B and TRPV1-overexpressing cells with salubrinal only are represented as squares and dots, respectively. Cell viability was determined as described under *Materials and Methods*. Data ($n = 6$) are relative to untreated controls.

protective processes (McCullough et al., 2001; Hu et al., 2004; Hyoda et al., 2006). The balance between cell death and survival ultimately depends upon the level of GADD153 expression and the coexpression of other pro- and anticytotoxic gene products that participate in ER stress responses.

Treatment of BEAS-2B cells with nonivamide promoted the phosphorylation of EIF2α at serine 52 (Fig. 4A). This was indicative of EIF2αK3 activation. EIF2α phosphorylation was associated with increased expression of GADD153 expression (Figs. 3A and 4, A and B). Increased concentrations of EIF2α-P and GADD153 correlated with the onset of cell death in BEAS-2B cells, as determined using dose- and temporal-response correlations with protein and mRNA (Fig. 4, A–C). These trends were reproduced using the TRPV1-overexpressing line. EIF2α phosphorylation and GADD153 expression were attenuated by LJO-328, but not by EGTA or ruthenium red. *n*-Benzylnonanamide, a pharmacologically inactive nonivamide analog, did not promote ER calcium release or induce GADD153 expression in BEAS-2B or any other cells tested, and it was nontoxic at concentrations equal to or in 2-fold excess of nonivamide (Fig. 2, A and B; Table 2). These data support our conclusion that TRPV1 activation promotes cytotoxicity via activation of EIF2αK3, phosphorylation of EIF2α, and expression of GADD153.

To substantiate the role of GADD153 in cell death, we cloned this gene and transiently transfected A549 cells with the expression construct. Performing transient transfection studies in the BEAS-2B and NHBE cells were hampered by variable transfection efficiency and high levels of toxicity due to transfection reagents. As such, we used A549 cells as the model for these experiments. We have previously shown that A549 cells respond to TRPV1-agonists similar to BEAS-2B cells (Reilly et al., 2003). Cells transfected with GADD153 exhibited reduced viability due to loss of cells from the culture wells (Fig. 5, A and B). Cytotoxicity and cell loss relative to controls were not observed with GADD153-L134A/L141A, ATF3, or p58^{IPK}, but toxicity was observed with ATF4. These results were consistent with the established roles of these proteins (Schroder and Kaufman, 2005). Specifically, ATF3 and p58^{IPK} limit ER stress responses by inhibiting ATF4-

TABLE 2
Induction of GADD153 expression by multiple TRPV1 agonists and inhibition by antagonists in various cell lines

Treatment (4 h)	GADD153 Induction (-Fold Control)				
	TRPV1-Overexpressing	BEAS-2B	NHBE	A549	HEK-293
Nonivamide, 1 μM	8.1 ± 0.8*				
Nonivamide, 100 μM		7.9 ± 0.5*	6.0 ± 0.4*	5.5 ± 0.3*	0.88 ± 0.07
Nonivamide, 200 μM					1.19 ± 0.06
Resiniferatoxin, 0.01 μM	7.9 ± 0.8*				
Resiniferatoxin, 7.5 μM		6.4 ± 0.8*	6.3 ± 0.3*	4.8 ± 0.4*	0.77 ± 0.08
Anandamide, 12.5 μM	7.4 ± 0.6*				
Anandamide, 25 μM		6.9 ± 0.5*		3.3 ± 0.2*	
n-Benzylnonanamide, 1 μM	1.3 ± 0.2				
n-Benzylnonanamide, 100 μM		2.2 ± 0.3	2.6 ± 0.2*	0.65 ± 0.07	0.78 ± 0.04
Capsaicin, 1 μM + 5-iodo-RTX, 1 μM	0.6 ± 0.4				
Capsaicin, 100 μM + 5-iodo-RTX, 30 μM		10.4 ± 0.9*	4.2 ± 0.4*		
Capsaicin, 1 μM + LJO-328, 20 μM	1.34 ± 0.03				
Capsaicin, 100 μM + LJO-328, 50 μM		1.4 ± 0.2	1.0 ± 0.1	0.75 ± 0.09	0.84 ± 0.07

* Statistically significant increase relative to control ($p < 0.05$, t test; $n = 3$).

dependent gene transcription and the phosphorylation of EIF2α by EIF2αK3, respectively. Conversely, ATF4 promotes GADD153 transcription, and GADD153 is procytotoxic. Additional support for GADD153 as the ultimate mediator of cytotoxicity was obtained by treating A549 cells that stably overexpressed the GADD153-L134A/L141A dominant-negative mutant (Matsumoto et al., 1996). Overexpression of GADD153-L134A/L141A markedly reduced cytotoxicity caused by nonivamide (Fig. 6A). Data in Figs. 5 and 6 imply that GADD153 was the primary cause of cytotoxicity in lung cells treated with TRPV1 agonists.

The effects of modifying the EIF2αK3/EIF2α signaling were also evaluated. Two approaches were used: stable overexpression of the EIF2α-S52A dominant-negative mutant in A549 cells (Srivastava et al., 1998) and pharmacological stabilization of EIF2α-P in BEAS-2B and TRPV1-overexpressing cells using salubrinal (Boyce et al., 2005). Interestingly, squelching of EIF2α phosphorylation (Fig. 6A) and inhibition of EIF2α dephosphorylation (Fig. 6B) protected cells from toxicity. Initially, these data seemed contradictory, but literature supports a dual role for EIF2α-P in regulating cell survival and death during ER stress. Thus, the results in Fig. 6, A and B, highlight this dual effect of the EIF2αK3/EIF2α pathway. However, the molecular basis for these antithetical responses remains enigmatic.

We also investigated whether ER stress represented a common mechanism of cytotoxicity for structurally diverse TRPV1 agonists. Table 2 shows that transcriptional activation of GADD153 occurred in BEAS-2B, A549, NHBE, and TRPV1-overexpressing cells treated with LD_{50} concentrations of nonivamide, resiniferatoxin, and anandamide. As predicted, TRPV1 agonists failed to induce GADD153 expression in the TRPV1-null HEK293 cell line (Table 2). Likewise, *n*-benzylnonanamide failed to elicit GADD153 expression, confirming the direct link between TRPV1 activation, GADD153 expression, and cell death. This conclusion was also supported by the inhibition of GADD153 expression by LJO-328 and 5-iodo-RTX (Table 2). The inability of 5-iodo-RTX to completely inhibit GADD153 expression in the BEAS-2B cell line was consistent with our previous findings that 5-iodo-RTX (like capsazepine) causes cytotoxicity at elevated concentrations (Reilly et al., 2003, 2005).

Collectively, the results presented by this study support the following mechanism of cytotoxicity for TRPV1-agonists in lung (and possibly other) cells. First, activation of intracellular TRPV1 leads to a decrease in ER calcium content, an accumulation of unfolded/partially folded proteins in the ER lumen, and an overall decrease in protein processing efficiency. As a result, EIF2αK3 is activated resulting in the phosphorylation of EIF2α and an increase in the expression of ATF4, GADD153, and other ER stress-related genes. Ultimately, increased transcription and expression of GADD153 causes cell death.

The translational facets of the results presented in this study are 2-fold. First, the near uniform response elicited by structurally diverse TRPV1 agonists in all four lung cell types suggests that this mechanism of toxicity is applicable to many other TRPV1 agonists. Specifically, environmental TRPV1 agonists that promote lung inflammation and injury (e.g., particle pollutants) and endogenous TRPV1 agonists (e.g., leukotrienes, H_2S) that are produced during inflammation or infection may also cause lung cell death and tissue damage via the EIF2αK3-dependent ER stress pathway. As such, future clinical research targeting TRPV1 and/or the EIF2αK3-dependent ER stress pathways may prove beneficial in the treatment and/or prevention diverse respiratory maladies. Second, our results indicate that the effects of a TRPV1 ligand on a cell will depend upon both the relative subcellular distribution of TRPV1 and the relative permeability of the ligand. Hence, it must be stressed that the subcellular location of TRPV1 should be established and multiple TRPV1 agonists and antagonists (preferably not capsazepine) should be used in future research studies evaluating the role of TRPV1 in specific biological outcomes. Although we have not specifically tested whether cell-impermeable agonists of TRPV1 (e.g., pH or environmental particle pollutants) exhibit different mechanisms of cytotoxicity, evidence supports this hypothesis. Specifically, inhibition of the cell surface TRPV1 in lung cells has no effect on cytotoxicity by TRPV1 agonists, despite inhibition of proinflammatory cytokine synthesis (Reilly et al., 2005), and sensory neurons, which primarily express TRPV1 on the cell surface, are protected against cytotoxicity by inhibiting cellular influx of calcium (Wood et al., 1988).

Overall, these results provide novel insight into mechanisms by which diverse exogenous and endogenous TRPV1 agonists affect lung cell physiology. These findings provide fundamental knowledge that will facilitate future basic sci-

ence and clinical research on TRPV1 in an array of physiological and pharmacological models, including models of acute lung injury and inflammatory lung injury.

Acknowledgments

We thank Dr. Manivannan Ethirajan (Department of Medicinal Chemistry, University of Utah, Salt Lake City, UT) for assistance with *n*-benzylnonanamide synthesis and Dr. David Ron (Skirball Institute, New York University Medical Center, New York City, NY) for helpful suggestions.

References

Agopyan N, Head J, Yu S, and Simon SA (2004) TRPV1 receptors mediate particulate matter-induced apoptosis. *Am J Physiol* **286:**L563–L572.

Bhatia M, Zhi L, Zhang H, Ng of SW, and Moore PK (2006) Role of substance P in hydrogen sulfide-induced pulmonary inflammation in mice. *Am J Physiol* **291:** L896–L904.

Billmire DF, Vinocur C, Ginda M, Robinson NB, Panitch H, Friss H, Rubenstein D, and Wiley JF (1996) Pepper-spray-induced respiratory failure treated with extracorporeal membrane oxygenation. *Pediatrics* **98:**961–963.

Boyce M, Bryant KF, Jousse C, Long K, Harding HP, Scheuner D, Kaufman RJ, Ma D, Coen DM, Ron D, et al. (2005) A selective inhibitor of eIF2alpha dephosphorylation protects cells from ER stress. *Science (Wash DC)* **307:**935–939.

Cribb AE, Peyrou M, Muruganandan S, and Schneider L (2005) The endoplasmic reticulum in xenobiotic toxicity. *Drug Metab Rev* **37:**405–442.

Geppetti P, Materazzi S, and Nicoletti P (2006) The transient receptor potential vanilloid 1: role in airway inflammation and disease. *Eur J Pharmacol* **533:**207–214.

Glinsukon T, Stitmunnaithum V, Toskulkao C, Buranawuti T, and Tangkrisanavinont V (1980) Acute toxicity of capsaicin in several animal species. *Toxicon* **18:** 215–220.

Heck A (1995) Accidental pepper spray discharge in an emergency department. *J Emerg Nurs* **21:**486.

Hu P, Han Z, Couvillon AD, and Exton JH (2004) Critical role of endogenous Akt/IAPs and MEK1/ERK pathways in counteracting endoplasmic reticulum stress-induced cell death. *J Biol Chem* **279:**49420–49429.

Hwang SW, Cho H, Kwak J, Lee SY, Kang CJ, Jung J, Cho S, Min KH, Suh YG, Kim D, et al. (2000) Direct activation of capsaicin receptors by products of lipoxygenases: endogenous capsaicin-like substances. *Proc Natl Acad Sci USA* **97:**6155–6160.

Hyoda K, Hosoi T, Horie N, Okuma Y, Ozawa K, and Nomura Y (2006) PI3K-Akt inactivation induced CHOP expression in endoplasmic reticulum-stressed cells. *Biochem Biophys Res Commun* **340:**286–290.

Jia Y, McLeod RL, and Hey JA (2005) TRPV1 receptor: a target for the treatment of pain, cough, airway disease and urinary incontinence. *Drug News Perspect* **18:** 165–171.

Johansen ME, Reilly CA, and Yost GS (2006) TRPV1 antagonists elevate cell surface populations of receptor protein and exacerbate TRPV1-mediated toxicities in human lung epithelial cells. *Toxicol Sci* **89:**278–286.

Knight DA and Holgate ST (2003) The airway epithelium: structural and functional properties in health and disease. *Respirology* **8:**432–446.

Li L, Bhatia M, Zhu YZ, Zhu YC, Ramnath RD, Wang ZJ, Anuar FB, Whiteman M, Salto-Tellez M, and Moore PK (2005) Hydrogen sulfide is a novel mediator of lipopolysaccharide-induced inflammation in the mouse. *FASEB J* **19:**1196–1198.

Lu PD, Jousse C, Marciniak SJ, Zhang Y, Novoa I, Scheuner D, Kaufman RJ, Ron D, and Harding HP (2004) Cytoprotection by pre-emptive conditional phosphorylation of translation initiation factor 2. *EMBO (Eur Mol Biol Organ) J* **23:**169–179.

Matsumoto M, Minami M, Takeda K, Sakao Y, and Akira S (1996) Ectopic expression of CHOP (GADD153) induces apoptosis in M1 myeloblastic leukemia cells. *FEBS Lett* **395:**143–147.

McCullough KD, Martindale JL, Klotz LO, Aw TY, and Holbrook NJ (2001) Gadd153 sensitizes cells to endoplasmic reticulum stress by down-regulating Bcl2 and perturbing the cellular redox state. *Mol Cell Biol* **21:**1249–1259.

Mitchell JE, Campbell AP, New NE, Sadofsky LR, Kastelik JA, Mulrennan SA, Compton SJ, and Morice AH (2005) Expression and characterization of the intracellular vanilloid receptor (TRPV1) in bronchi from patients with chronic cough. *Exp Lung Res* **31:**295–306.

Morice AH, Kastelik JA, and Thompson R (2001) Cough challenge in the assessment of cough reflex. *Br J Clin Pharmacol* **52:**365–375.

Oyadomari S and Mori M (2004) Roles of CHOP/GADD153 in endoplasmic reticulum stress. *Cell Death Differ* **11:**381–389.

Reilly CA, Johansen ME, Lanza DL, Lee J, Lim JO, and Yost GS (2005) Calcium-dependent and independent mechanisms of capsaicin receptor (TRPV1)-mediated cytokine production and cell death in human bronchial epithelial cells. *J Biochem Mol Toxicol* **19:**266–275.

Reilly CA, Taylor JL, Lanza DL, Carr BA, Crouch DJ, and Yost GS (2003) Capsaicinoids cause inflammation and epithelial cell death through activation of vanilloid receptors. *Toxicol Sci* **73:**170–181.

Ricciardolo FL, Gaston B, and Hunt J (2004) Acid stress in the pathology of asthma. *J Allergy Clin Immunol* **113:**610–619.

Schröder M and Kaufman RJ (2005) ER stress and the unfolded protein response. *Mutat Res* **569:**29–63.

Seki N, Shirasaki H, Kikuchi M, Sakamoto T, Watanabe N, and Himi T (2006) Expression and localization of TRPV1 in human nasal mucosa. *Rhinology* **44:**128–134.

Srivastava SP, Kumar KU, and Kaufman RJ (1998) Phosphorylation of eukaryotic translation initiation factor 2 mediates apoptosis in response to activation of the double-stranded RNA-dependent protein kinase. *J Biol Chem* **273:**2416–2423.

Steffee CH, Lantz PE, Flannagan LM, Thompson RL, and Jason DR (1995) Oleoresin capsicum (pepper) spray and "in-custody deaths". *Am J Forensic Med Pathol* **16:**185–192.

Szallasi A, Cruz F, and Geppetti P (2006) TRPV1: a therapeutic target for novel analgesic drugs? *Trends Mol Med* **12:**545–554.

Tominaga M, Caterina MJ, Malmberg AB, Rosen TA, Gilbert H, Skinner K, Raumann BE, Basbaum AI, and Julius D (1998) The cloned capsaicin receptor integrates multiple pain-producing stimuli. *Neuron* **21:**531–543.

Trevisani M, Gazzieri D, Benvenuti F, Campi B, Dinh QT, Groneberg DA, Rigoni M, Emonds-Alt X, Creminon C, Fischer A, et al. (2004) Ethanol causes inflammation in the airways by a neurogenic and TRPV1-dependent mechanism. *J Pharmacol Exp Ther* **309:**1167–1173.

Trevisani M, Patacchini R, Nicoletti P, Gatti R, Gazzieri D, Lissi N, Zagli G, Creminon C, Geppetti P, and Harrison S (2005) Hydrogen sulfide causes vanilloid receptor 1-mediated neurogenic inflammation in the airways. *Br J Pharmacol* **145:**1123–1131.

Van Der Stelt M and Di Marzo V (2004) Endovanilloids. Putative endogenous ligands of transient receptor potential vanilloid 1 channels. *Eur J Biochem* **271:**1827–1834.

van Rijswijk JB and Gerth van Wijk R (2006) Capsaicin treatment of idiopathic rhinitis: the new panacea? *Curr Allergy Asthma Rep* **6:**132–137.

Vargaftig BB and Singer M (2003) Leukotrienes mediate murine bronchopulmonary hyperreactivity, inflammation, and part of mucosal metaplasia and tissue injury induced by recombinant murine interleukin-13. *Am J Respir Cell Mol Biol* **28:**410–419.

Veronesi B, Oortgiesen M, Carter JD, and Devlin RB (1999) Particulate matter initiates inflammatory cytokine release by activation of capsaicin and acid receptors in a human bronchial epithelial cell line. *Toxicol Appl Pharmacol* **154:**106–115.

Watanabe N, Horie S, Michael GJ, Spina D, Page CP, and Priestley JV (2005) Immunohistochemical localization of vanilloid receptor subtype 1 (TRPV1) in the guinea pig respiratory system. *Pulm Pharmacol Ther* **18:**187–197.

Wek RC, Jiang HY, and Anthony TG (2006) Coping with stress: eIF2 kinases and translational control. *Biochem Soc Trans* **34:**7–11.

Wood JN, Winter J, James IF, Rang HP, Yeats J, and Bevan S (1988) Capsaicin-induced ion fluxes in dorsal root ganglion cells in culture. *J Neurosci* **8:**3208–3220.

Zhang K and Kaufman RJ (2006) The unfolded protein response: a stress signaling pathway critical for health and disease. *Neurology* **66:**S102–S109.

Address correspondence to: Dr. Christopher A. Reilly, Department of Pharmacology and Toxicology, 30 S. 2000 E., Room 201 Skaggs Hall, University of Utah, Salt Lake City, UT 84112. E-mail: chris.reilly@pharm.utah.edu

CHAPTER 3

STRUCTURE ACTIVITY RELATIONSHIPS FOR CAPSAICIN ANALOGUES AND TRPV1-MEDIATED HUMAN LUNG EPITHELIAL CELL TOXICITY

3.1 Abstract

Capsaicinoid compounds activate transient receptor potential vanilloid-1 (TRPV1). Activation of intracellular TRPV1 in human lung cells causes calcium efflux from the endoplasmic reticulum (ER), activation of the unfolded protein response/ER stress, and cell death via increased expression of pro-apoptotic GADD153. In this study, variants of capsaicin and its analogue nonivamide were synthesized and used to probe the relationship between TRPV1 receptor binding, activation, ER calcium release, changes in GADD153 expression, and cell death in TRPV1-overexpressing BEAS-2B, BEAS-2B, and primary NHBE lung cells. The vanilloid ring pharmacophore of capsaicin is 3-methoxy-4-hydroxybenzylamide. Removal, substitution, methylation, or repositioning of the 3-MEO- or 4-OH group on the vanilloid ring pharmacophore of nonivamide markedly reduced analogue potency and toxicity using calcium flux, GADD153 induction, and cytotoxicity as quantitative measures. Molecular modeling of binding interactions between TRPV1 and the various analogues verified that the inactive analogues do not form 'productive' ligand receptor complexes. Demethylation of the 3-MeO- group to produce the *n*-(3,4-dihydroxybenzyl)nonanamide analogue slightly reduced cytotoxicity in TRPV1-overexpressing and NHBE cells, but drastically increased toxicity in BEAS-

2B cells. This indicates a decrease in TRPV1-binding and activation, and co-activation of non-TRPV1-mediated cell death processes, presumably involving redox cycling of the catechol and increased production of reactive oxygen species. This conclusion was confirmed by an attenuation of cell death by *n*-acetylcysteine (NAC) co-treatment. All three cell types responded similarly to the analogues, but NHBE cells appeared to have greater capacity to detoxify the catechol analogue. This study further defines how capsaicinoids interact with TRPV1 to alter cellular function, and provide strong support for TRPV1-mediated ER stress as an important mechanism of cell death in lung cells exposed to capsaicinoid compounds and other TRPV1 agonists.

3.2 Introduction

The capsaicin receptor, TRPV1, is a popular pharmacological target due to its functional diversity and many hypothesized roles in pathology and disease (*1, 2*). Endogenous and exogenous noxious stimuli activate TRPV1, including heat, acidic pH, and a variety of chemical irritants (*2-4*). The prototypical agonist of TRPV1 is capsaicin (N-[(4-hydroxy-3-methoxyphenyl)methyl]-8-methylnon-6-enamide), the pungent compound in chili peppers that elicits a burning sensation upon contact.

TRPV1 is functionally expressed in sensory (C- and Aδ-fibers) neurons and a variety of non-neuronal cell types. Activation of TRPV1-expressing sensory nerves in the airways elicits cough, dyspnea, and neurogenic inflammation characterized by plasma extravasation and edema. In lung epithelial cells, the physiological functions of TRPV1 remain poorly understood. Accumulating evidence suggests that TRPV1 helps regulate host defense/innate immunity through regulation of proinflammatory responses characterized by marked upregulation of a number of Th1-type cytokine and chemokine

genes following exposure to injurious agents, including TRPV1 agonists (*15-17*). It is proposed that the influx of neutrophils into the lung following exposure to TRPV1 agonists is mediated, in part, by TRPV1 activation in epithelial cells.

Rats exposed to capsaicin aerosols also exhibit alveolar damage and significant cell damage and cell loss in the conducting airways (*18*). In cultured human lung epithelial cells, capsaicin and structurally related compounds activate TRPV1, leading to dose- and time-dependent cytokine release, ER stress, and cell death (*16, 18, 19*). Increases in IL-6 and IL-8 are predominantly associated with activation of cell surface TRPV1, while activation of ER associated TRPV1 causes ER stress, leading to activation of the PERK pathway, GADD153 induction, and cell death (*15, 16, 18, 19*). Blocking TRPV1 activation with cell-permeable antagonists such as LJO-328 ameliorates ER stress, but inhibition of calcium influx via cell surface TRPV1 only attenuates cytokine gene induction, not lung cell death. TRPV1 antagonists do not protect cells with low TRPV1 expression from cytotoxicity, despite attenuating ER stress (*16, 18, 19*).

Previous structure-activity relationships determined that the essential structural properties of capsaicin for TRPV1 activation required substituents in specific positions on the aromatic ring, presence of the amide bond, and a narrow range of carbons in the hydrophobic hydrocarbon ‘tail’ (*5-7*). For the A-region of nonivamide (vanilloid ring), compounds with the parent capsaicin structure of 3-methoxy-4-hydroxybenzyl were the most potent agonists. Substitutions at positions 2, 5 and 6 on the ring reduced or ablated activity. If 4-OH was removed, activity was lost; alkylation of 4-OH also reduced or removed activity. Removal of or changing the substituent at the 3-position reduced or abolished activity. Switching the 3-MEO- and 4-OH groups reduced activity, and

catechol compounds were equipotent *in vitro* but were not as potent in a functional analgesia model (*7*). For the B-region of nonivamide (amide bond), features required for activity were sp3 hybridization of the nitrogen, potential for hydrogen bonding, and the presence of a single bridging carbon to the vanilloid ring. Thiourea analogues were the most potent (*6*). For the C-region of nonivamide (hydrophobic tail), the most important features were length (8-12 carbons) and hydrophobicity, as substitution with polar groups decreased potency (*5*). Use of these criteria also led to the synthesis and characterization of capsazepine, the first selective antagonist of TRPV1 (*8*). More recent site-directed mutagenesis studies of TRPV1 and molecular modeling of the identified capsaicin binding site have verified the necessity of the structural features first described by Walpole and Wrigglesworth (*9-14*).

For this study, a series of capsaicin/nonivamide analogues with modified vanilloid ring pharmacophores were synthesized to assess and differentiate between TRPV1-mediated and nonspecific cell death in lung cell culture models and for future use in studies of TRPV1-mediated lung injury in animal models. The ability of these modified capsaicinoids to bind and activate TRPV1, induce ER stress, and cause cell death, as well as the ability of these chemicals to function as antagonists of TRPV1, was investigated.

3.3 Methods

3.3.1 Chemicals

Nonivamide (*n*-vanillylnonanamide or *n*-(4-hydroxy-3-methoxybenzyl)nonanamide), sulfinpyrazone, ionomycin, *n*-acetylcysteine, DMSO, 3-hydroxy-4-methoxybenzylamine-HCl, 3,4-dihydroxybenzylamine-HBr,

nonanoyl chloride, methanol, sodium methoxide, ethyl acetate and hexane were purchased from Sigma-Aldrich (St. Louis, MO). Nonivamide and capsaicin have indistinguishable toxicity profiles in the human lung cells used in this study, thus nonivamide was used as the prototype TRPV1 agonist. LJO-328 was provided by Dr. Jeewoo Lee (Seoul National University, Seoul, Korea). PCR primers for TRPV1, GADD153 and β2M were synthesized by the University of Utah Core Facilities (Salt Lake City, UT).

3.3.2 Synthesis of Capsaicinoid Analogues

n-Benzylnonanamide was synthesized as described previously (*19*). *n*-(3-hydroxy-4-methoxybenzyl)nonanamide and *n*-(3,4-dihydroxybenzyl)nonanamide were synthesized by reacting 3-hydroxy-4-methoxybenzylamine-HCl and 3,4-dihydroxybenzylamine-HBr with a 5-fold molar excess of nonanoyl chloride in 0.1N NaOH at room temperature. The precipitates were collected by vacuum filtration over a paper filter, rinsed with saturated sodium carbonate and water, and air-dried. The crude acylated products were dissolved in dry methanol and reacted with 0.5 M sodium methoxide at room temperature under argon for 2 hours. The mixture was neutralized with amberlite IR120(H^+), filtered, dried under vacuum, and the crude product was purified over a silica gel column eluted with ethyl acetate:hexane (1:5 v/v). Product purity (>95%) and structure were determined by HPLC with UV detection at 230 nm, LC/MS^2, and [^{1}H]NMR.

3.3.3 Cell Culture

Immortalized human bronchial epithelial cells (BEAS-2B) were purchased from American Type Culture Collection (Manassas, VA), and TRPV1-overexpressing BEAS-

2B (TRPV1-OE) cells were generated as described previously (*18*). BEAS-2B and TRPV1-OE cells were cultured in LHC-9 media (Invitrogen, Carlsbad, CA). Normal Human Bronchial Epithelial (NHBE) cells, a primary cell line, were purchased from Lonza (Walkersville, MD) and cultured in BEGM media. Culture flasks for NHBE, BEAS-2B and TRPV1-OE cells were coated with LHC basal media fortified with 30 μg/mL collagen, 10 μg/mL fibronectin, and 10 μg/mL bovine serum albumin. Cells were maintained between 30 to 90% maximum density and were subcultured every 2-4 days depending on cell growth rates.

3.3.4 Cytotoxicity/Dose Response Assays

Cells were subcultured into 96-well plates and grown to ~90% confluence. Cells were treated for 24 hours at 37ºC with increasing concentrations of chemical. Treatment solutions were prepared using LHC-9 media for BEAS-2B and TRPV1-OE cells (Invitrogen, Carlsbad, CA). For NHBE cells, agonist and antagonists were prepared in Opti-MEM I Reduced Serum Medium (Invitrogen, Carlsbad, CA) without fetal bovine serum. Cell treatment solutions contained ≤ 0.5% DMSO. Cell viability was assessed using the Dojindo cell counting kit-8 (Dojindo Laboratories, Gaithersburg MD), according to supplier's recommendations. Toxicity data are expressed as the percentage of viable cells relative to untreated controls, calculated using the absorbance at 450 nm minus the absorbance at 630 nm.

3.3.5 Fluorometric Calcium Assays

TRPV1-OE cells were used to evaluate calcium flux as a consequence of TRPV1 activation. TRPV1-OE cells were sub-cultured into 96-well culture plates and grown to approximately 90% maximum density. Cells were loaded with the fluorogenic calcium

indicator Fluo-4-acetoxymethyl ester (Fluo-4 AM, 2.5 μM) (Invitrogen, Carlsbad, CA) for 60 minutes at room temperature (about 22º C), in the presence of 200 μM sulfinpyrazone in LHC-9 media. Cells were washed twice and incubated at room temperature for an additional 20 minutes in sulfinpyrazone containing media to permit methyl ester hydrolysis and activation of Fluo-4 in cells. Changes in cellular fluorescence in response to agonist and antagonist treatments were measured using a NOVOStar plate reader (BMG Labtech, Germany) with excitation at 485 nm and emission at 520 nm. Baseline fluorescence readings were subtracted from the fluorescence measured, and each treatment was performed in triplicate. Ionomycin (10 μM) produces maximum calcium movement into cells and was used as a positive control to normalize responses. Data in Table 3.1 are expressed as percent of ionomycin fluorescence ± standard deviation.

3.3.6 Quantitative Real-Time PCR Analysis of Gene Expression

Cells were subcultured into 6-well cell culture plates and grown to ~90% density. Cells were then treated with TRPV1 agonists and antagonists for 4 hours at 37ºC to determine GADD153 induction. Total RNA was extracted from cells using the Invitrogen PureLink Micro-to-Midi Total RNA Purification System (Invitrogen, Carlsbad, CA), and 1 μg of the total RNA was transcribed into cDNA using Superscript III (Invitrogen, Carlsbad, CA). cDNA was diluted 1:100 in filter-sterilized Milli-Q H_2O for all samples. cDNA was amplified by PCR using RT^2 SYBR Green qPCR Master Mix from SABiosciences (Frederick, MD) following manufacturer instructions in 25 μL reaction volumes on a Chromo 4 Real Time Detection System (Bio-Rad, Hercules, CA) using MJ Opticon Monitor 3 software. The PCR program used consisted of an initial 10-

minute incubation at 95ºC, followed by 40 cycles of 95ºC for 15 seconds, 55ºC for 30 seconds**,** then 72ºC for 30 seconds. Experiments were performed in triplicate with a copy number standard curve for both the housekeeping gene (β-2 macroglobulin, β2M) and the genes of interest. Primer sequences for human β2M were:

sense, 5' –GATGAGTATGCCTGCCGTGTG – 3';

antisense, 5' –CAATCCAAATGCGGCATCT – 3'. Primer sequences for human TRPV1 were: sense, 5'- CTGCGGACCCACTCCAAAA-3';

antisense, 5'-CCTCGTGAGGGCAATCCAC-3'. Primer sequences for human GADD153 were: sense, 5'-AGAACCAGGAAACGGAAACAGA-3';

antisense 5'-TCTCCTTCATGCGCTGCTTT-3'.

3.3.7 Molecular Modeling

Chemical structures of capsaicin and capsaicinoid analogues were optimized using Gaussian03 software. Structures were then docked into a constrained PDB structure of TRPV1 transmembrane helices 3 and 4 (*10*) using AutoDock software. The most highly populated energy cluster conformations of the docked structures were visualized in Chimera.

3.3.8 Statistical Analysis

Statistical analysis was performed using 95% confidence intervals as the limit for significance with $p < 0.05\%$. All results are represented as mean ± standard error of the mean unless otherwise indicated. For comparisons of two groups, unpaired student's t-test was used for statistical analysis. To compare more than two groups, one-way ANOVA analysis was performed with Newman-Keuls Multiple Comparison Test post-hoc testing performed, as indicated in figure legends. Statistical analyses were performed

using GraphPad Prism version 4.02 for Windows (GraphPad Software, San Diego, California, www.graphpad.com).

3.4 Results

A series of capsaicinoid analogues were synthesized to probe the relationship between TRPV1 binding, activation, ER stress and cell death. Structural attributes of each analogue are presented in Figure 3.1.

TRPV1 transcription was quantified using RT-PCR in TRPV1-OE, BEAS-2B, and NHBE cells (Figure 3.2). TRPV1-OE cells expressed approximately 10 times more copies of TRPV1 mRNA than BEAS-2B cells, and approximately 45 times more copies than NHBE cells, using β2M as a normalization factor. β2M did not vary significantly between cell types.

The ability of the analogues to activate TRPV1 was evaluated using fluorometric calcium flux assays (Figure 3.3). Previous studies have shown that ER calcium release was a precursor to GADD153 induction and epithelial lung cell death (*19*). TRPV1-OE cells treated with increasing concentrations of nonivamide and *n*-(3,4-dihydroxybenzyl)nonanamide exhibited statistically significant increases in cytosolic calcium flux (15-20 fold) relative to untreated cells. The EC_{50} values were 1.5 μM and 9.6 μM, respectively. All other nonivamide variants were essentially inactive even at concentrations ~150x the EC_{50} for nonivamide. Calcium flux dose-response curves for all analogues are shown in Figure 3.3. Calcium flux data at 2, 20 and 100 μM are also shown in Table 3.1.

Molecular modeling techniques were used to model molecular interactions between capsaicinoid analogues and TRPV1 transmembrane domains 3 and 4. Previous

research has shown that capsaicin binds between transmembrane domains 3 and 4 to activate TRPV1, likely interacting with residues Y511, S512, L547, W549, and T550 (*9-14, 20*). Capsaicinoid analogue structures were optimized as described in *Methods*. Representative figures for the docking analysis of nonivamide, *n*-benzylnonanamide *n*-(3-hydroxy-4-methoxybenzyl)nonanamide and *n*-(4-hydroxybenzyl)nonanamide are shown in Figure 3.4, panels a-e.

The dose-response cytotoxicity profile of each analogue was determined. Cytotoxicity (LC_{50}) data for each cell type and analogue are presented in Table 3.2. TRPV1-OE cells were most sensitive to nonivamide and *n*-(3,4-dihydroxybenzyl)nonanamide with LC_{50} values of 1 and 3.4 μM, respectively. All other analogues exhibited cytotoxicity at concentrations above 60-70 μM. BEAS-2B cells were also sensitive to nonivamide and *n*-(3,4-dihydroxybenzyl)nonanamide with LC_{50} values of 114 and 16.1 μM respectively, and were sensitive to most other analogues only at concentrations greater than the LC_{50} for nonivamide. NHBE cells were sensitive to most of the analogues at concentrations between 150 μM and 200 μM, with LC_{50} for nonivamide of 160 μM, consistent with a lower level of TRPV1 expression relative to TRPV1-OE and BEAS-2B cells. Results in Table 3.2 generally indicate that decreased TRPV1 activation correlated with decreased toxicity for all lung cell types tested, but also show that the toxicity of *n*-benzylnonanamide, *n*-(3-methoxybenzyl)nonanamide, and 3-methoxy-4-(nonamidomethyl)phenyl sulfate are the result of non-TRPV1-mediated events since the LC_{50} values in all three cell types was similar. Finally, NHBE cells were less sensitive to *n*-(3,4-dihydroxybenzyl)nonanamide than BEAS-2B and TRPV1-OE cells.

Previous studies have show that activation of TRPV1 in BEAS-2B and TRPV1-OE cells leads to ER stress, PERK pathway activation, and GADD153 expression (*19*). GADD153 mRNA expression was used as a quantifiable marker of ER stress activation by the capsaicinoid analogues. Results for GADD153 induction in TRPV1-OE cells treated at 2, 20 and 100 μM, and BEAS-2B and NHBE cells treated at 200 μM are shown in Table 3.3. Significant GADD153 induction was observed in TRPV1-OE cells treated with 2 μM nonivamide for 4 hours. At 20 μM, statistically significant increases in GADD153 were observed with nonivamide and *n*-(3,4-dihydroxybenzyl)nonanamide), while at 100 μM, induction was observed with nonivamide, *n*-(3,4-dihydroxybenzyl)nonanamide, *n*-(3,4-dimethoxybenzyl)nonanamide, *n*-(4-hydroxybenzyl)nonanamide and *n*-(3-hydroxy-4-methoxybenzyl)nonanamide, in agreement with results from cytotoxicity (Table 3.2) and calcium flux (Figure 3.3, Table 3.1) endpoints. BEAS-2B cells showed increased GADD153 mRNA after 4 hour treatments with 200 μM nonivamide, *n*-(3-methoxybenzyl)nonanamide, *n*-(3,4-dihydroxybenzyl)nonanamide, *n*-(4-hydroxybenzyl)nonanamide *n*-(4-trifluoromethylbenzyl)nonanamide and 3-methoxy-4-(nonamidomethyl)phenyl sulfate, again correlating with the ability of these compounds to cause cell death. NHBE cells treated for 4 hours at 200 μM had statistically significant GADD153 induction in cells treated with 200 μM nonivamide and *n*-(3,4-dihydroxybenzyl)nonanamide, but increases caused by the other analogues were not statistically significant, due to high variability. The NHBE data were consistent with the TRPV1-OE and BEAS-2B response data.

Statistical analysis confirmed significant inverse correlations between loss of cell viability and GADD153 expression in all three cell types (Figure 3.5). For TRPV1-OE cells, correlation statistics were performed to compare cell viability at 2.5, 25 and 100 μM with GADD153 induction at 2, 20 and 100 μM, respectively. Cell viability and GADD153 induction in TRPV1-OE cells after treatment with analogues at 100 μM was not statistically correlated, but it was at 2 and 20 μM. At 100 μM analogues likely mediate cell death through non-TRPV1-mediated and calcium-independent pathways that may or may not alter GADD153 expression levels. For BEAS-2B and NHBE cells, correlation statistics were used to compare cell viability after treatment for 24 hours with 200 μM analogue and GADD153 induction after a 4 hour treatment of 200 μM analogue. In BEAS-2B and NHBE cells, cell viability results were inversely correlated to GADD153 induction.

Correlation statistics were also performed to investigate the relationship between cell viability and calcium flux in TRPV1-OE cells (Figure 3.6). Calcium flux results at 2, 20, and 100 μM were compared to cell viability at 2.5, 25, and 100 μM, respectively. In TRPV1-OE cells, calcium flux at 2 μM was not correlated to cell death, but statistically significant inverse correlation was found at 20 and 100 μM. Correlation statistics were also performed to investigate the relationship between calcium flux and GADD153 induction in TRPV1-OE cells with paired concentrations of 2 μM, 20 μM and 100 μM (Figure 3.7). For all three concentrations, calcium flux and GADD153 induction was significantly correlated.

Alternate non-TRPV1-mediated mechanisms of toxicity were evaluated for *n*-(3,4-dihydroxybenzyl)nonanamide. To determine the extent to which the toxicity of *n*-

(3,4-dihydroxybenzyl)nonanamide was TRPV1 mediated, TRPV1-OE cells were co-treated with *n*-(3,4-dihydroxybenzyl)nonanamide and the TRPV1 antagonist LJO-328 (Figure 3.8). Unlike nonivamide, the toxicity of *n*-(3,4-dihydroxybenzyl)nonanamide was not attenuated by LJO-328 co-treatment. Based on the structure, it was hypothesized that *n*-(3,4-dihydroxybenzyl)nonanamide may redox cycle leading to reactive oxygen species formation and cell death. Co-treatment with *n*-(3,4-dihydroxybenzyl)nonanamide and *n*-acetylcysteine (NAC) showed that NAC attenuated cell death after treatment of TRPV1-OE with 10 μM *n*-(3,4-dihydroxybenzyl)nonanamide. NAC was not protective against cytotoxicity in BEAS-2B cells treated with 25 μM *n*-(3,4-dihydroxybenzyl)nonanamide.

The less potent analogues were also evaluated as potential antagonists of nonivamide toxicity to test whether they compete for TRPV1 binding. Co-treatment of TRPV1-OE cells with nonivamide and increasing concentrations of *n*-benzylnonanamide demonstrated that *n*-benzylnonanamide attenuated cell death at concentrations between 50 and 100 μM (Figure 3.9). All other analogues failed to protect against nonivamide-induced cytotoxicity.

3.5 Discussion

TRPV1 has rapidly emerged as a promising therapeutic target. Better characterization of this receptor, and its associated functions in various cells and tissues, is key to understanding its role in physiology, pathology and disease. TRPV1 is expressed in many tissue and cell types, and it can be difficult to translate results from one model to another. We have designed and characterized a set of capsaicinoid analogues to probe TRPV1 function in an effort to better identify specific and non-

specific outcomes that can be used to study TRPV1 function in the lung, and to extrapolate results across models.

To examine the structure activity relationships of the capsaicin analogues with TRPV1, calcium flux, GADD153 induction and cytotoxicity were evaluated in three different epithelial lung cell lines. We used these parameters as indications of TRPV1 activation because they each represent a step in a proposed mechanism of TRPV1-mediated cell death for these lung cells. TRPV1-mediated calcium flux is commonly used to quantify TRPV1 activation, and causes ER stress (*21*). Previous work has shown that TRPV1 activation induces GADD153 expression as a marker of ER stress (*19*) and that this pro-apoptotic gene product was a prerequisite to cell death (*22-24*). By measuring calcium flux, GADD153 induction and cell death, three different consequences of TRPV1 activation were simultaneously evaluated to examine how they correlated and whether or not they represent an alternative pathway, leading to cell death for nonivamide, because these cells were not protected from cell death by TRPV1 antagonists.

Data indicate that capsaicinoid analogues with specific structural features caused significant calcium flux, GADD153 induction, and cell death in primary and immortalized human lung epithelial cells in a TRPV1-dependent manner. TRPV1-OE cells were highly susceptible to capsaicinoid analogues with both a 4-hydroxy moiety and an adjacent 3-position methoxy or hydroxy group (i.e., nonivamide and *n*-(3,4-dihydroxybenzyl)nonanamide), with nonivamide being most potent and cytotoxic. The presence of only a 4-hydroxy group was not sufficient to activate TRPV1 and removing the 4-hydroxy moiety from the vanilloid ring, masking it by methylation or sulfation, or

switching the 4-hydroxy and 3-methoxy moieties, ablated TRPV1 activation and cytotoxicity in TRPV1-OE cells, with similar results in BEAS-2B and NHBE cells. These results show that the 4-hydroxy and adjacent 3-methoxy moieties are requisite structural features for maximum TRPV1 activation, ER stress, and cell death in all three lung cell types regardless of their level of TRPV1 expression and indicate a correlation between TRPV1 activation and toxicity. These data agree with previous structure activity relationship analyses indicating that presence of a group at the 3-position, in addition to a 4-position hydroxy, are essential for the formation of an optimum and productive ligand-receptor complex (*7*).

Quantitative real-time PCR results confirmed that TRPV1-OE cells expressed the most TRPV1 mRNA (Figure 3.2). These results were expected since TRPV1-OE cells were engineered to over-express TRPV1 under the control of a CMV promoter (*18*). The TRPV1-OE cells were most sensitive to select analogues and to other known TRPV1 agonists indicating that TRPV1 expression is a primary determinant of toxicity in cells. A similar evaluation of mRNA comparisons was previously carried out in our laboratory using TRPV1-OE, BEAS-2B and A549 cells (*18*) showing similar relationships between TRPV1 mRNA abundance and LC_{50}.

Molecular modeling studies to investigate interactions between TRPV1 and capsaicin analogues also agreed with previous literature reports of predicted capsaicin-TRPV1 ligand-receptor interactions. The structures of TRPV1 used for molecular modeling are often based off of a structurally similar voltage-dependent potassium (K_v) channel with 6 transmembrane domains since they were described as having similar topology in 1998 by Vannier *et al.* (*25*). It has been hypothesized that the TRPV1-

capsaicin binding interaction induces a conformational change in the receptor, which opens the pore-loop and allows ions to flow through (*10*). It has also been proposed that transmembrane domains 3 and 4 form a paddle structure, similar to potassium ion channels, and the paddle shifts to permit capsaicin and vaniolloid agonist binding on the intracellular side of the channel (*10, 11, 26*). Mutation studies by Jordt and Julius (2002) indicate that human TRPV1 residue Y511 confers capsaicin sensitivity to the receptor, which was identified because chickens lack the corresponding residue and pain responses to capsaicin (*12*). Additional studies predict that capsaicin and other vanilloid agonists interact with TRPV1 transmembrane domains 3 and 4 at residues Y511, S512, L547, W549 and T550. (*9-14, 20*) The vanilloid ring of capsaicin is hypothesized to have pi stacking interactions with W549, and the hydrophobic tail of the molecule likely interacts with Y511 forming a chemical tether between the two helices that causes a structural change, rendering the channel more susceptible to opening at a given temperature.

Our results show that nonivamide likely interacts with TRPV1 similarly to capsaicin, at residues Y511 and W549 (Figure 3.4, panel a). The predicted binding interactions between TRPV1 and *n*-benzylnonanamide did not exhibit the same characteristics as nonivamide and its "nonproductive" interactions correlated with a lack of agonist activity. *N*-benzylnonanamide did appear to interact with TRPV1 to some extent, presumably by binding to the helices by associating with Y511 as indicated by its ability to attenuate the toxicity of nonivamide. Docking studies of *n*-(3-hydroxy-4-methoxybenzyl)nonanamide also appeared to lack favorable interactions, with the vanilloid ring primarily interacting also with Y511. Docking of *n*-(4-hydroxybenzyl)nonanamide showed two conformational clusters which were highly

populated. The lowest energy cluster at -8.5 kcal/mole was associated with a conformation in which the analogue was aligned between transmembrane domains 3 and 4 but did not form hydrogen bonds with W549 or Y511. The most highly populated cluster at -7.5 kcal/mole showed the analogue backed into the binding site, but did not form any predicted hydrogen bonds, in agreement with the results showing minimal potency for this analogue.

Previous studies determined EC_{50} values for nonivamide in BEAS-2B, TRPV1-OE, and NHBE cells, providing a positive control for TRPV1 activation in these experiments (*15*). In our model, nonivamide provides results identical to those seen with the prototypical TRPV1 agonist, capsaicin. Based on this, we expected to nonivamide to have high relative potency in comparison to the other analogues in terms of calcium flux, GADD153 induction and cytotoxicity. As expected, nonivamide induced significant calcium flux in TRPV1-OE cells, and significantly increased GADD153 expression in all three cell types indicative of ER stress. Nonivamide also caused significant cell death in a dose-dependent manner, which is consistent with prior studies. (*15, 19*)

The benefit of working with TRPV1-OE cells is that TRPV1-mediated effects are magnified in these cells. This facilitated comparisons with the other cell types, characterizing the responses as meaningful and TRPV1-mediated. If results were inconsistent between TRPV1-OE and other cell types, we focused on TRPV1-independent mechanisms. For example, if an analogue was highly toxic in BEAS-2B and/or NHBE cells, but was relatively nontoxic in TRPV1-OE cells, the toxicity of that analogue was not likely predominately TRPV1-mediated. To illustrate, the 3-methoxy-4-(nonamidomethyl)phenyl sulfate analogue was prepared in hopes that it would not be cell

permeable and would not cause significant TRPV1-mediated cell death. However, this compound was equally toxic in all three cell types, with similar LC_{50} values of about 60-90 μM. Based on the similarities in cytotoxicity across cell types and inconsistent results in other markers (i.e., calcium flux, GADD153 induction) of TRPV1 activation, these results indicate 3-methoxy-4-(nonamidomethyl)phenyl sulfate toxicity was TRPV1-independent. The results for *n*-(3-methoxybenzyl)nonanamide and *n*-(4-hydroxybenzyl)nonanamide in Table 3.3 show a similar trend, suggesting they too are cytotoxic by alternative mechanisms.

The capsaicinoid variant that produced significant cytotoxicity was *n*-(3,4-dihydroxybenzyl)nonanamide. Similar to nonivamide, *n*-(3,4-dihydroxybenzyl)nonanamide induced significant calcium flux and, induced GADD153 in all three cell types when treated at concentrations above its LC_{50}, and caused cell death. The relative EC_{50} values of *n*-(3,4-dihydroxybenzyl)nonanamide and nonivamide in calcium flux experiments was ~10 μM as compared to ~2 μM indicating that nonivamide was ~5x more potent in eliciting calcium flux. In TRPV1-OE and NHBE cells, the LC_{50} for *n*-(3,4-dihydroxybenzyl)nonanamide was close to that for nonivamide itself. Interestingly, in BEAS-2B cells, *n*-(3,4-dihydroxybenzyl)nonanamide was ~6 times more toxic than nonivamide, indicating that *n*-(3,4-dihydroxybenzyl)nonanamide toxicity was not completely TRPV1-mediated. This conclusion was supported by results showing that the TRPV1 antagonist LJO-328 did not attenuate calcium flux or GADD153 induction (data not shown) or cell killing due to the *n*-(3,4-dihydroxybenzyl)nonanamide (Figure 3.8). We have yet to determine the specific nature through which this analogue, which is also a CYP450 -derived metabolite (i.e.,

CYP1A2 and 2C19) of capsaicin, is toxic to cells, but data showing an attenuation of toxicity by *n*-acetylcysteine (Figure 3.9) suggest it involves redox cycling and oxidative stress which may also contribute to GADD153 induction via the Nrf2/Keap1 pathway (*27*).

Two analogues were essentially nonfunctional in these assays. *N*-benzylnonanamide may function as a weak TRPV1 antagonist by virtue of its ability to potentially compete for Y511, but it did not activate TRPV1. *N*-(3,4-dimethoxybenzyl)nonanamide may be a good negative control for future studies when receptor blockade is not desired, but the remaining analogues may be weak agonists of TRPV1 and may prove useful in structure related metabolism studies of nonivamide, capsaicin and related compounds and the relevance of metabolism to alter responses to related channels.

In conclusion, all cell types showed statistically significant inverse correlations between cell viability and GADD153 induction, confirming the hypothesis that TRPV1 activation causes ER stress, leading to cell death. In all of the cell types used, there are additional cellular events that may modulate GADD153 expression and cell death, but the results herein confirm that GADD153 induction/ER stress after treatment with various capsaicinoid analogues is TRPV1-mediated.

Collectively, a more thorough understanding of capsaicinoid-TRPV1 structure activity relationships was achieved and the results more clearly define how TRPV1 functions in lung cells, how capsaicinoid variants and metabolites alter cellular function. The conclusions of this study support our previously proposed model of TRPV1-

mediated cell death in lung cells, which should help elucidate mechanisms of capsaicinoid action and TRPV1 function in many other cell types of diverse origin.

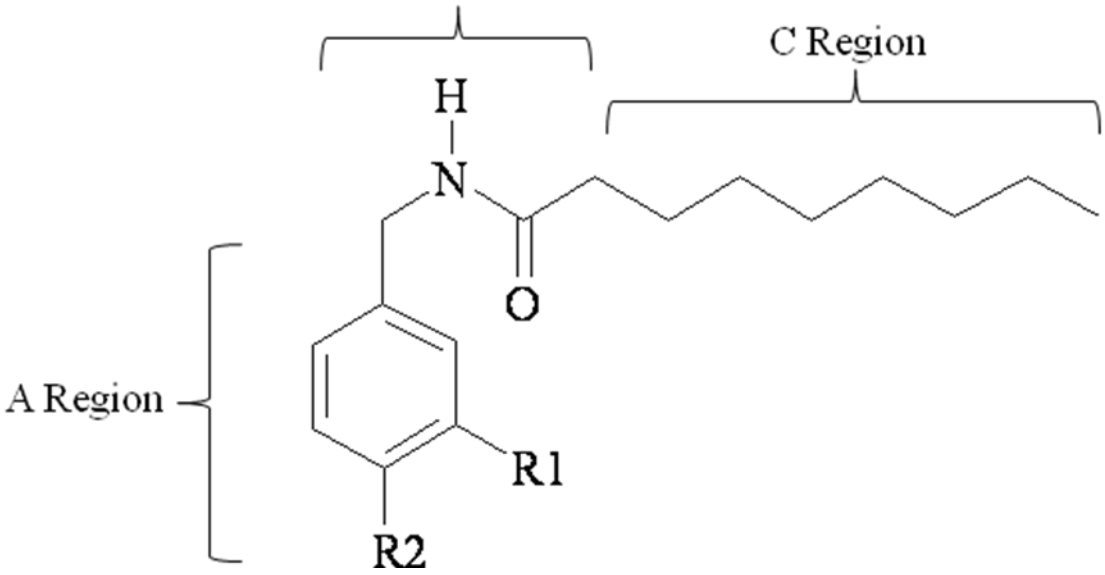

Analogue	Figure Abbreviation	Vanilloid Ring Moieties	
		R1 Group (3 Position)	R2 Group (4 Position)
n-(3-methoxy-4-hydroxybenzyl)nonanamide	Nonivamide	OCH_3	OH
n-benzylnonanamide	N-benzyl	H	H
n-(3-methoxybenzyl)nonanamide	3-MEOH	OCH_3	H
n-(3,4-dimethoxybenzyl)nonanamide	3-MEOH, 4-MEOH	OCH_3	OCH_3
n-(3-hydroxy-4-methoxybenzyl)nonanamide	3-OH, 4-MEOH	OH	OCH_3
n-(3,4-dihydroxybenzyl)nonanamide	3-OH, 4-OH	OH	OH
3-methoxy-4-(nonamidomethyl)phenyl sulfate	SO_4	OCH_3	SO_4
n-(4-trifluoromethylbenzyl)nonanamide	CF_3	H	CF_3
n-(4-hydroxybenzyl)nonanamide	4-OH	H	OH

Figure 3.1. Structures of capsaicinoid analogues.

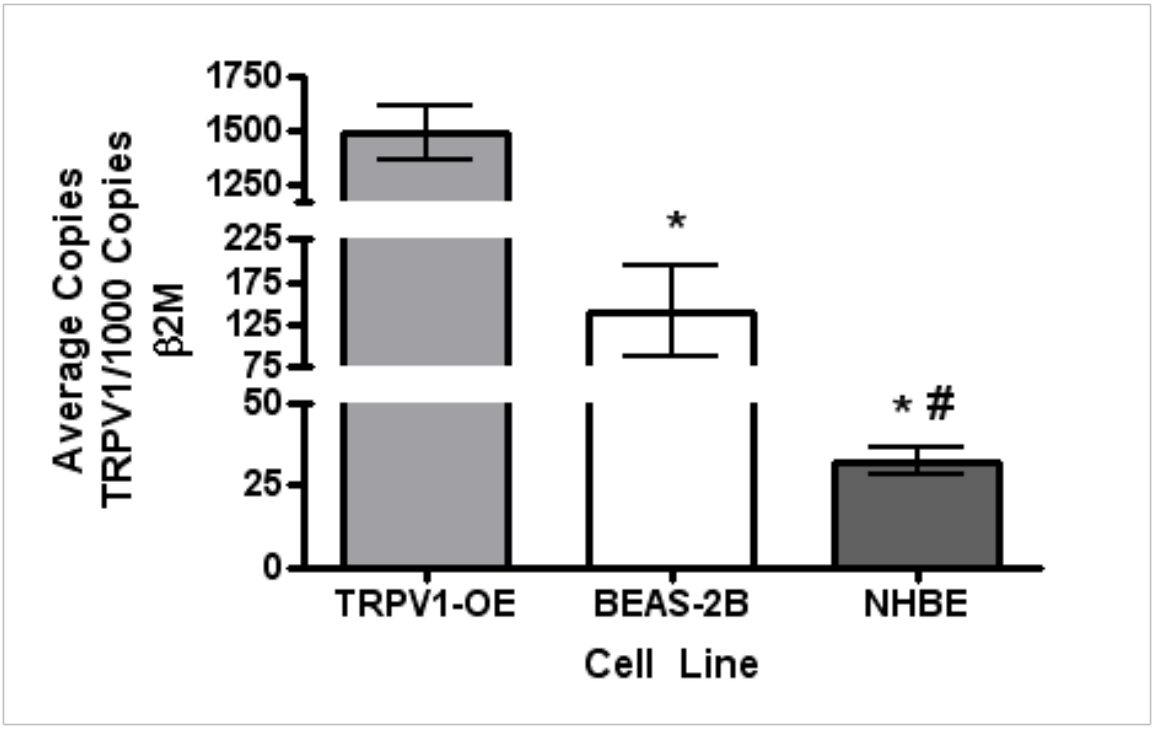

Figure 3.2. Quantification of TRPV1 mRNA in different lung cell types. Copies of TRPV1 were normalized to copies of β2M, a housekeeping gene. Data are represented as average copies TRPV1/1,000 copies β2M with error bars indicating ± standard error of the mean. *, $p<0.0001$ compared to TRPV1-OE, #, $p=0.044$ compared to BEAS-2B, unpaired *t* test. N=3.

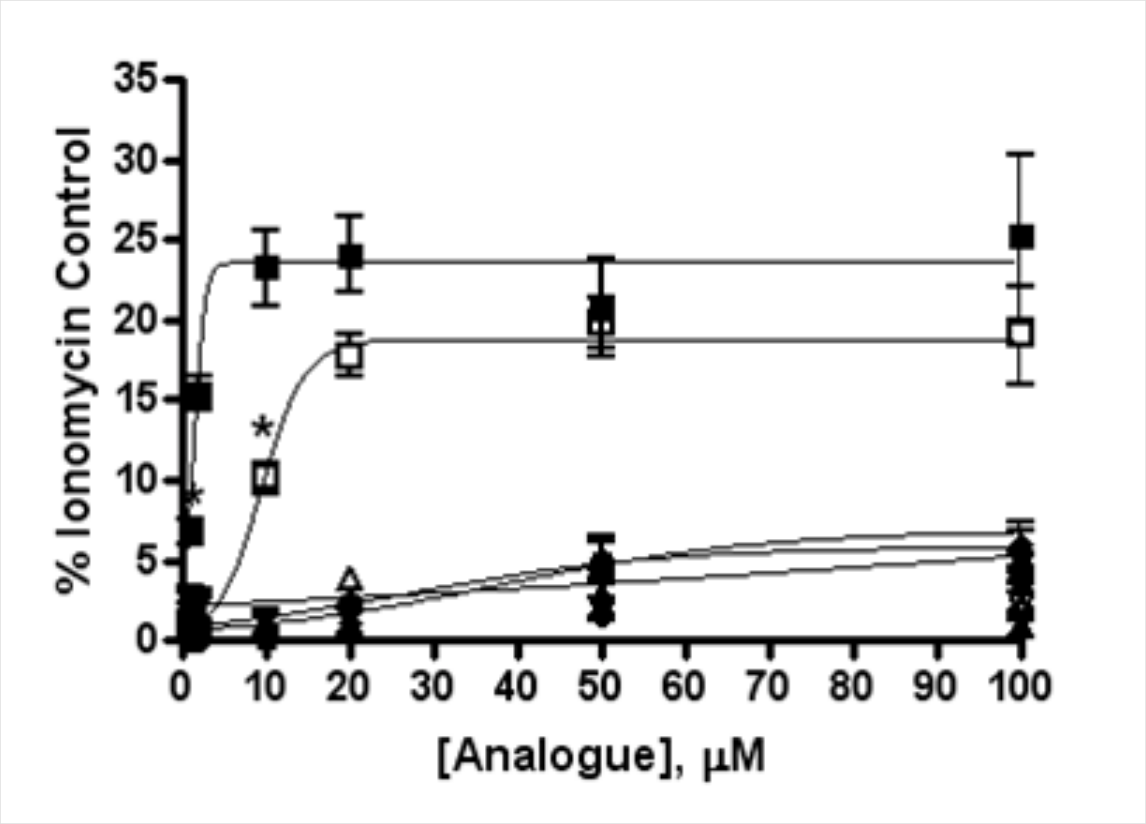

Figure 3.3. Calcium flux dose-response in TRPV1-OE cells after treatment with capsaicinoid analogues. Calcium flux was measured on a NOVOStar plate reader as described in *Methods*. Filled squares: nonivamide, open squares: *n*-(3,4-dihydroxybenzyl)nonanamide, filled circles: *n*-(3-hydroxy-4-methoxybenzyl)nonanamide, open triangles: 3-methoxy-4-(nonamidomethyl)phenyl sulfate, filled triangles indicate *n*-benzylnonanamide, inverted filled triangles: *n*-(3-methoxybenzyl)nonanamide, filled diamonds: *n*-(3,4-dimethoxybenzyl)nonanamide, open inverted triangles: *n*-(4-trifluoromethylbenzyl)nonanamide, and open diamonds: *n*-(4-hydroxybenzyl)nonanamide. * indicates lowest concentration of analogue causing statistically significant calcium flux, $p<0.05$ by one-way ANOVA. Data are represented as % ionomycin fluorescence ± standard error of the mean. N=3.

Figure 3.4. Molecular modeling. Representative molecular modeling images of (a) nonivamide, (b) *n*-benzylnonanamide, (c) *n*-(3-hydroxy-4-methoxybenzyl)nonanamide, and for *n*-(4-hydroxybenzyl)nonanamide (d) lowest energy cluster (-8.5 kcal/mole) and (e) most highly populated cluster (-7.5 kcal/mole). Analogues were docked between transmembrane domains 3 and 4 of TRPV1. Potential hydrogen bonding interactions were determined by the software, and inter-atom distances are indicated with angstrom distances between the residues and atoms.

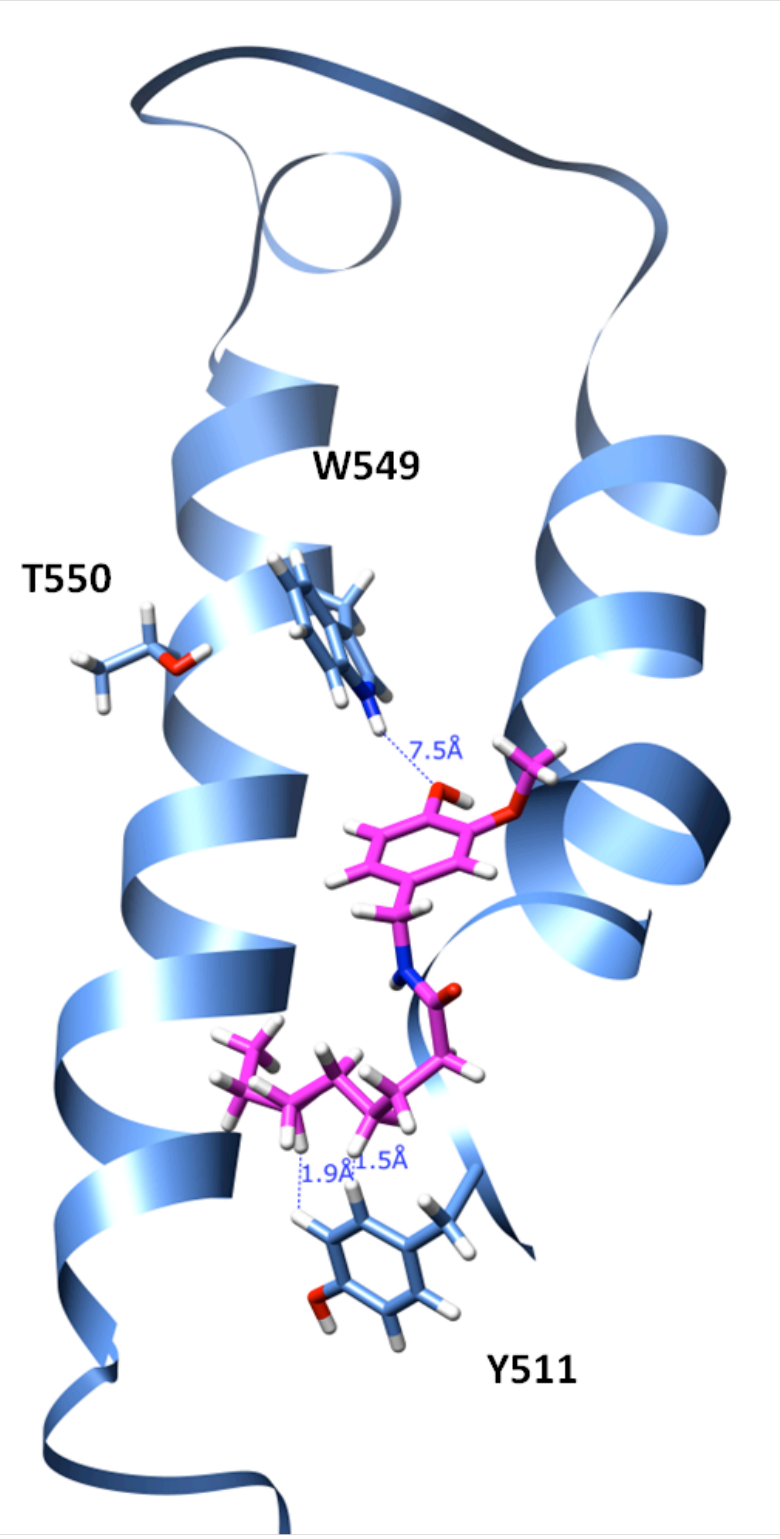

Figure 3.4.a.

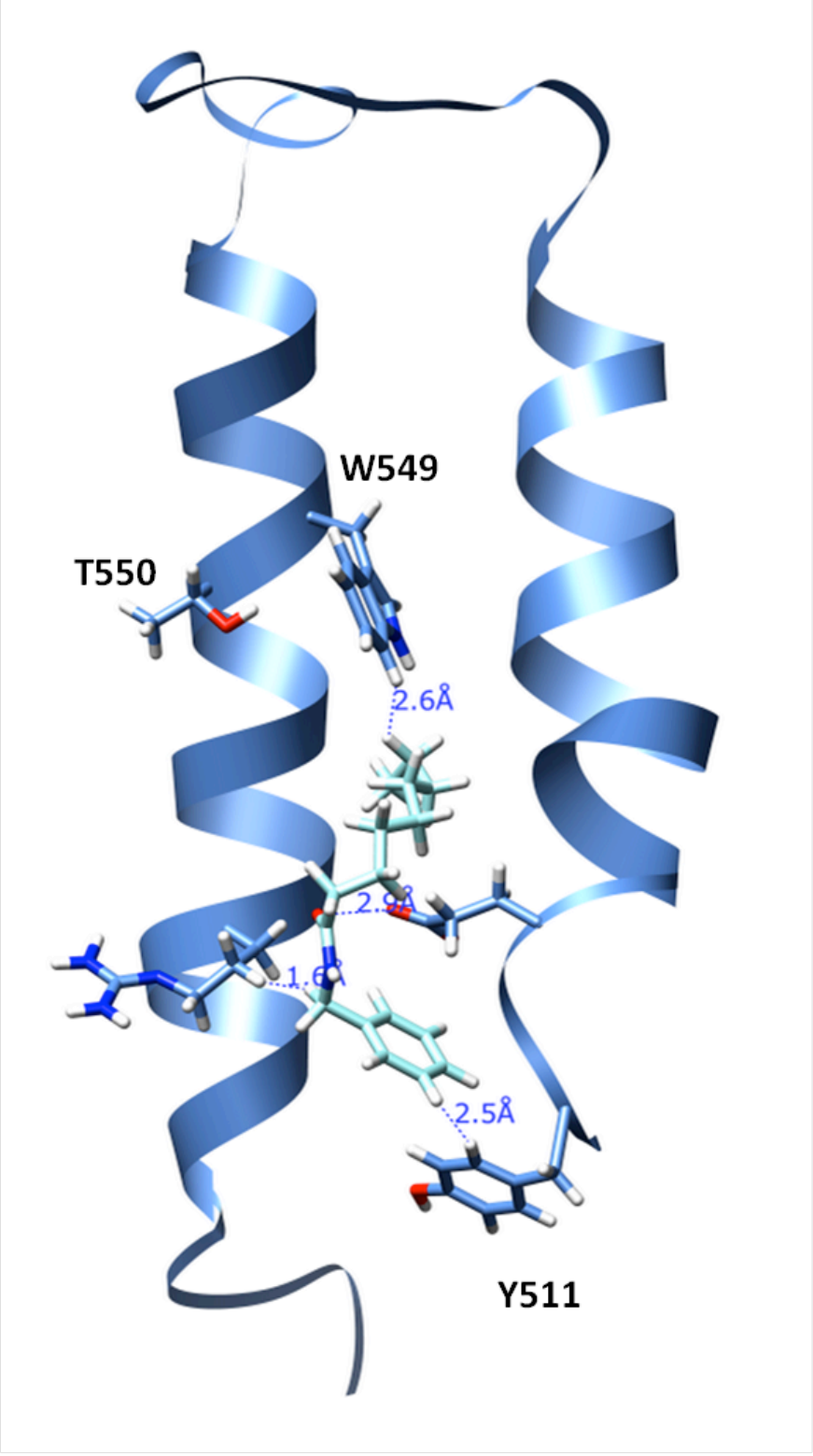

Figure 3.4.b.

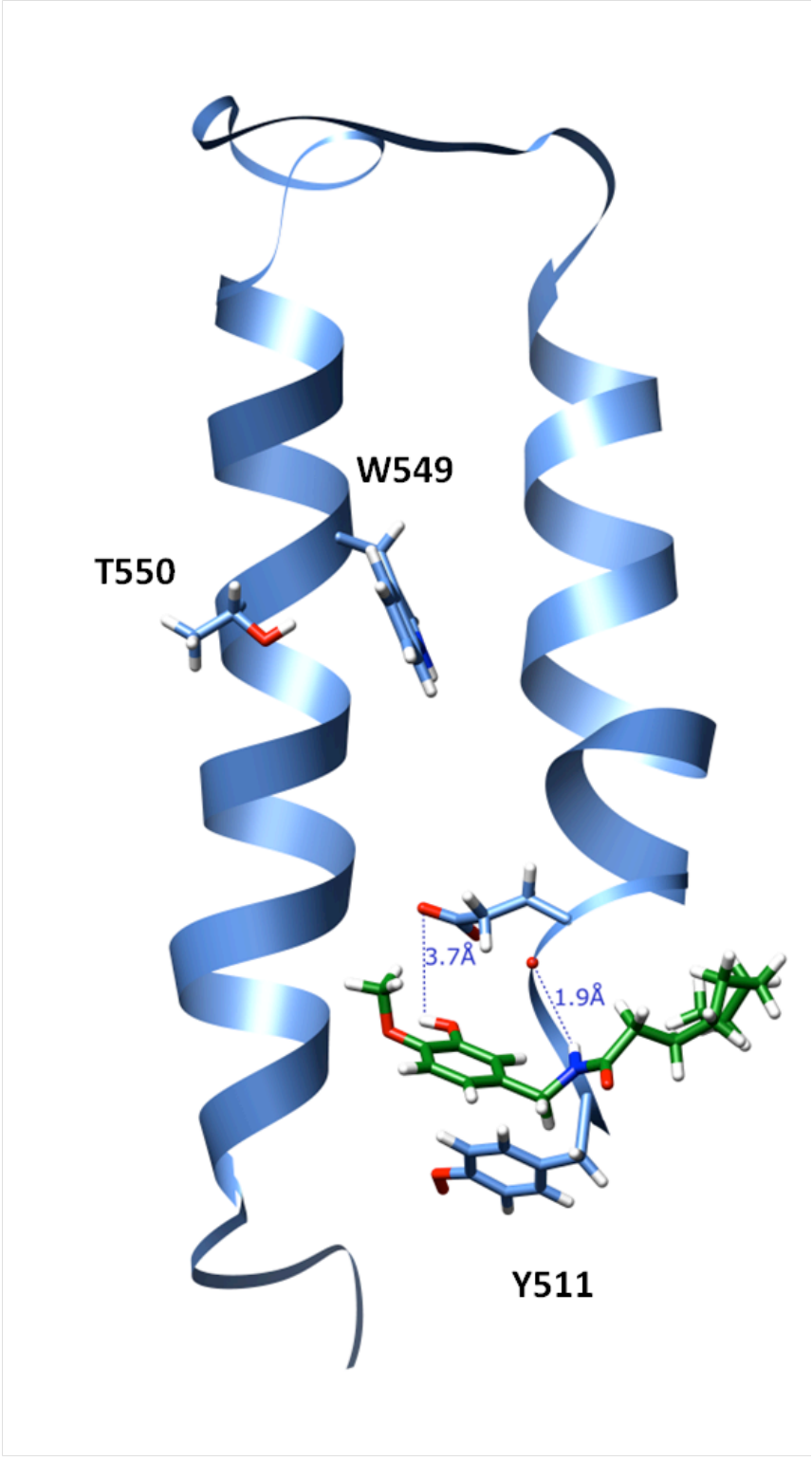

Figure 3.4.c.

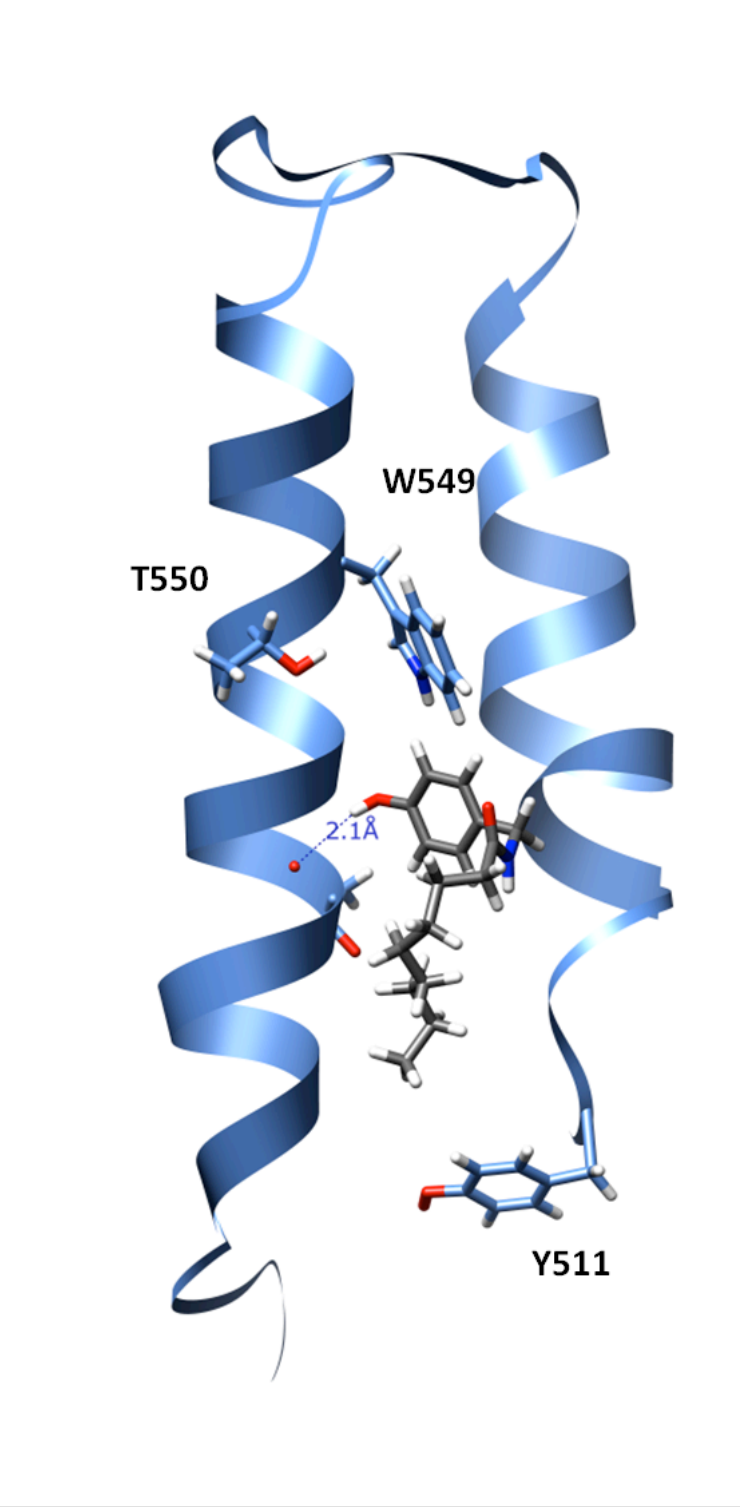

Figure 3.4.d.

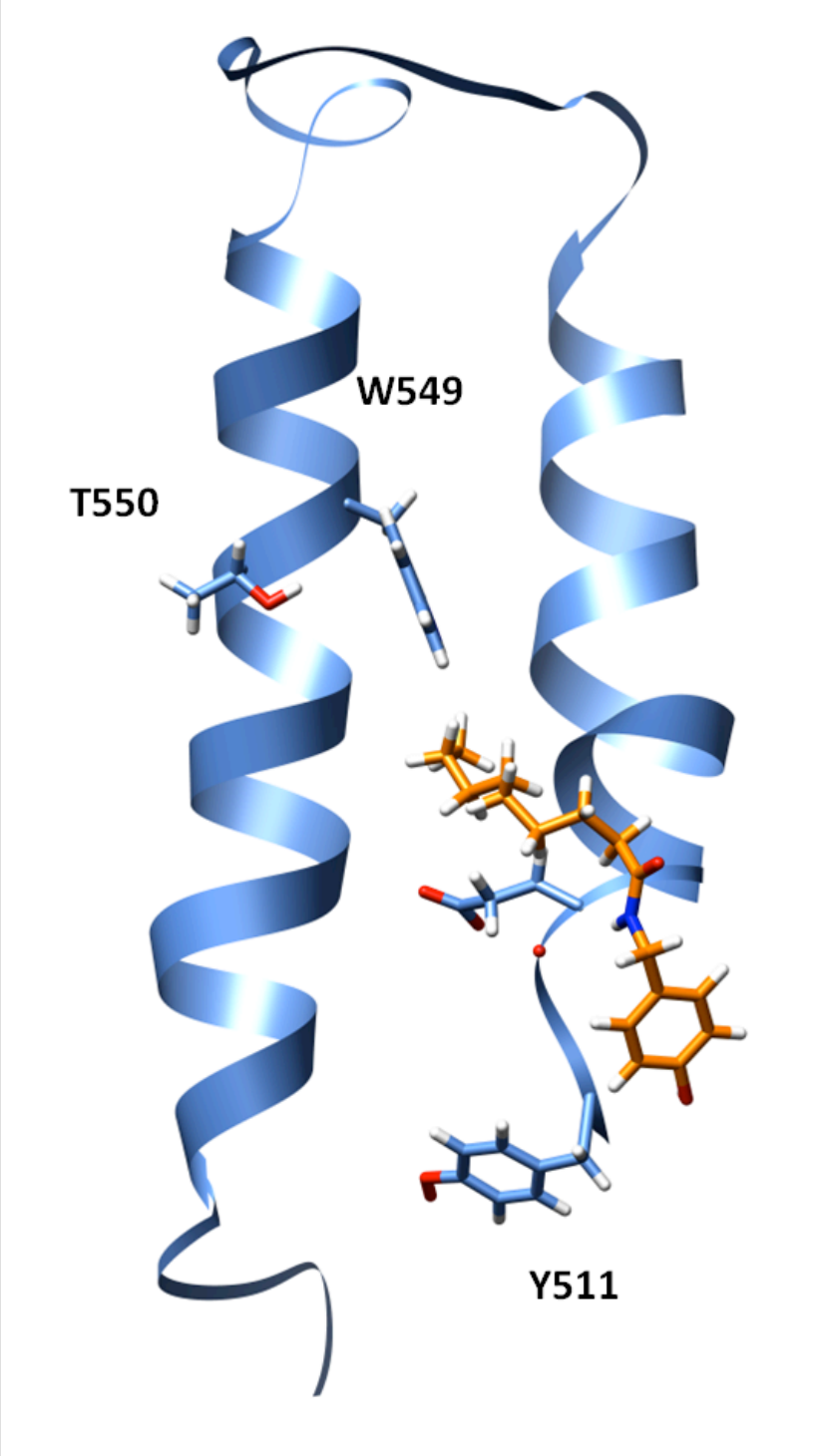

Figure 3.4.e.

Figure 3.5. Inverse correlation of cell viability and GADD153 induction. Cell viability was assayed after 24-hour treatment as described in *Methods*. GADD153 induction was measured using quantitative PCR after 4-hour treatment. TRPV1-OE cell viability after treatment with 2.5 μM, 25 μM, and 100 μM analogue was compared to GADD153 induction after treatment with 2 μM, 20 μM, and 100 μM analogue respectively (panels a, b and c). (d) BEAS-2B cell viability after 200 μM analogue treatment compared to GADD153 induction after treatment with 200 μM analogue. (e) NHBE cell viability after 200 μM analogue treatment compared to GADD153 induction after treatment with 200 μM analogue. For all cell types, statistical analysis to determine significant inverse correlation is represented by the Pearson correlation value 'r' and is presented in the Figure panel.

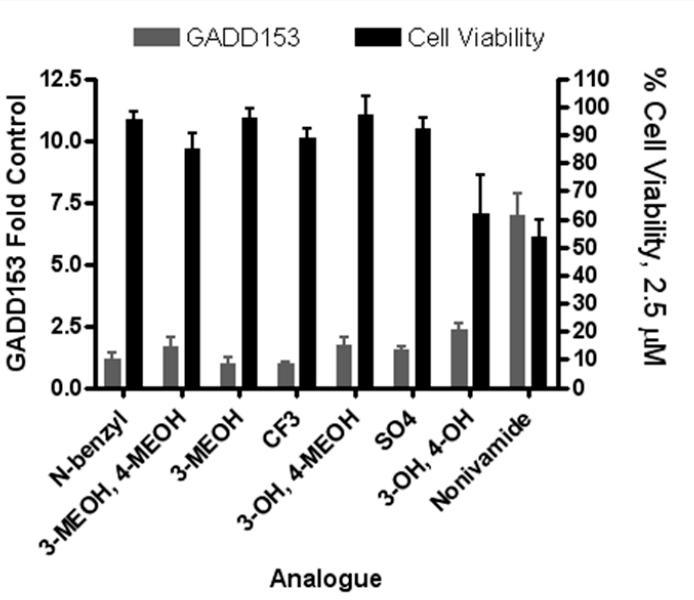

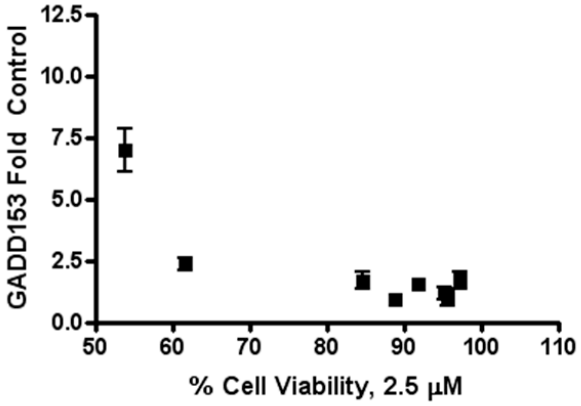

Parameter	GADD153
Number of XY Pairs	8
Pearson r	-0.8254
95% confidence interval	-0.9674 to -0.2884
P value (two-tailed)	0.0116
P value summary	*
Is the correlation significant? (alpha=0.05)	Yes
R squared	0.6813

Figure 3.5.a.

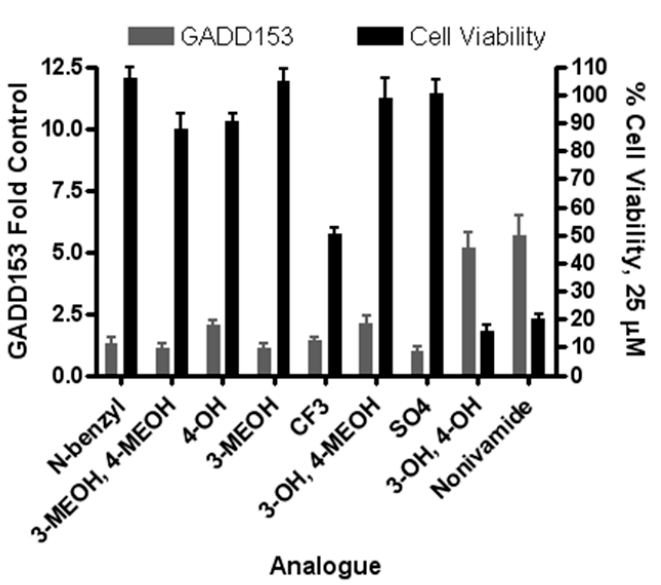

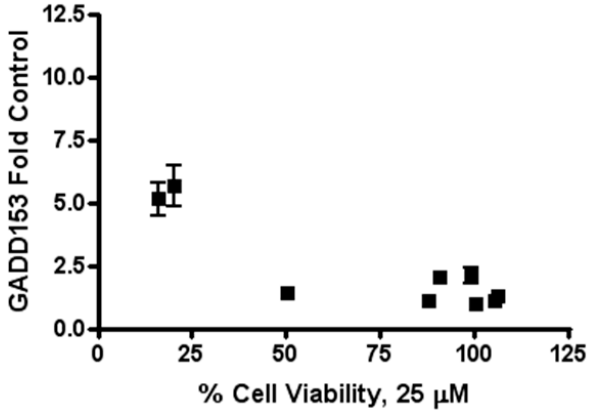

Parameter	GADD153
Number of XY Pairs	9
Pearson r	-0.8703
95% confidence interval	-0.9724 to -0.4884
P value (two-tailed)	0.0023
P value summary	**
Is the correlation significant? (alpha=0.05)	Yes
R squared	0.7574

Figure 3.5.b.

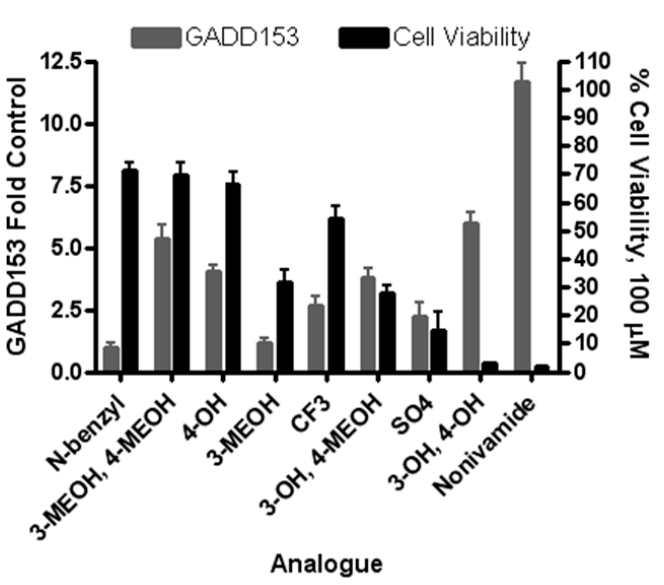

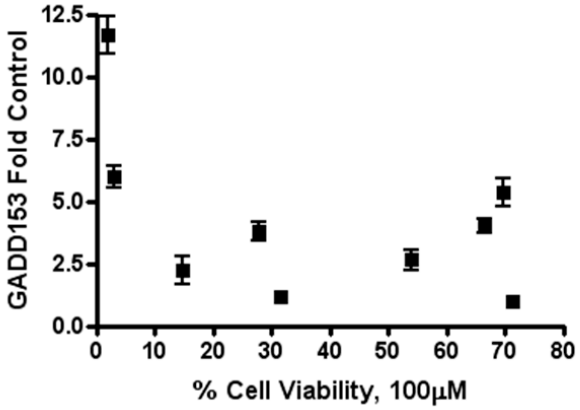

Parameter	GADD153
Number of XY Pairs	9
Pearson r	-0.4868
95% confidence interval	-0.8698 to 0.2622
P value (two-tailed)	0.1839
P value summary	ns
Is the correlation significant? (alpha=0.05)	No
R squared	0.2370

Figure 3.5.c.

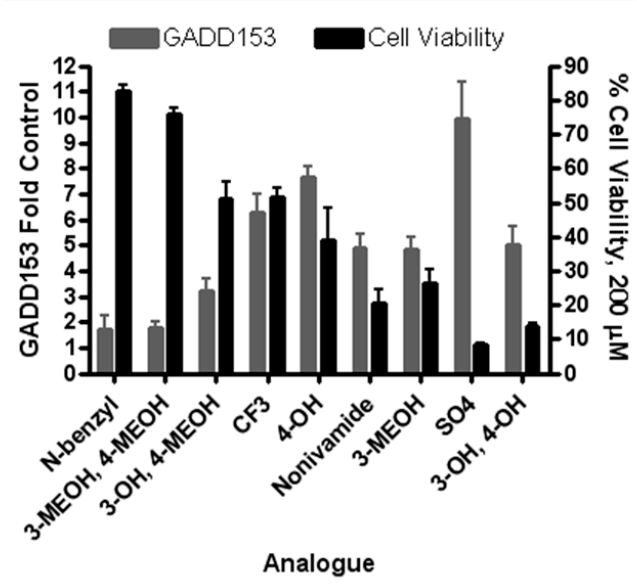

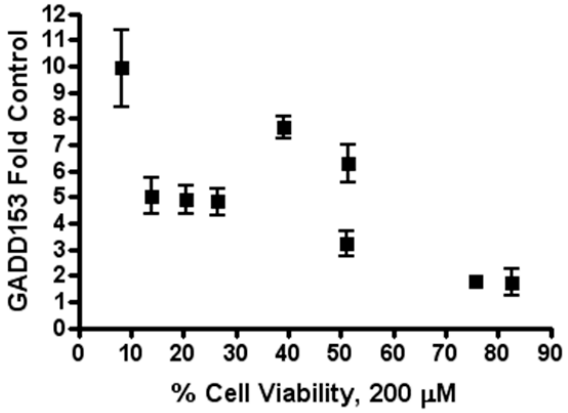

Parameter	GADD153
Number of XY Pairs	9
Pearson r	-0.7342
95% confidence interval	-0.9400 to -0.1366
P value (two-tailed)	0.0243
P value summary	*
Is the correlation significant? (alpha=0.05)	Yes
R squared	0.5391

Figure 3.5.d.

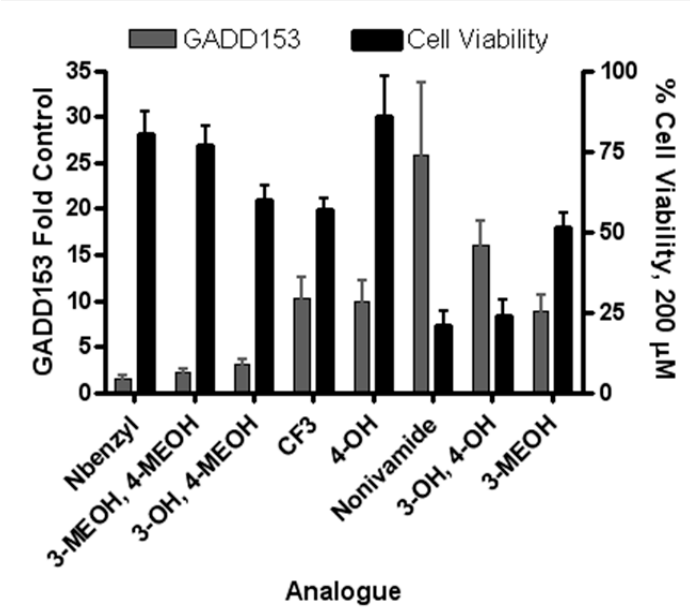

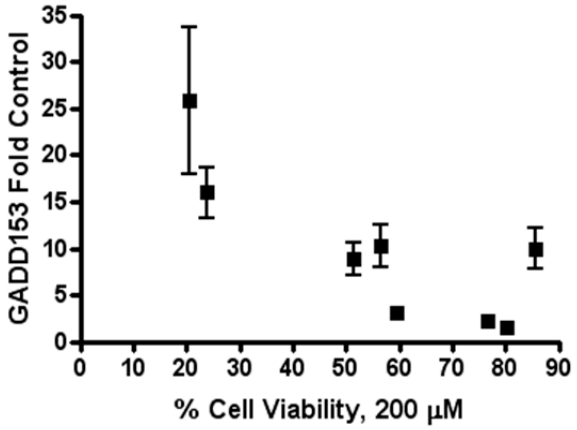

Parameter	GADD153
Number of XY Pairs	8
Pearson r	-0.8119
95% confidence interval	-0.9647 to -0.2505
P value (two-tailed)	0.0144
P value summary	*
Is the correlation significant? (alpha=0.05)	Yes
R squared	0.6592

Figure 3.5.e.

Figure 3.6. Inverse correlation of cell viability and calcium flux in TRPV1-OE cells. Cell viability was assayed after 24-hour treatment as described in *Methods*. Calcium flux was measured using a NOVOstar plate reader as described in *Methods*. TRPV1-OE cell viability after 2.5 μM, 25 μM, and 100 μM analogue treatment was compared to maximum calcium flux after 2 μM, 20 μM, and 100 μM analogue treatment, respectively (panels a, b and c). Statistical analysis to determine significant inverse correlation is represented by the Pearson correlation value 'r' and is presented in the figure.

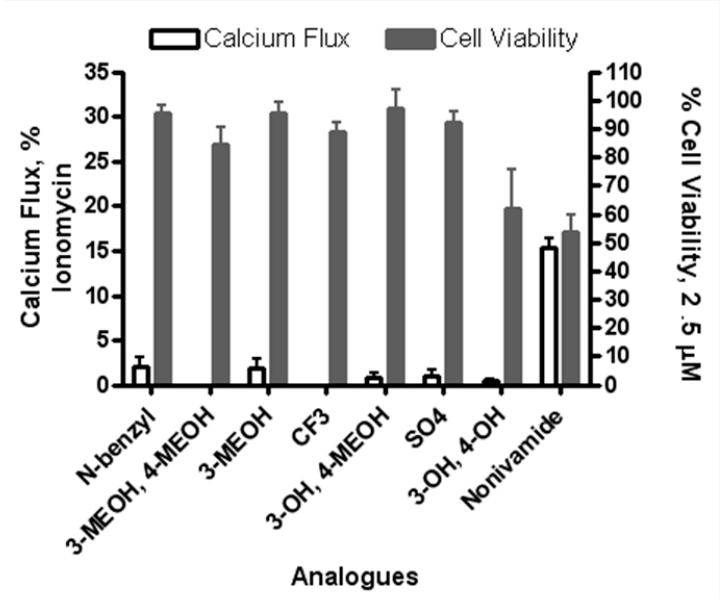

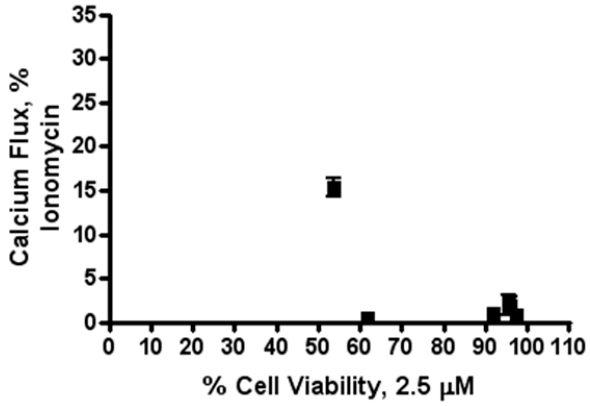

Number of XY Pairs	8
Pearson r	-0.6682
95% confidence interval	-0.9334 to 0.06921
P value (two-tailed)	0.0701
P value summary	ns
Is the correlation significant? (alpha=0.05)	No
R squared	0.4464

Figure 3.6.a.

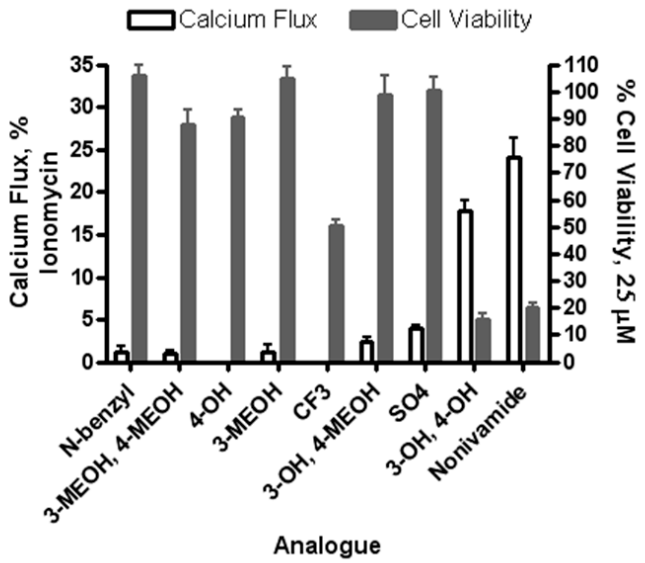

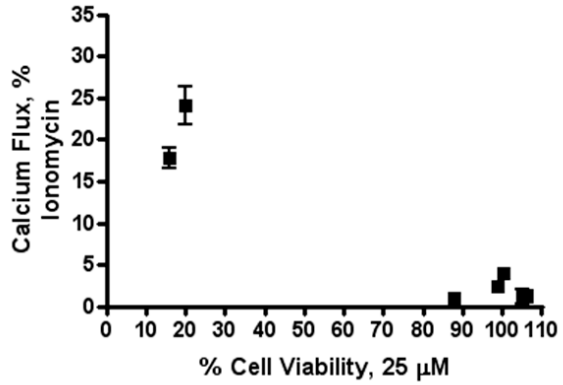

Parameter	Calcium Flux
Number of XY Pairs	9
Pearson r	-0.8248
95% confidence interval	-0.9620 to -0.3551
P value (two-tailed)	0.0062
P value summary	**
Is the correlation significant? (alpha=0.05)	Yes
R squared	0.6803

Figure 3.6.b.

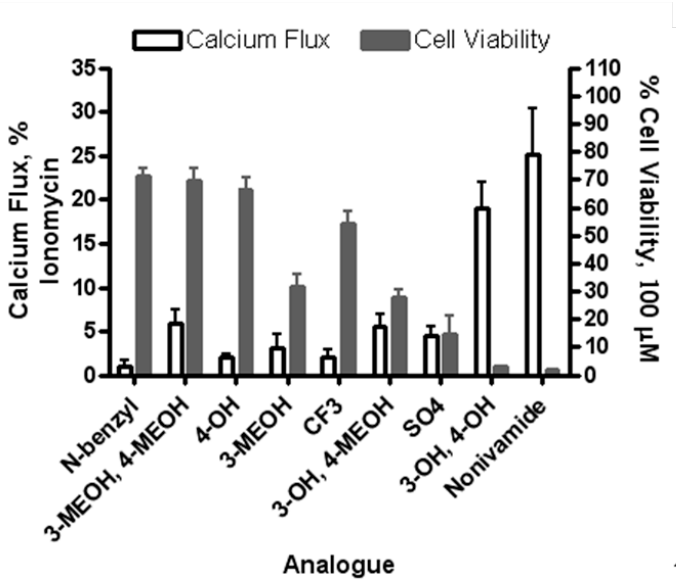

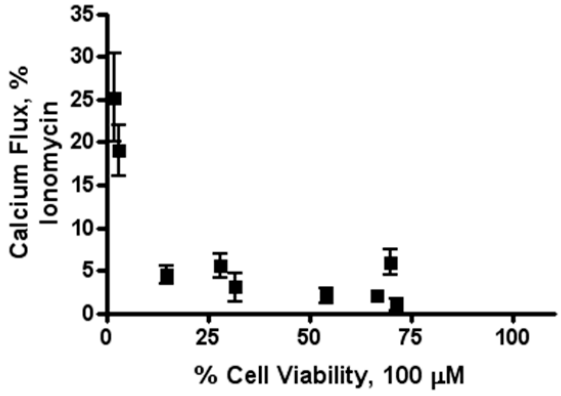

Parameter	Calcium Flux
Number of XY Pairs	9
Pearson r	-0.7416
95% confidence interval	-0.9419 to -0.1525
P value (two-tailed)	0.0222
P value summary	*
Is the correlation significant? (alpha=0.05)	Yes
R squared	0.5500

Figure 3.6.c.

Figure 3.7. Correlation of calcium flux and GADD153 induction in TRPV1-OE cells. Calcium flux was measured using a NOVOstar plate reader as described in *Methods*. GADD153 induction was measured using quantitative PCR after 4-hour treatment. TRPV1-OE maximum calcium flux and GADD153 induction were compared after 2 μM, 20 μM and 100 μM analogue treatment (panels a, b and c). Statistical analysis to determine significant correlation is represented by the Pearson correlation value 'r' and is presented in the figure.

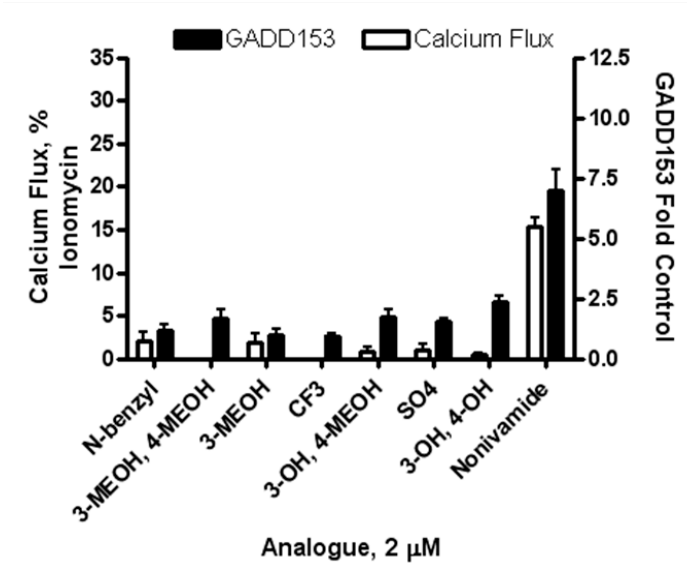

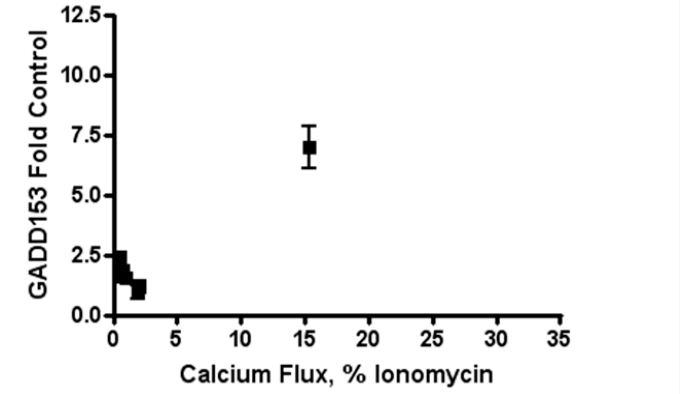

Number of XY Pairs	8
Pearson r	0.9501
95% confidence interval	0.7425 to 0.9912
P value (two-tailed)	0.0003
P value summary	***
Is the correlation significant? (alpha=0.05)	Yes
R squared	0.9027

Figure 3.7.a.

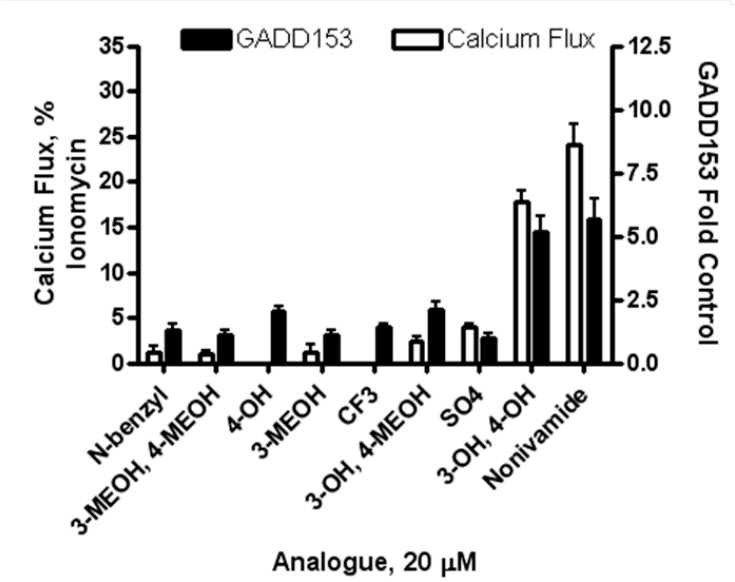

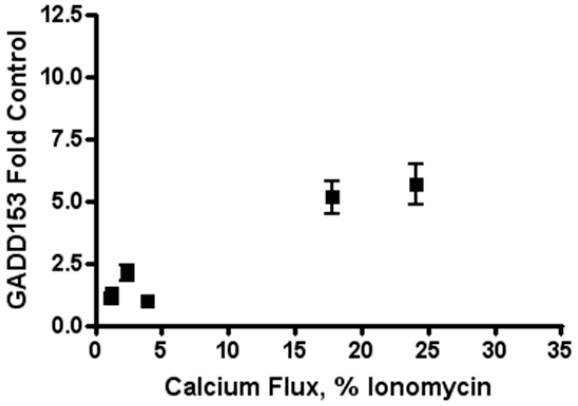

Parameter	GADD153
Number of XY Pairs	9
Pearson r	0.9498
95% confidence interval	0.7735 to 0.9897
P value (two-tailed)	P<0.0001
P value summary	***
Is the correlation significant? (alpha=0.05)	Yes
R squared	0.9020

Figure 3.7.b.

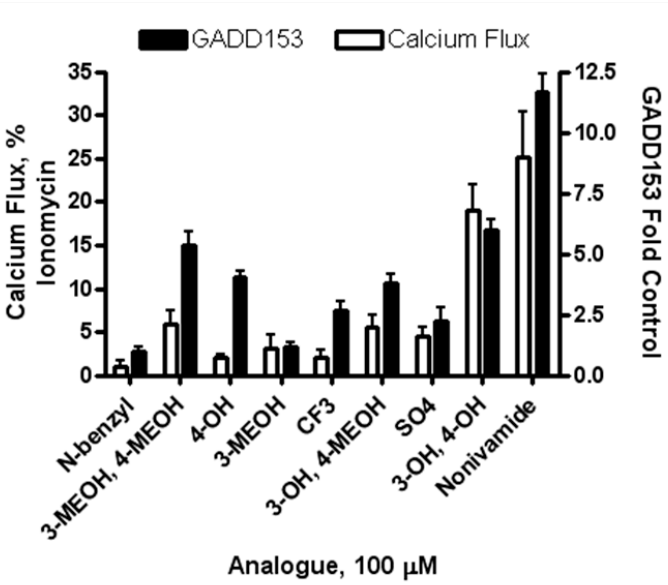

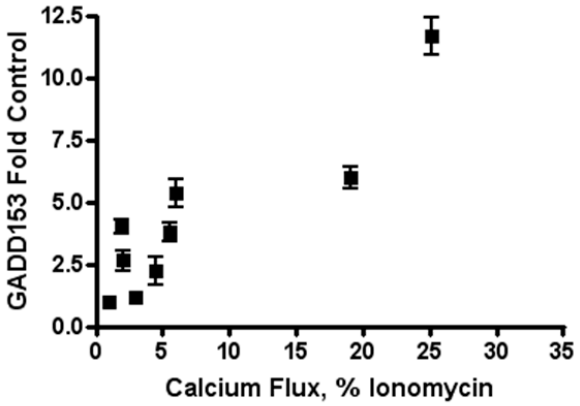

Parameter	GADD153
Number of XY Pairs	9
Pearson r	0.8978
95% confidence interval	0.5787 to 0.9785
P value (two-tailed)	0.0010
P value summary	**
Is the correlation significant? (alpha=0.05)	Yes
R squared	0.8061

Figure 3.7.c.

Figure 3.8. Treatment of TRPV1-OE cells with LJO-328 and NAC to modulate *n*-(3,4-dihydroxybenzyl)nonanamide induced toxicity. Cell viability was assayed after 24-hour treatment as described in *Methods*. (a) TRPV1-OE cell viability dose-response after treatment with LJO-328 (open triangles), nonivamide (filled squares), *n*-(3,4-dihydroxybenzyl)nonanamide (filled circles) alone, LJO-328 with nonivamide (open squares), LJO-328 with *n*-(3,4-dihydroxybenzyl)nonanamide (open circles). (b) TRPV1-OE and BEAS-2B cells treated with *n*-(3,4-dihydroxybenzyl)nonanamide (10 and 25 μM, respectively), alone or in the presence of NAC (2.5 mM). * indicates statistically significantly different ($p<0.05$) from treatment with *n*-(3,4-dihydroxybenzyl)nonanamide alone, # indicates statistically significant ($p<0.05$) from treatment with NAC alone as determined using one-way ANOVA. Data are represented as mean cell viability % of untreated control ± standard error of the mean, N=3.

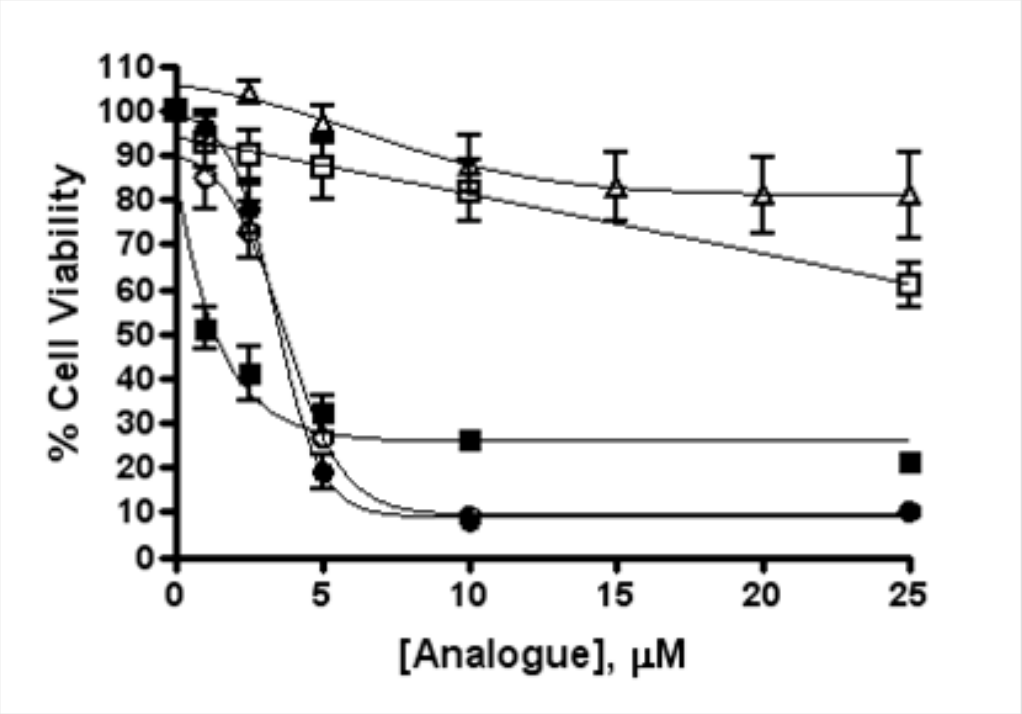

Figure 3.8.a.

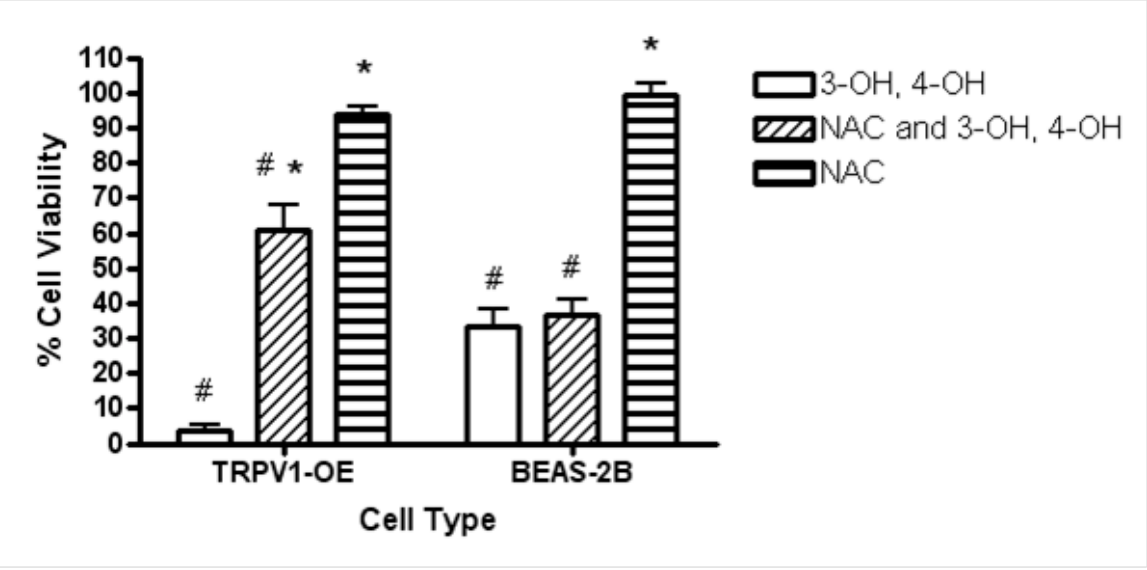

Figure 3.8.b.

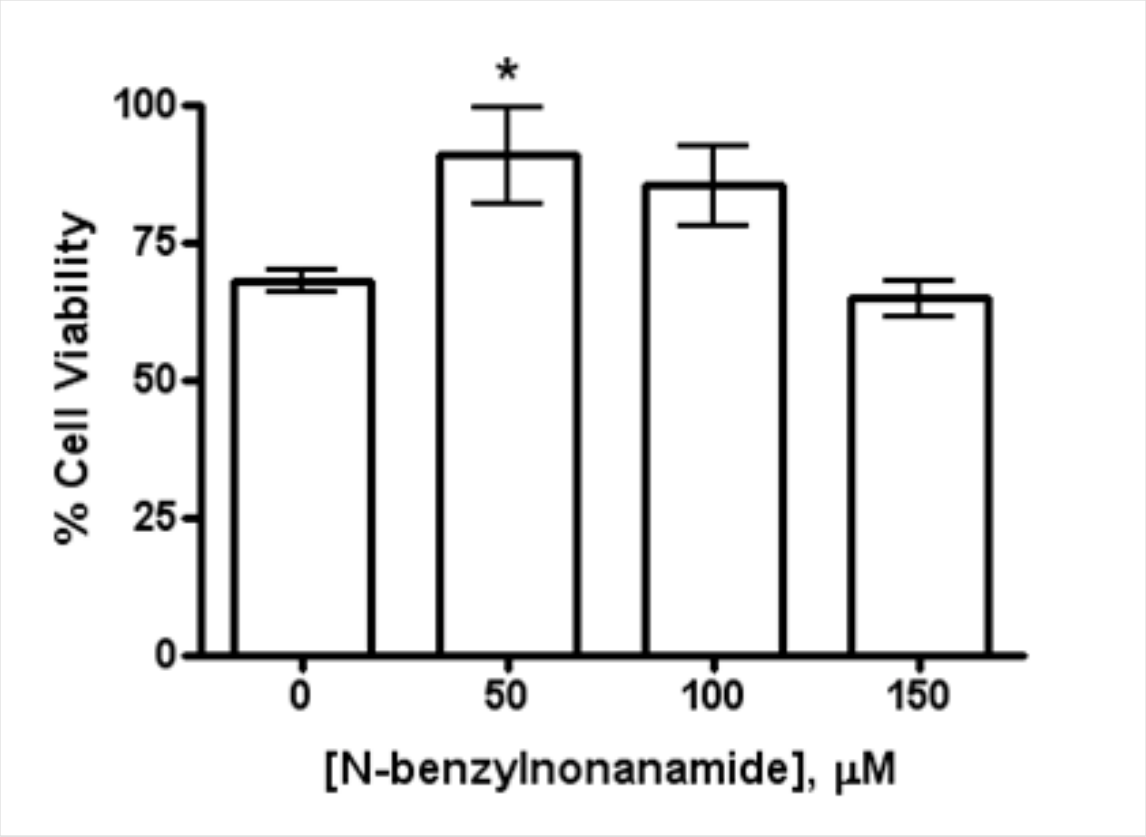

Figure 3.9. Evaluation of antagonist activity of *n*-benzylnonanamide. Comparison of cell viability at 1.5 μM nonivamide alone (0 μM n-benzylnonanamide), or cells treated with both compounds. One-way ANOVA was used to determine stastical significance between the groups with Dunnett's multiple comparison test post-hoc testing. *$p < 0.01$ compared to nonivamide alone. Data are represented as average % cell viability as compared to

Table 3.1
Calcium Flux in TRPV1-OE Cells in Response to Various Capsaicinoid Agonists at 2, 20 and 100 μM.

Analogue	Calcium Flux, % Ionomycin ± S.D.		
	2 μM	20 μM	100 μM
Nonivamide	15.4 ± 3.2 *	34.1 ± 6.9 *	25.2 ± 15.5 *
n-benzylnonanamide	2.0 ± 3.5	1.2 ± 2.3	1.0 ± 2.2
n-(3-methoxybenzyl)nonanamide	1.9 ± 2.8	1.2 ± 2.6	3.0 ± 4.8
n-(3,4-dimethoxybenzyl)nonanamide	-0.1 ± 0.4	1.1 ± 1.0	6.0 ± 4.3
n-(3-hydroxy-4-methoxybenzyl)nonanamide	0.8 ± 1.6	2.4 ± 1.7	5.5 ± 4.1
n-(3,4-dihydroxybenzyl)nonanamide	0.5 ± 0.6	17.8 ± 3.8 *	19.0 ± 5.2 *
3-methoxy-4-(nonamidomethyl)phenyl sulfate	1.0 ± 2.0	3.9 ± 1.2	4.5 ± 3.1
n-(4-trifluoromethylbenzyl)nonanamide	-0.4 ± 0.5	-0.1 ± 1.0	2.1 ± 2.6
n-(4-hydroxybenzyl)nonanamide	0.1 ± 0.6	-0.3 ± 0.6	2.0 ± 1.3

Calcium flux was assayed using a NOVOstar plate reader as described in *Methods*. Maximal baseline responses were subtracted from the maximal response after treatments were added. Data are shown as calcium flux for each of 3 concentrations in TRPV1-OE cells. Data are represented as % ionomycin calcium flux ± standard deviation.

Table 3.2

LC_{50} Values in Various Cell Types after Treatment with Capsaicinoid Analogues

Analogue	μM LC_{50} (95% CI)		
	TRPV1-OE	BEAS-2B	NHBE
Nonivamide	1.0 (0.7-1.4)	114.6 (103.5-127.1)	160.0 (156.0-164.4)
n-benzylnonanamide	> 250	> 250	> 200
n-(3-methoxybenzyl)nonanamide	116.4 (102.3-132.7)	100.5 (95.3-106.2)	106.2 (6.1-170.6)
n-(3,4-dimethoxybenzyl)nonanamide	> 250	> 250	> 200
n-(3-hydroxy-4-methoxybenzyl)nonanamide	75.0 (62.1-90.8)	217.3 (164.8-285.8)	180.7 (120.8-270.4)
n-(3,4-dihydroxybenzyl)nonanamide	3.4 (2.6-4.3)	16.1 (13.6-19.2)	157.0 (121.3-203.2)
3-methoxy-4-(nonamidomethyl)phenyl sulfate	63.1 (46.7-85.5)	87.3 (84.1-90.8)	57.7 (45.5-72.9)
n-(4-trifluoromethylbenzyl)nonanamide	112.7 (84.5-150.0)	184.1 (144.9-233.9)	173.8 (108.9-277.3)
n-(4-hydroxybenzyl)nonanamide	147.9 (121.9-179.5)	163.7 (135.2-198.2)	165.2 (113.2-241.5)

Data are represented as the calculated EC_{50} for each analogue in each cell type ± 95% confidence interval.

Table 3.3

GADD153 Expression in Various Cell Types after Treatment with Capsaicinoid Analogues

Analogue	GADD153 Induction (Average Fold Control ± S.D.)				
	TRPV1-OE			BEAS-2B	NHBE
	2 μM	20 μM	100 μM	200 μM	200 μM
Nonivamide	7.0 ± 2.7 *	5.7 ± 2.5 *	11.7 ± 2.2 *	4.9 ± 1.5 *	25.8 ± 23.5 *
n-benzylnonanamide	1.2 ± 0.8	1.3 ± 0.7	1.0 ± 0.5	1.7 ± 1.5	1.6 ± 1.0
n-(3-methoxybenzyl)nonanamide	1.0 ± 0.9	1.1 ± 0.5	1.2 ± 0.6	4.8 ± 1.4 *	8.9 ± 5.2
n-(3,4-dimethoxybenzyl)nonanamide	1.7 ± 1.0	1.1 ± 0.5	5.4 ± 1.7 *	1.8 ± 0.6	2.2 ± 1.3
n-(3-hydroxy-4-methoxybenzyl)nonanamide	1.7 ± 1.0	2.1 ± 0.9	3.8 ± 1.1 *	3.2 ± 1.4	3.1 ± 1.6
n-(3,4-dihydroxybenzyl)nonanamide	2.3 ± 0.8	5.1 ± 2.0 *	6.0 ± 1.3 *	5.0 ±2.0 *	16.0 ± 8.2 *
3-methoxy-4-(nonamidomethyl)phenyl sulfate	1.5 ± 0.5	1.0 ± 0.5	2.2 ± 1.6	9.9 ± 4.4 *	8.9 ± 3.6
n-(4-trifluoromethylbenzyl)nonanamide	0.9 ± 0.4	1.4 ± 0.4	2.6 ± 1.2	6.3 ± 2.2 *	10.3 ± 6.8
n-(4-hydroxybenzyl)nonanamide	1.9 ± 0.4	2.0 ± 0.5	4.0 ± 0.8 *	7.6 ± 1.3 *	10.0 ± 6.6

Cells were treated with capsaicinoid analogues for 4 hours (previously determined to be the peak induction after nonivamide treatment). TRPV1-OE cells were treated at 2 μM, 20 μM and 100 μM, and NHBE and BEAS-2B cells were treated at 200 μM. Data are expressed as mean ± standard deviation.

3.6 References

1. Jia, Y., and Lee, L. Y. (2007) Role of TRPV receptors in respiratory diseases, *Biochim Biophys Acta 1772*, 915-927.

2. Szallasi, A., Cortright, D. N., Blum, C. A., and Eid, S. R. (2007) The vanilloid receptor TRPV1: 10 years from channel cloning to antagonist proof-of-concept, *Nat Rev Drug Discov 6*, 357-372.

3. Caterina, M. J., Schumacher, M. A., Tominaga, M., Rosen, T. A., Levine, J. D., and Julius, D. (1997) The capsaicin receptor: a heat-activated ion channel in the pain pathway, *Nature 389*, 816-824.

4. Tominaga, M., Caterina, M. J., Malmberg, A. B., Rosen, T. A., Gilbert, H., Skinner, K., Raumann, B. E., Basbaum, A. I., and Julius, D. (1998) The cloned capsaicin receptor integrates multiple pain-producing stimuli, *Neuron 21*, 531-543.

5. Walpole, C. S., Wrigglesworth, R., Bevan, S., Campbell, E. A., Dray, A., James, I. F., Masdin, K. J., Perkins, M. N., and Winter, J. (1993) Analogues of capsaicin with agonist activity as novel analgesic agents; structure-activity studies. 3. The hydrophobic side-chain "C-region", *J Med Chem 36*, 2381-2389.

6. Walpole, C. S., Wrigglesworth, R., Bevan, S., Campbell, E. A., Dray, A., James, I. F., Masdin, K. J., Perkins, M. N., and Winter, J. (1993) Analogues of capsaicin with agonist activity as novel analgesic agents; structure-activity studies. 2. The amide bond "B-region", *J Med Chem 36*, 2373-2380.

7. Walpole, C. S., Wrigglesworth, R., Bevan, S., Campbell, E. A., Dray, A., James, I. F., Perkins, M. N., Reid, D. J., and Winter, J. (1993) Analogues of capsaicin with agonist activity as novel analgesic agents; structure-activity studies. 1. The aromatic "A-region", *J Med Chem 36*, 2362-2372.

8. Walpole, C. S., Bevan, S., Bovermann, G., Boelsterli, J. J., Breckenridge, R., Davies, J. W., Hughes, G. A., James, I., Oberer, L., Winter, J., and et al. (1994) The discovery of capsazepine, the first competitive antagonist of the sensory neuron excitants capsaicin and resiniferatoxin, *J Med Chem 37*, 1942-1954.

9. Fernandez-Ballester, G., and Ferrer-Montiel, A. (2008) Molecular modeling of the full-length human TRPV1 channel in closed and desensitized states, *J Membr Biol 223*, 161-172.

10. Gavva, N. R., Klionsky, L., Qu, Y., Shi, L., Tamir, R., Edenson, S., Zhang, T. J., Viswanadhan, V. N., Toth, A., Pearce, L. V., Vanderah, T. W., Porreca, F., Blumberg, P. M., Lile, J., Sun, Y., Wild, K., Louis, J. C., and Treanor, J. J. (2004)

Molecular determinants of vanilloid sensitivity in TRPV1, *J Biol Chem 279*, 20283-20295.

11. Johnson, D. M., Garrett, E. M., Rutter, R., Bonnert, T. P., Gao, Y. D., Middleton, R. E., and Sutton, K. G. (2006) Functional mapping of the transient receptor potential vanilloid 1 intracellular binding site, *Mol Pharmacol 70*, 1005-1012.

12. Jordt, S. E., and Julius, D. (2002) Molecular basis for species-specific sensitivity to "hot" chili peppers, *Cell 108*, 421-430.

13. Salazar, H., Jara-Oseguera, A., Hernandez-Garcia, E., Llorente, I., Arias, O., II, Soriano-Garcia, M., Islas, L. D., and Rosenbaum, T. (2009) Structural determinants of gating in the TRPV1 channel, *Nat Struct Mol Biol 16*, 704-710.

14. Sutton, K. G., Garrett, E. M., Rutter, A. R., Bonnert, T. P., Jarolimek, W., and Seabrook, G. R. (2005) Functional characterisation of the S512Y mutant vanilloid human TRPV1 receptor, *British journal of pharmacology 146*, 702-711.

15. Johansen, M. E., Reilly, C. A., and Yost, G. S. (2006) TRPV1 antagonists elevate cell surface populations of receptor protein and exacerbate TRPV1-mediated toxicities in human lung epithelial cells, *Toxicol Sci 89*, 278-286.

16. Reilly, C. A., Johansen, M. E., Lanza, D. L., Lee, J., Lim, J. O., and Yost, G. S. (2005) Calcium-dependent and independent mechanisms of capsaicin receptor (TRPV1)-mediated cytokine production and cell death in human bronchial epithelial cells, *J Biochem Mol Toxicol 19*, 266-275.

17. Veronesi, B., Carter, J. D., Devlin, R. B., Simon, S. A., and Oortgiesen, M. (1999) Neuropeptides and capsaicin stimulate the release of inflammatory cytokines in a human bronchial epithelial cell line, *Neuropeptides 33*, 447-456.

18. Reilly, C. A., Taylor, J. L., Lanza, D. L., Carr, B. A., Crouch, D. J., and Yost, G. S. (2003) Capsaicinoids cause inflammation and epithelial cell death through activation of vanilloid receptors, *Toxicol Sci 73*, 170-181.

19. Thomas, K. C., Sabnis, A. S., Johansen, M. E., Lanza, D. L., Moos, P. J., Yost, G. S., and Reilly, C. A. (2007) Transient receptor potential vanilloid 1 agonists cause endoplasmic reticulum stress and cell death in human lung cells, *J Pharmacol Exp Ther 321*, 830-838.

20. Myers, B. R., Bohlen, C. J., and Julius, D. (2008) A yeast genetic screen reveals a critical role for the pore helix domain in TRP channel gating, *Neuron 58*, 362-373.

21. Schroder, M., and Kaufman, R. J. (2005) ER stress and the unfolded protein response, *Mutat Res 569*, 29-63.

22. Matsumoto, M., Minami, M., Takeda, K., Sakao, Y., and Akira, S. (1996) Ectopic expression of CHOP (GADD153) induces apoptosis in M1 myeloblastic leukemia cells, *FEBS Lett 395*, 143-147.

23. McCullough, K. D., Martindale, J. L., Klotz, L. O., Aw, T. Y., and Holbrook, N. J. (2001) Gadd153 sensitizes cells to endoplasmic reticulum stress by down-regulating Bcl2 and perturbing the cellular redox state, *Mol Cell Biol 21*, 1249-1259.

24. Oyadomari, S., and Mori, M. (2004) Roles of CHOP/GADD153 in endoplasmic reticulum stress, *Cell Death Differ 11*, 381-389.

25. Vannier, B., Zhu, X., Brown, D., and Birnbaumer, L. (1998) The membrane topology of human transient receptor potential 3 as inferred from glycosylation-scanning mutagenesis and epitope immunocytochemistry, *J Biol Chem 273*, 8675-8679.

26. Jiang, Y., Lee, A., Chen, J., Ruta, V., Cadene, M., Chait, B. T., and MacKinnon, R. (2003) X-ray structure of a voltage-dependent K+ channel, *Nature 423*, 33-41.

27. Ishii, T., Ishikawa, M., Miyoshi, N., Yasunaga, M., Akagawa, M., Uchida, K., and Nakamura, Y. (2009) Catechol type polyphenol is a potential modifier of protein sulfhydryls: development and application of a new probe for understanding the dietary polyphenol actions, *Chem Res Toxicol 22*, 1689-1698.

CHAPTER 4

CONTRIBUTIONS OF TRPV1, ENDOVANILLOIDS AND ENDOPLASMIC RETICULUM STRESS TO LUNG CELL DEATH *IN VITRO* AND LUNG INJURY *IN VIVO*

4.1 Abstract

Endogenous agonists of the TRPV1 receptor (endovanilloids) have been implicated as mediators of lung inflammation and injury during experimental sepsis and other causes of systemic inflammation. The current study tests the hypothesis that pulmonary inflammation and lung injury elicited by lipopolysaccharides (LPS; endotoxin) occur via the formation of pneumotoxic endovanilloids that activate TRPV1 in the lung. In human lung cells, plasma membrane and endoplasmic reticulum (ER) populations of TRPV1 differentially regulate cytokine gene expression and cell death after TRPV1 activation. Calcium efflux from the ER initiates the unfolded protein/ER stress response, leading to cell death via EIF2αK3 activation, G_1/S arrest, and increased expression of proapoptotic growth arrest and DNA damage inducible gene 153 (GADD153, CHOP or DDIT3). Treatment of human primary lung bronchial and bronchiolar epithelial, alveolar, and microvascular endothelial cells with nonivamide caused cytooxicity with LC_{50} values inversely proportional to TRPV1 expression, and induced GADD153 expression. Treatment of mice i.p. with LPS promoted systemic

inflammation and caused lung injury in mice in a TRPV1 and ER stress dependent manner. All responses to LPS were attenuated by cotreating mice with the TRPV1 antagonist LJO-328 (5mg/kg, i.p) and in TRPV1-/- mice. These results provide compelling evidence that TRPV1 and pneumotoxic endovanilloids promote lung injury associated with systemic inflammation, and validate previous mechanistic findings on TRPV1 mediated lung cell toxicities *in vitro*. These results also highlight the possibility that modulation of TRPV1 may ameliorate lung injury due to systemic inflammation associated with sepsis or other causes.

4.2 Introduction

Lung injury and its most severe manifestation, acute respiratory distress syndrome (ARDS), cause severe morbidity and mortality. Lung injury is defined as pulmonary edema and cellular damage resulting from loss of alveolar and vascular endothelial cell function and/or viability (*1-4*). Damage to the alveolar-capillary unit increases the flux of plasma fluid and protein into the alveolar spaces and inhibits O_2/CO_2 exchange (*3-5*). Studies have clearly shown that stimulation of the host immune system during sepsis/systemic endotoxemia causes lung injury, but the precise molecular mechanisms coupling infection and/or inflammation with lung injury remain poorly defined (*1, 3, 4*).

It has been shown that endotoxemia and other common causes of lung injury induce the synthesis of a variety of small molecule immune system modulators including hydrogen sulfide (H_2S), anandamide, leukotrienes (LTs), hydroxy- and hydroperoxyeicosatetraenoic acids (HETEs and HPETEs), and prostaglandins (*6-12*). These substances contribute to lung injury and the deleterious sequelae associated with

sepsis and burn injury (*7, 10-12*). Several of these substances are potent agonists of the TRPV1 (transient receptor potential vanilloid 1) receptor (*7, 9, 12-14*).

TRPV1 is a transmembrane ligand gated calcium channel activated by capsaicin, the compound found in chili peppers that elicits a burning sensation. TRPV1 is also activated by temperatures >43^{o}C, pH <6.2 (at 37^{o}C) and a variety of exogenous and endogenous compounds (*15-19*). Known endogenous TRPV1 agonists (endovanilloids) include anandamide, leukotriene B_4, 12(S)-HPETE and similar eicosanoids, and H_2S.

TRPV1 is expressed by tachykinin rich sensory neurons and various non-neuronal cells of the lung. Activation of TRPV1 in C- and Aδ-fibers in the lung causes pulmonary neurogenic inflammation, largely via the release of substance P and neurokinin A, two substances known to promote vascular leakage and edema (*7, 14, 20-26*). TRPV1 is also expressed by non-neuronal cells. In these cells TRPV1 is expressed on the plasma membrane and on the endoplasmic reticulum (ER) (*27-30*). Activation of TRPV1 on the plasma membrane of lung cells causes calcium influx and has been linked to increased immunomodulatory cytokine transcription and secretion. TRPV1-mediated increases in IL-6 and IL-8 likely promote pulmonary inflammation, neutrophilia and injury associated with capsaicin inhalation in rats (*31*). Conversely, activation of ER TRPV1 causes ER calcium depletion, ER stress, and cell death, which likely contributes to the extensive damage to epithelial cells throughout the airways and lungs of rats exposed to capsaicin aerosols (*32*). The neuronal release of tachykinins and the release of cytokines from epithelial cells, coupled with ER stress associated cell cycle arrest and cell death, presumably cause lung inflammation and injury by TRPV1 agonists.

There are several reports that multiple endovanilloids are produced during experimental sepsis and that ER stress is observed in damaged lungs of LPS-treated mice (*7, 8, 10, 12, 14, 31-37*). However, the possibility that TRPV1 and endovanilloids were responsible for the initiation of ER stress in lung cells was not investigated. The hypothesis for this work is that lung injury resulting from systemic exposure to LPS is mediated, in part, by endovanilloids and TRPV1. This research utilizes a multi-faceted strategy including the assessment of TRPV1 activation, GADD153 expression (a marker for ER stress), and cell death in cultured primary human lung cells known to be targeted during sepsis, and an assessment of the contribution of TRPV1 and endovanilloids in lung injury *in vivo* in TRPV1-/- (knockout) mice treated with LPS.

4.3 Methods

4.3.1 Chemicals

Nonivamide (*n*-vanillylnonanamide), LPS (0110:B4), and anandamide (*n*-arachadonoylethanolamine) were purchased from Sigma-Aldrich (St. Louis, MO). AM-251 was purchased from Cayman Chemicals (Ann Arbor, MI). Nonivamide and capsaicin have indistinguishable toxicity profiles in the human lung cells used in this study, but nonivamide is available in higher purity so it is used in experiments as the prototypical TRPV1 agonist. LJO-328 was provided by Dr. Jeewoo Lee (Seoul National University, Seoul, Korea). PCR primers for mouse and human GADD153 and β-actin were synthesized by Integrated DNA Technologies (Coralville, IA). PCR primers for TRPV1 and β2M were synthesized by the University of Utah Core Facilities (Salt Lake City, UT). All other general chemicals and reagents were purchased from established suppliers.

4.3.2 Cell Culture

Immortalized human bronchial epithelial cells (BEAS-2B) were purchased from American Type Culture Collection (Manassas, VA), and TRPV1 overexpressing BEAS-2B (TRPV1-OE) cells were generated as described previously (*31*). BEAS-2B and TRPV1-OE cells were cultured in LHC-9 media (BioSource International, Camarillo, CA). Primary human lung microvascular endothelial (HMVEC-L), small airway epithelial cells (SAEC) and normal human bronchial epithelial (NHBE) cells were purchased from Lonza (Walkersville, MD). HMVEC-L cells were cultured in supplemented EGM-MV media, SAEC cells were cultured in SAGM media, and NHBE cells were cultured in BEGM media (Lonza, Walkersville, MD). Culture flasks for SAEC, NHBE, BEAS-2B and TRPV1-OE cells were coated with LHC basal media fortified with 30 μg/mL collagen, 10 μg/mL fibronectin, and 10 μg/mL bovine serum albumin. Cells were maintained between 30 and 90% maximum density.

4.3.3 Cytotoxicity/Dose Response Assays

Cells were subcultured into 96 well plates and grown to ~90% confluence. Cells were treated for 24 hours at 37ºC with increasing concentrations of chemical. Treatment solutions were prepared in LHC-9 media for BEAS-2B and TRPV1-OE cells and in OptiMEM I reduced serum media (Invitrogen, Carlsbad, CA) for NHBE, HMVEC-L and SAEC cells. Cell viability was quantified using the Dojindo cell counting kit-8 (Dojindo Laboratories, Gaithersburg MD), according to supplier's recommendations.

4.3.4 Semiquantitative Reverse Transcriptase PCR Analysis of GADD153 Gene Expression

Cells were subcultured into 6 well cell culture plates and grown to ~90% density. HMVEC-L and NHBE cells were treated with nonivamide for varying durations at 37ºC. Total RNA was extracted from cells using the Invitrogen PureLink Micro-to-Midi Total RNA Purification System (Invitrogen, Carlsbad, CA), and 2.5 μg of the total RNA was transcribed into cDNA using Superscript III (Invitrogen, Carlsbad, CA). cDNA corresponding to GADD153 and β -actin was amplified by PCR using 1 μL of the cDNA synthesis reaction, gene specific primers and GoTaq Green PCR Master Mix (Promega, Madison, WI). The PCR program used to examine the expression of both human and mouse GADD153 consisted of an initial 2 minute incubation at 94ºC, followed by 28 cycles of 94ºC for 30 seconds, 54ºC for 30 seconds, and72ºC for 1 minute. The program ended with 10 minutes at 72ºC. PCR products were resolved on 1% SB buffer agarose gels. Images were captured using a Gel-Doc imaging system (Bio-Rad, Hercules, CA). Product quantification was achieved by determining band intensities for each PCR product relative to β-actin, the internal PCR control, using the Gel-Doc density analysis tools in the Quantity One software program (Bio-Rad). Primers for human GADD153 were: sense, 5'- GACCTGCAAGAGGTCCTGTC-3’; antisense, 5’-TCGCCTCTACTTCCCTGGTC-3’; the PCR product was 395 nucleotides. Primer sequences for human β-actin were: sense, 5’-GACAACGGCTCCGGCATGTGGCA-3’; antisense, 5’-TGAGGATGCCTCTCTTGCTCTG-3’; the PCR product is 183 nucleotides. Primer sequences for mouse GADD153 and β-actin are presented below.

4.3.5 Quantitative Real-Time PCR Analysis of TRPV1 and GADD153 Expression in Human Cells

Total RNA was isolated using the Invitrogen PureLink Micro-to-Midi Total RNA Purification System (Invitrogen, Carlsbad, CA). cDNA was prepared by using 1 μg of the total RNA transcribed into cDNA using Superscript III (Invitrogen, Carlsbad, CA). Real time PCR was performed using 1 μL cDNA diluted 1:100 and RT^2 SYBR Green qPCR Master Mix from SABiosciences (Frederick, MD) on a Chromo 4 Real Time Detection System (Bio-Rad, Hercules, CA) using MJ Opticon Monitor 3 software. The PCR program used consisted of an initial 10 minute incubation at 95ºC, followed by 40 cycles of 95ºC for 15 seconds, 55ºC for 30 seconds**,** then 72ºC for 30 seconds. Experiments were performed in triplicate with a copy number standard curve for both the housekeeping gene (beta-2 macroglobulin, β2M) and the genes of interest (TRPV1 and GADD153). cDNA was diluted 1:100 for all samples. Primer sequences for human β2M were: sense, 5' –GATGAGTATGCCTGCCGTGTG – 3';

antisense, 5' –CAATCCAAATGCGGCATCT – 3'. Primer sequences for human TRPV1 were: sense, 5'- CTGCGGACCCACTCCAAAA-3';

antisense, 5'-CCTCGTGAGGGCAATCCAC-3'.

Primer sequences for human GADD153 were:

sense, 5'-AGAACCAGGAAACGGAAACAGA-3'; a

antisense, 5'-TCTCCTTCATGCGCTGCTTT-3'.

4.3.6 Animals

Experiments were performed on 20-25 g male CF1, C57BL/6 mice, and TRPV1 -/- null C57BL/6 mice. Mice were maintained in the University of Utah vivarium and

Institutional Animal Care and Use Committee (IACUC) authorization was obtained for all procedures and experimental protocols.

4.3.7 LPS Induced Lung Injury

Intraperitoneal injection of LPS was used as the immune system stimulant. LPS (E.coli 0111:B4) was prepared in 0.9% saline, or in 98.4% saline, 1% ethanol, 0.5% Tween 20, and 0.1% DMSO for experiments where LJO-328 co-treatment was used. Mice were injected intraperitoneally (i.p.) with vehicle alone, 10 mg/kg or 15 mg/kg LPS, LPS 10 or 15 mg/kg with 5 mg/kg LJO-328, or 5 mg/kg LJO-328. Animals were treated for 12 hours during which lung injury developed. Animals were terminally anesthetized by i.p. injection of pentobarbital (100 mg/kg in 50% DMSO), and exsanguinated via cardiac puncture. Bronchial alveolar lavage (BAL) was performed using 0.4 mL saline, and the lungs were collected for gene expression analysis. Lung injury was also assessed histologically and by assaying changes in BAL protein content and lung water weight, as described below.

4.3.8 Quantification of Lactate Dehydrogenase (LDH) in BAL Fluid

Contents of the lung airspace were collected by lavage. The trachea was cannulated using a blunt ended 22 gauge needle attached to a 1 mL syringe. The lungs were gently infused with 0.4 mL of sterile saline and the fluid was recovered by gently pulling back on the syringe, repeated twice. The fluid was clarified by centrifugation at 1000 x g for 2 minutes at 4° C and the supernatant was assayed for soluble LDH activity and total protein content. LDH activity was quantified using the TOX-7 assay kit (Sigma-Aldrich, St. Louis, MO). Total protein was quantified using the Bicinchoninic Acid

(BCA) Assay Kit (Pierce, Rockford, IL). Data for LDH activity are expressed as units/total mg of protein in the BAL fluid.

4.3.9 Quantification of GADD153 Expression in Mouse Lung

Lungs were removed and trimmed to remove the heart, trachea, bronchi, and connective tissues. Lungs were placed in RNALater RNA Stabilization Reagent (Qiagen, Valencia, CA) at 4ºC for 24 hours and stored at -20ºC until analysis. Tissues were homogenized and total RNA was isolated using the Invitrogen PureLink Micro-to-Midi Total RNA Purification System (Invitrogen, Carlsbad, CA). 2.5 μg of the total RNA was transcribed into cDNA using Superscript III (Invitrogen, Carlsbad, CA). cDNA corresponding to GADD153 and β -actin was amplified by PCR using 1 μL of the cDNA synthesis reaction, gene specific primers and GoTaq Green PCR Master Mix (Promega, Madison, WI). The PCR program used to examine the expression of mouse GADD153 was identical to the program used to quantify GADD153 mRNA in primary human cells. Primer sequences used for mouse GADD153 were: sense, 5'- GCAGCCATGGCAGCTGAGTCCCTGCCTTCC -3';
antisense, 5'- CAGACTCGAGGTGATGCCCACTGTTCATGC -3'. Primer sequences used for mouse β-actin are: sense, 5'- GTGACGAGGCCCAGAGCAAGAG -3'; antisense, 5'- AGGGGCCGGACTCATCGTACTC -3'.

4.3.9 Quantification of Excess Lung Water Weight

Net changes in lung tissue mass were determined. Mice were sacrificed and lungs were collected during necropsy. The left lobe from each animal was weighed and heated for 48 hours at 55°C. The lungs were weighed again and the change in mass was used to

quantify fluid accumulation and cellular infiltration in the lung as a consequence of LPS treatment. Data are expressed as the change in lung wet weight to dry weight.

4.3.10 Statistical Analysis

Statistical analysis was performed using 95% confidence intervals as the limit for significance. All results, excluding lung histopathology, are represented as mean ± standard deviation or mean with the 95% confidence interval (C.I.). Post-hoc testing was performed in individual experiments as indicated in figure legends.

4.4 Results

Cellular sensitivity to TRPV1 agonists depends on the relative amount of TRPV1 expression, which varies by cell type and anatomical location. TRPV1 mRNA expression was quantified in TRPV1 overexpressing BEAS-2B cells (TRPV1-OE), BEAS-2B, A549, NHBE, SAEC, and HMVEC-L cell types using quantitative real time PCR techniques. TRPV1 expression was inversely correlated with LC_{50} values for the TRPV1 agonist nonivamide (Figure 4.2).

Primary human lung cells, chosen to mimic cells of the lung known to be targeted for damage during acute lung injury/ARDS (i.e., microvascular endothelial and alveolar type II cells), were treated with nonivamide to establish a dose response curve and determine the cytotoxic potential of capsaicin in these cells. Primary human HMVEC-L, SAEC and NHBE cells were sensitive to nonivamide with LC_{50}s of 150 μM, 160 μM and 160 μM, respectively (Figure 4.3 panel A). Cell death due to nonivamide treatment was partially attenuated with LJO-328 cotreatment in HMVEC-L cells (data not shown). Preliminary data indicate that GADD153 mRNA is induced in NHBE and HMVEC-L

cells in a time-dependent manner after treatment with nonivamide at LC_{50} concentrations (Figure 4.3 panel B).

The role of TRPV1 in lung injury *in vivo* was investigated using a mouse model of septic/inflammatory lung injury. LPS endotoxin was injected intraperitoneally into mice. A hallmark of lung injury is the accumulation of inflammatory cells and fluid in the lung. To determine the extent to which LPS treatment induced inflammation and edema in the lung, lungs were weighed and dried to quantify excess water weight and residual cellular material. Mice treated with LPS exhibited a significant increase in water weight, approximately 12 mg H_2O, relative to controls. Increases in water weight were attenuated ~50% by LJO-328 co-treatment (Figure 4.4).

Lung cell damage after LPS treatment was also quantified using an assay to determine soluble LDH activity in BAL fluid. Comparison of wild type LPS-treated mice, wild type mice co-treated with LPS (10 mg/kg) and the TRPV1 antagonist LJO-328 (5 mg/kg) for 12 hours demonstrated significant attenuation of LPS-induced increases in BAL LDH by LJO-328 (Figure 4.5, panel A). Comparison between wild type and TRPV1 -/- mice treated with LPS (15 mg/kg) for 12 hours demonstrated that TRPV1-/- mice had significantly lower BAL LDH activity compared to wild-type mice, in agreement with the prior results using LJO-328 (Figure 4.5, panel B).

GADD153 mRNA expression was also quantified as an indicator of TRPV1 activation and ER stress induction in damaged lungs of LPS treated animals. GADD153 mRNA levels were significantly induced in LPS treated mice compared to vehicle treated mice. In animals co-treated with LPS and LJO-328, GADD153 expression was reduced to near control levels, as it was in TRPV1 -/- mice (Figure 4.6, panels A and B).

Histopathological assessment of lung injury was performed on lung slices to gauge the severity of lung injury. Representative images are presented in Figure 4.7. Lungs of vehicle treated mice showed mild inflammation, occasional macrophages, and minimal bronchial or alveolar exudates. Lungs of LPS treated mice exhibited occasional emphysematous alveoli, increased numbers of macrophages, some neutrophils, and occasional alveoli containing eosinophilic proteinacious exudates. Lungs of LPS treated TRPV1-/- mice showed only mild inflammatory infiltrates with some eosinophilic material, similar to controls. Similar results were observed in LJO-328 cotreated mice (data not shown).

Capsaicin is the prototypical TRPV1 agonist, but endogenous TRPV1 agonists also have the ability to activate TRPV1. The endovanilloid anandamide was evaluated as a mediator of TRPV1 dependent lung injury using lung cells. HMVEC-L, SAEC, and NHBE cells were sensitive to anandamide with LC_{50} values of approximately 14 μM, 20 μM, and 31 μM, respectively (Figure 4.8, panel A). TRPV1-OE and BEAS-2B cells exhibited LC_{50} values of ~22 μM and ~18 μM, respectively. For both TRPV1-OE and BEAS-2B cells, anandamide induced cytotoxicity was not significantly blocked by LJO-328 or AM-251 co-treatment. (Figure 4.8, panels B and C) Similar results were produced when GADD153 induction was examined after treatment with anandamide alone or in the presence of LJO-328 or AM-251. (Figure 8, panel D) These results indicate anandamide is likely toxic to human lung cells via non TRPV1 dependent mechanisms and that other endovanilloids may be involved in LPS induced responses in the lung.

4.5 Discussion

As research has progressed on the etiology of inflammation induced lung injury, a role for TRPV1 and endogenous agonists as potential mediators of injury has emerged. Although the exact mechanisms of cell death and damage in lung injury are not fully understood, continued investigation of this process is vital to the development of better models, new therapies, and ultimately the survival of thousands of patients each year.

To better characterize TRPV1 and associated functions in the lung, TRPV1 expression and responses of primary human lung cells to the prototypical agonist nonivamide were studied. Microvascular, alveolar, and even bronchial epithelial cells are among cells targeted for damage during systemic inflammation arising from conditions such as sepsis and trauma. Treatment of SAEC, HMVEC-L, and NHBE cells with nonivamide produced cytotoxicity (Figure 4.3 panel A). SAEC, HMVEC-L and the primary BEAS-2B cognate NHBE cells were roughly equally sensitive to nonivamide (LC_{50} ~150 μM), consistent with their relative levels of TRPV1 expression (Figure 4.2). Preliminary data indicate that nonivamide induces GADD153 in HMVEC-L and NHBE cells in a time dependent manner (Figure 4.3 panel B).

Injury of cells in the intact lung during sepsis/systemic endotoxemia is indeed much more complex than the simple *in vitro* cell culture studies described above. However, we postulated that the results observed *in vitro* would be reflected in the intact lung if pneumotoxic endovanilloids contributed to lung injury. Preliminary data from our lab have indicated that intratracheal administration of capsaicin to mice induces GADD153 in the whole lung at least 2 fold as compared to PBS treated animals (data not shown). Experiments using the LPS model of lung injury confirmed that TRPV1 played a

role in lung injury due to LPS treatment. Both TRPV1 antagonism using LJO-328 and TRPV1 knockout decreased inflammation and edema as evidenced by histological assessment of lung morphology, and by statistically lower LDH and lung water weight in LPS treated mice. Histopathological results also provided some indication of alveolar-capillary damage/edema and inflammatory cell recruitment in the lungs of LPS treated mice. It is anticipated that future immunohistochemical analysis of these lung slices for diagnostic markers of lung injury and ER stress will further confirm these results. Additionally, evaluation of inflammatory cytokine induction in BAL and optimization of time points and treatment doses should provide additional compelling results and support for our hypothesis on TRPV1 and endovanilloids as mediators of lung injury. A limitation of our results is that previous use and characterization of the LPS-model of induced sepsis has shown reproducible results, but that C57BL/6 mice experience a relatively mild inflammatory and lung injury response in comparison to other strains of mice and animal species (*2*). We have observed differences in susceptibility between the CF1 and C57BL/6 mouse strains, which is reflected in the doses used and results presented herein.

Responses to the prototype TRPV1 agonist capsaicin and the endovanilloid anandamide were compared to gain insight into whether endogenous TRPV1 agonists could cause lung injury through TRPV1 activation in lung cells. The results showing similar LC_{50} values for anandamide in all cell types independent of TRPV1 expression, as well as the inability of TRPV1 and CB1/2 antagonists to block anandamide toxicity in TRPV1-OE and BEAS-2B cells indicated that anandamide toxicity was not completely TRPV1 mediated. Since the *in vitro* data indicate anandamide is likely toxic via non

TRPV1 dependent mechanisms, anandamide is not likely the endovanilloid responsible for the observed TRPV1 mediated responses *in vivo*.

Collectively, these results provide novel insights into the role of TRPV1 and endogenous TRPV1 agonists as mediators of lung injury in the context LPS induced inflammation. These studies couple *in vitro* mechanistic results showing that TRPV1 agonists cause lung cell death through ER stress with results that LPS induced lung injury and GADD153 expression *in vivo* are a consequence of TRPV1 activation by endogenous agonists such as anandamide, but indicates that endovanilloids other than anandamide likely play a more prominent role *in vivo*.

4.6 Footnotes

We would like to thank Dr. Alan R. Light, PhD for the generous gift of C57BL/6 and TRPV1 knockout mice. We would also like to acknowledge the University of Utah Anti-epileptic Drug Development Program for providing CF1 mice, Dr. Jack L. Taylor, DVM, PhD for evaluating the histology slides, and Dr. Randal O. Dull, MD, PhD for assistance with the design and interpretation of results from the animal lung injury studies. This work was funded by NIH grant HL069813.

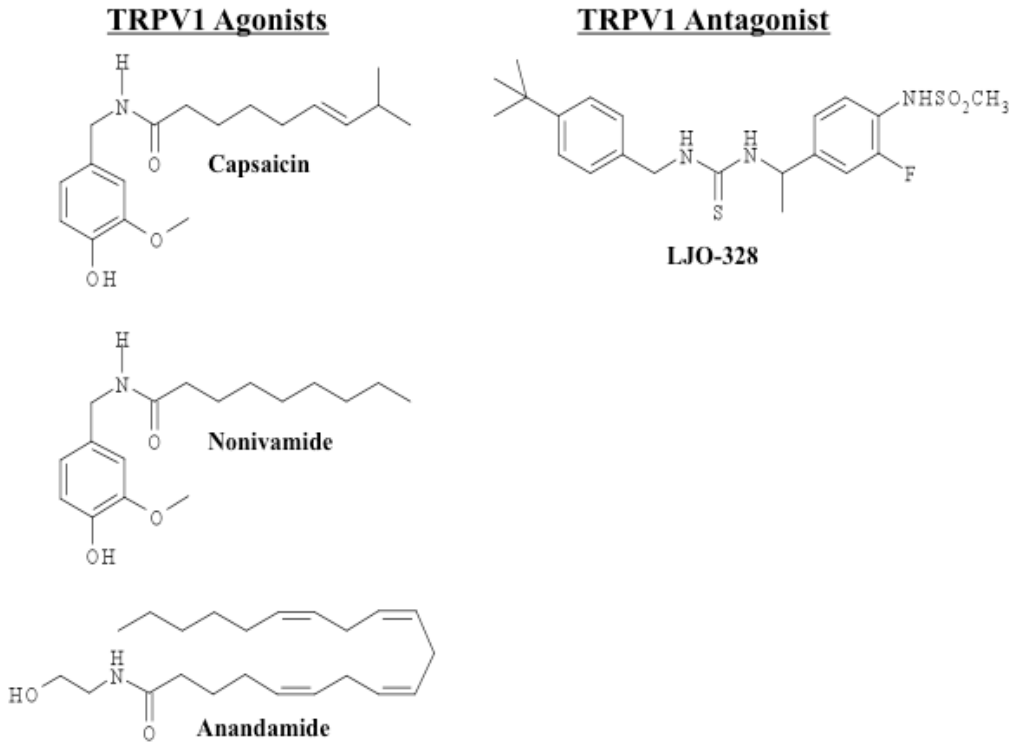

Figure 4.1. Structures of TRPV1 agonists and antagonists.

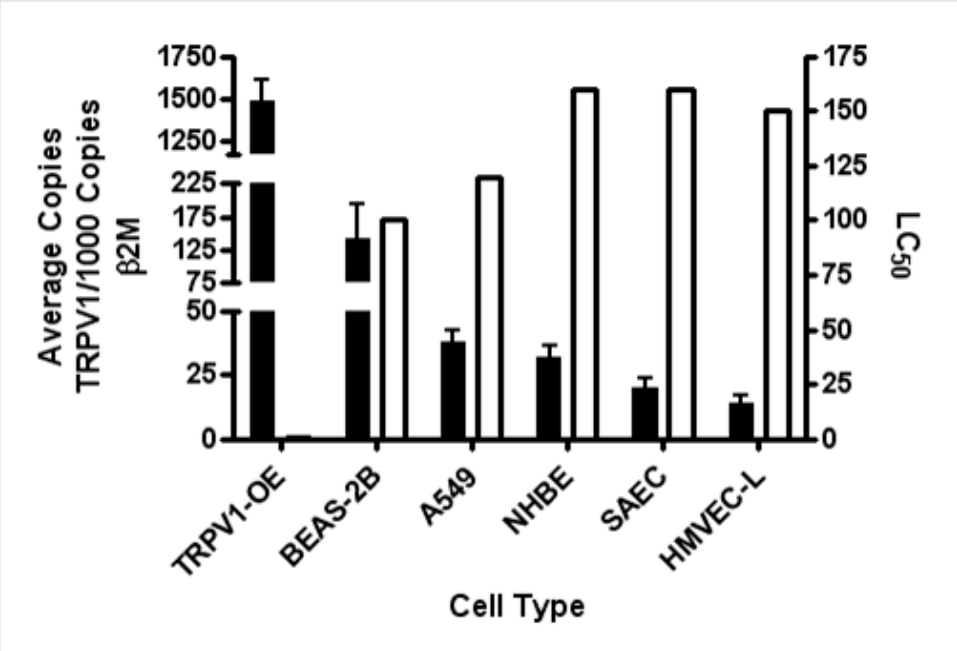

Figure 4.2. Quantitative real-time PCR copies of TRPV1 fold β2M control in a variety of cell types compared to their approximate nonivamide LC_{50} concentrations. Cytotoxicity assays and real-time PCR were carried out as described in *Methods*. Average copies TRPV1 and LC_{50} values in these cells were significantly inversely correlated with a Pearson 'r' value of -0.9424, p=0.0049.

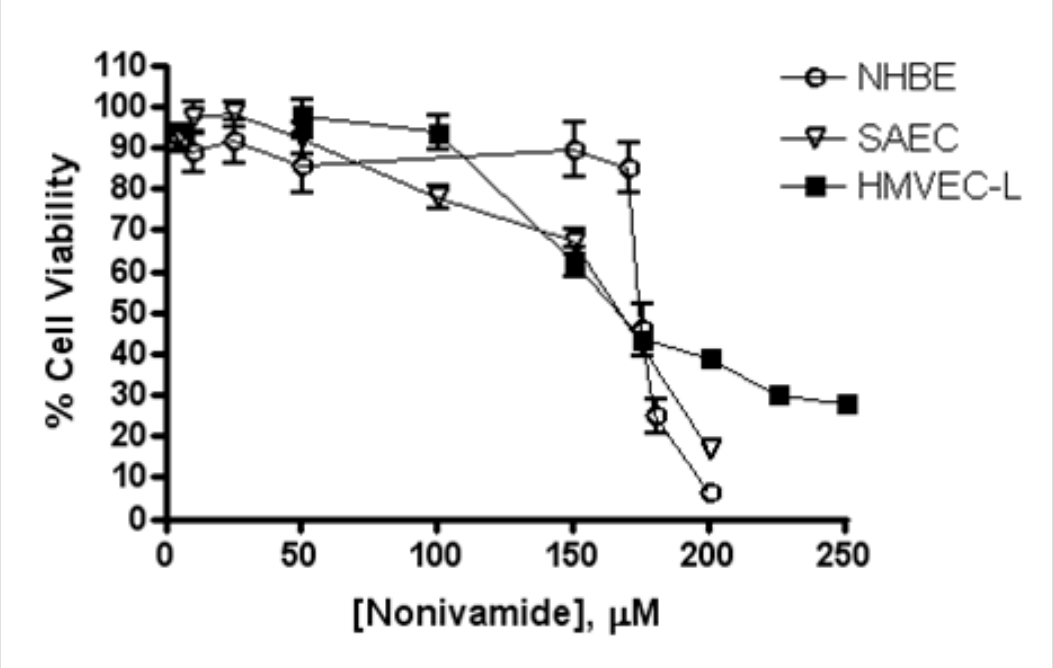

Panel A.

Figure 4.3. Dose-response cytotoxicity for nonivamide in NHBE, SAEC and HMVEC-L cells and nonivamide-induced GADD153 expression in NHBE and HMVEC-L cells. **Panel A.** NHBE, SAEC and HMVEC-L cells were sensitive to nonivamide at concentrations above 150 µM. NHBE cells are represented with open circles, SAEC cells are represented by open triangles and HMVEC-L cells are represented with closed squares. Data are shown as % viability of untreated control cells. **Panel B**. *Preliminary Data*. Semi-quantitative GADD153 mRNA expression was examined in NHBE and HMVEC-L cells treated with approximate LC_{50} concentrations of nonivamide (160 and 175 µM, respectively) at varying time points. Data are presented as fold control relative to β-actin loading control, N=1.

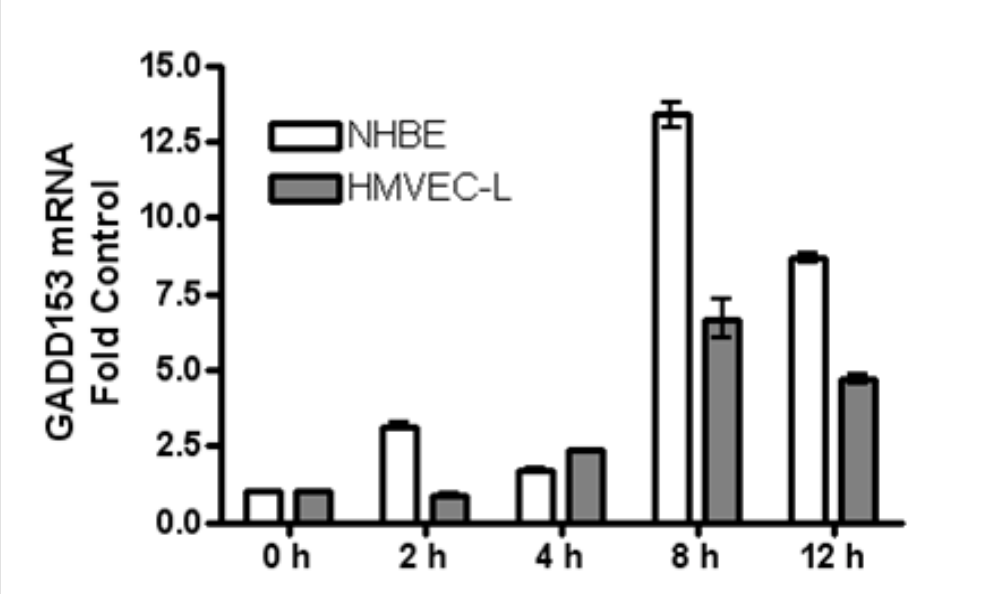

Figure 4.3 Panel B.

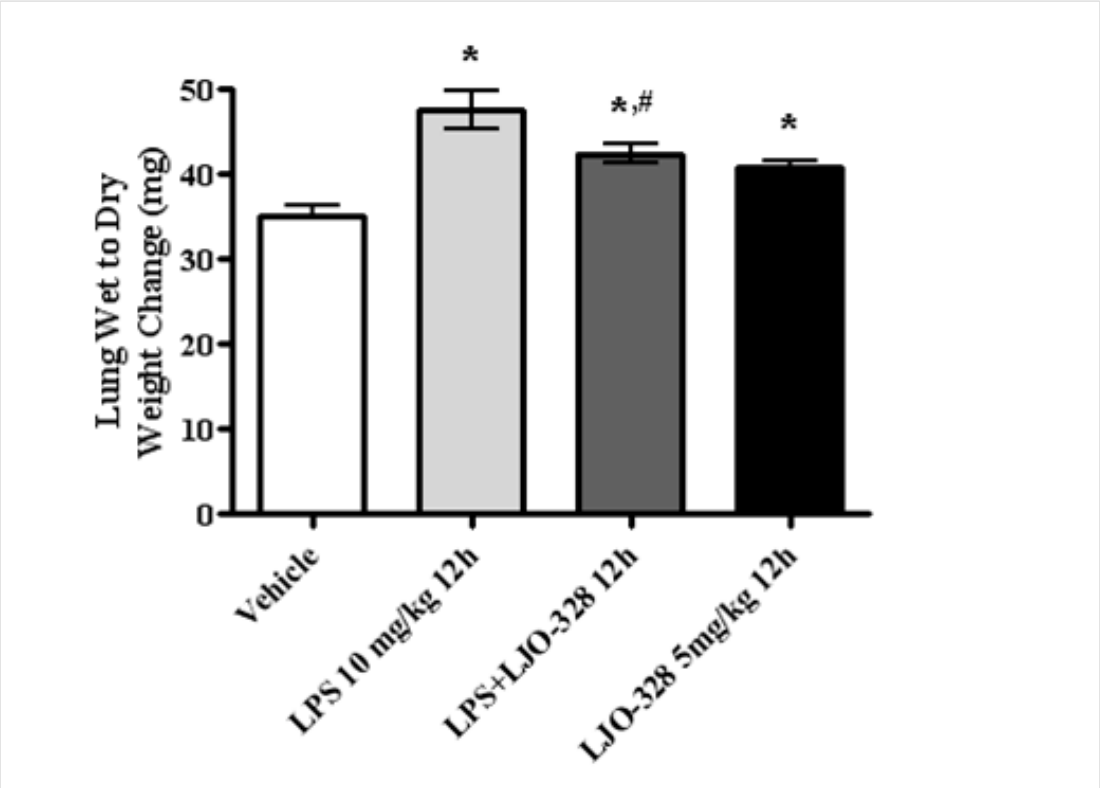

Figure 4.4. Changes in mouse lung water weight. The change in weight indicates edema and cellular accumulation in lungs of CF1 mice treated with vehicle (white bars, n=6), LPS (10 mg/kg) (light grey bars, n=6), LPS (10 mg/kg) and LJO-328 (5 mg/kg) (dark grey bars, n=6) and LJO-328 (5 mg/kg) (black bars, n=6) alone. Statistical differences ($p<0.05$) between the vehicle, LPS-treated, LPS+LJO-328, and LJO-328 treated groups were observed (*). # indicates statistical differences between LPS treated and LPS + LJO-328 treated groups. Statistical analyses were performed by one-way ANOVA and Newman-Keuls post-tests.

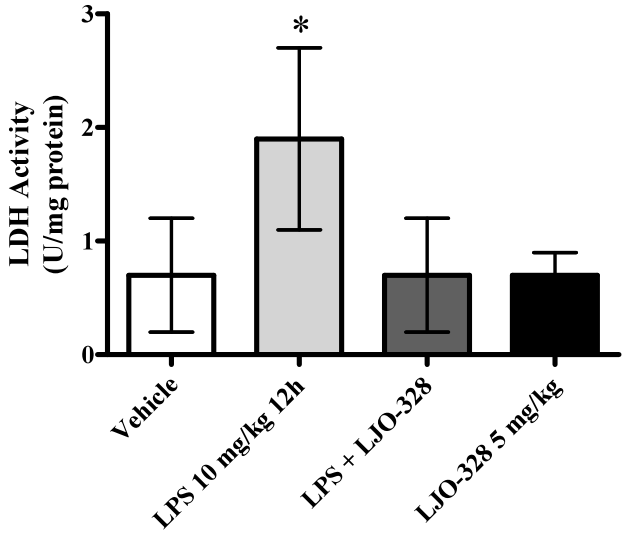

Panel A.

Figure 4.5. Panel A. LDH activity in BAL from CF1 mice. LDH activity is shown for vehicle treated CF1 mice (white bars, n=6), LPS (10 mg/kg) treated mice (light grey bars, n=6), mice co-treated with both LPS (10 mg/kg) and LJO-328 (5 mg/kg) (dark grey bars, n=6), and mice treated with LJO-328 alone (black bars, n=6) was examined. LPS treated wild-type mice had statistically significant increases (*) in BAL LDH. **Panel B**. Soluble LDH activity in BAL from LPS-treated C57BL/6 mice was evaluated in vehicle treated mice (white bars, n=5), LPS treated wild-type mice (light grey bars, n=5) and LPS treated TRPV1-/- mice (dark grey bars, n=3). Statistically significant differences (#) were observed between LPS treated wild-type mice and LPS treated TRPV1 -/- mice at the 95% C.I. using one-way ANOVA analysis and Newman-Keuls post-test. * indicates statistical differences between LPS treated and vehicle control groups.

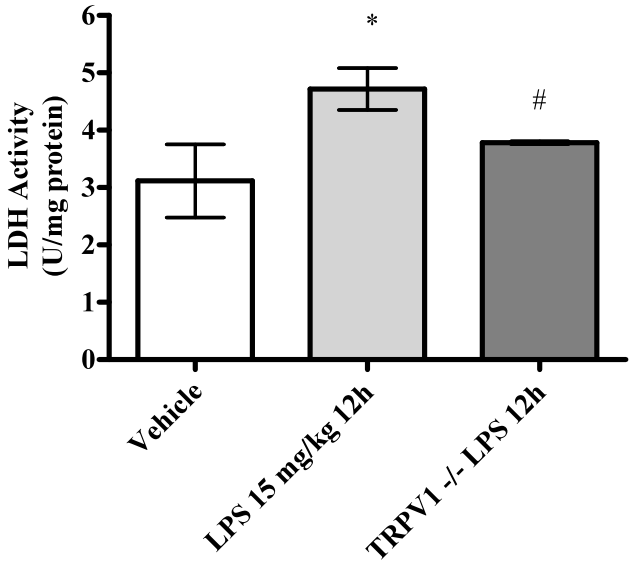

Figure 4.5 Panel B.

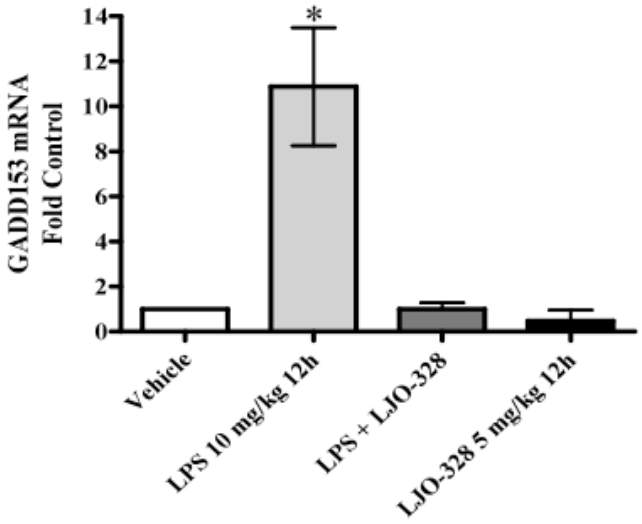

Panel A.

Figure 4.6. Expression of GADD153 mRNA in mouse lungs. Treatment groups are described in each panel and data are expressed as fold control relative to β-actin loading control. **Panel A.** LPS resulted in a statistically significant increase in GADD153 mRNA induction relative to vehicle treatment, $p < 0.05$ using one-way ANOVA and Dunnett's multiple comparison test, n=6 for each group. **Panel B.** Statistically significant decreases (*) in the GADD153 PCR products were seen in LPS treated TRPV1-/- mice compared to wild-type C57BL/6 mice using one-way ANOVA and Newman-Keuls post-testing, $p < 0.05$. For vehicle and LPS treatment groups, n=5. For TRPV1-/- , n=3. # indicates statistical differences between LPS treated and LPS treated TRPV1-/- groups.

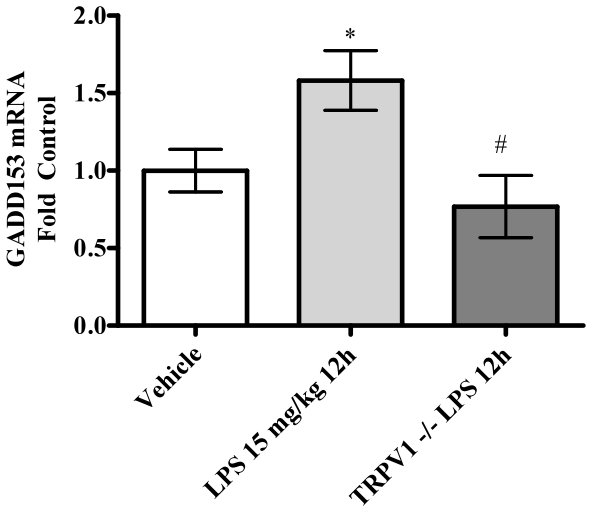

Figure 4.6 Panel B.

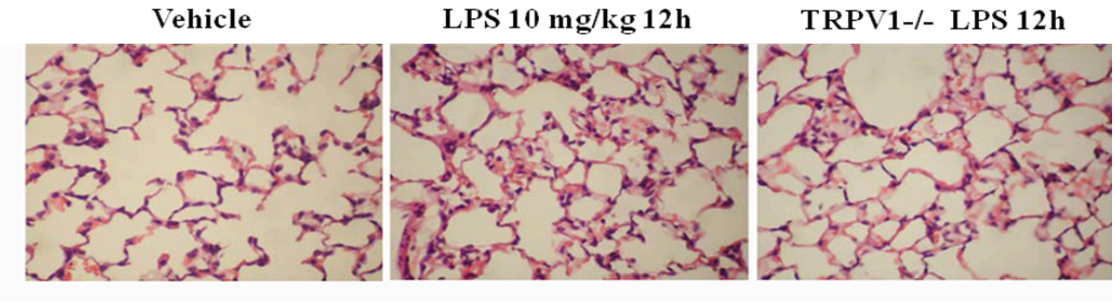

Figure 4.7. Mouse lung histology. Lungs were fixed *in situ* by infusing with 10% neutral-buffered formalin, removed, and placed in fixative solution. 5 μm sections were prepared, stained with eosin and hematoxylin, and analyzed. Representative mouse lung sections are shown for vehicle treated wild-type C57BL/6 mice, wild-type mice treated with 10 mg/kg LPS for 12 hours, and TRPV1-/- mice treated with 10 mg/kg LPS for 12 hours.

Figure 4.8. Anandamide dose response and GADD153 induction in several lung cell types. **Panel A. A**nandamide dose response curves for NHBE, SAEC and HMVEC-L cells. NHBE, SAEC and HMVEC-L cells were sensitive to anandamide at concentrations above 10 μM. NHBE cells are represented with open circles, SAEC cells are represented by open triangles and HMVEC-L cells are represented with closed squares. Data are shown as % viability of untreated control cells. TRPV1-OE (**panel B**) and BEAS-2B (**panel C**) cells were treated with anandamide alone or in the presence of LJO-328 (TRPV1 antagonist) or AM-251 (CB1/2 receptor antagonist) for 24 hours as described in *Methods.* None of the groups were significantly different from each other as determined using one-way ANOVA: for TRPV1-OE cells, $p=0.44$ and for BEAS-2B cells $p=0.73$. **Panel D**. TRPV1-OE and BEAS-2B cells were treated treated with anandamide (AEA) alone (25 μM) indicated by closed squares; or in the presence of LJO-328 (20 μM TRPV1-OE or 50 μM BEAS-2B) indicated by open triangles, or AM-251 (2.5 μM both cell types) indicated by open circles. * denotes value significantly elevated over untreated control, and ≠ denotes a value significantly elevated over anandamide alone, using one-way ANOVA analysis with Newman-Keuls multiple comparison post-hoc testing, $p<0.05$.

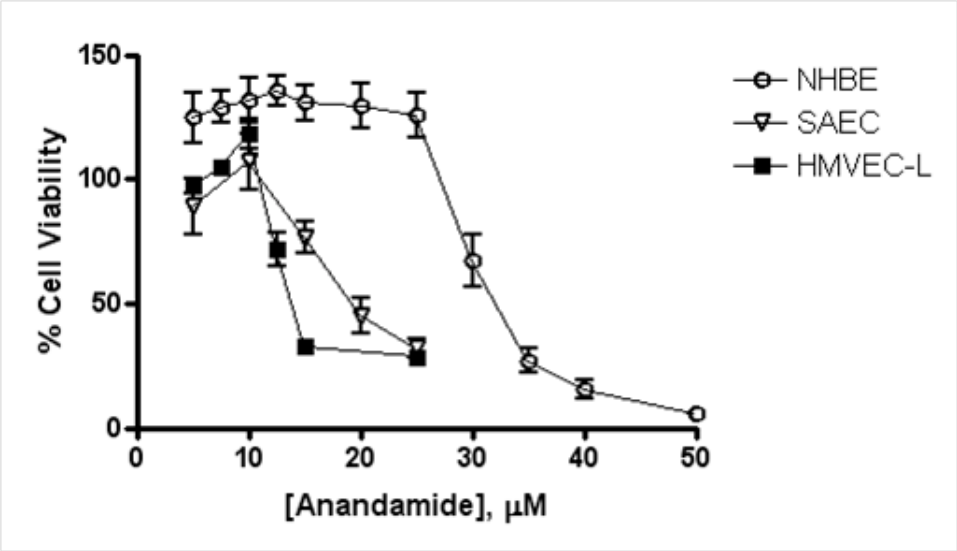

Figure 4.8 A.

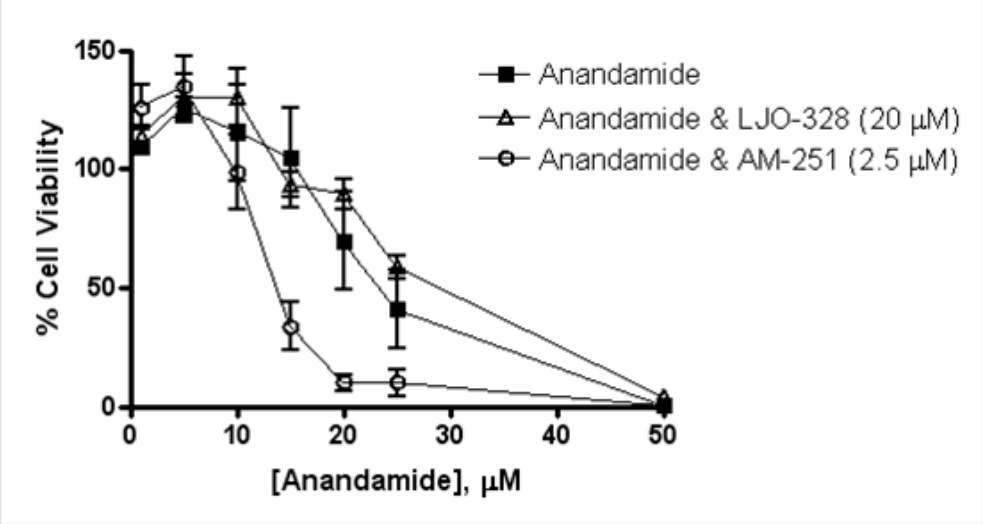

Figure 4.8 B.

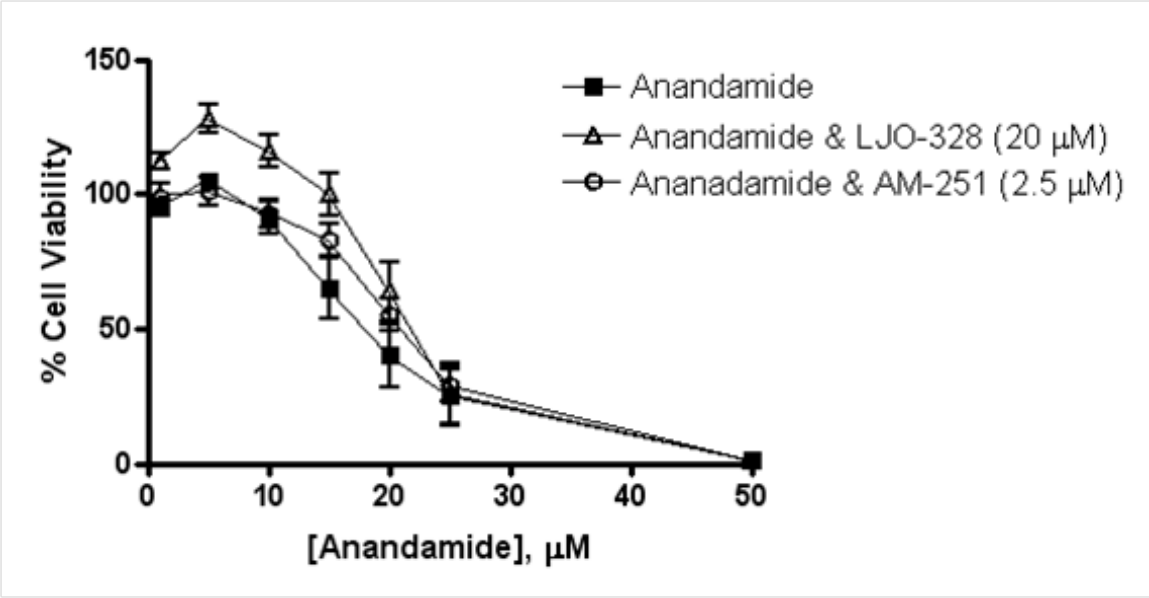

Figure 4.8 C.

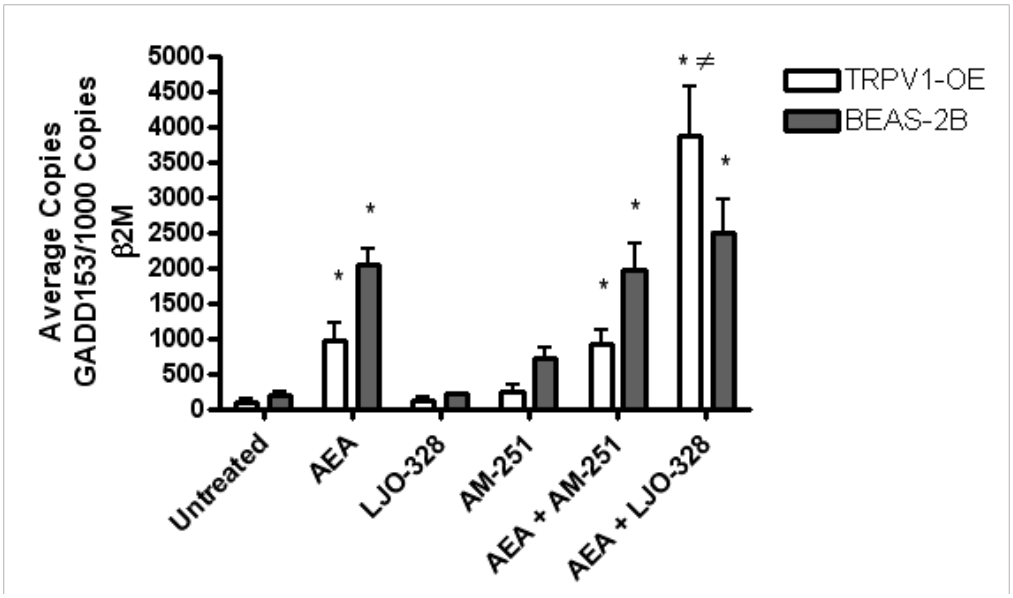

Figure 4.8 D.

4.7 References

1. Matthay, M. A., Zimmerman, G. A., Esmon, C., Bhattacharya, J., Coller, B., Doerschuk, C. M., Floros, J., Gimbrone, M. A., Jr., Hoffman, E., Hubmayr, R. D., Leppert, M., Matalon, S., Munford, R., Parsons, P., Slutsky, A. S., Tracey, K. J., Ward, P., Gail, D. B., and Harabin, A. L. (2003) Future research directions in acute lung injury: summary of a National Heart, Lung, and Blood Institute working group, *Am J Respir Crit Care Med 167*, 1027-1035.

2. Matute-Bello, G., Frevert, C. W., and Martin, T. R. (2008) Animal models of acute lung injury, *Am J Physiol Lung Cell Mol Physiol 295*, L379-399.

3. Ware, L. B., and Matthay, M. A. (2000) The acute respiratory distress syndrome, *N Engl J Med 342*, 1334-1349.

4. Wheeler, A. P., and Bernard, G. R. (2007) Acute lung injury and the acute respiratory distress syndrome: a clinical review, *Lancet 369*, 1553-1564.

5. Perl, M., Lomas-Neira, J., Chung, C. S., and Ayala, A. (2008) Epithelial cell apoptosis and neutrophil recruitment in acute lung injury-a unifying hypothesis? What we have learned from small interfering RNAs, *Mol Med 14*, 465-475.

6. Ang, S. F., Moochhala, S. M., and Bhatia, M. (2010) Hydrogen sulfide promotes transient receptor potential vanilloid 1-mediated neurogenic inflammation in polymicrobial sepsis, *Crit Care Med 38*, 619-628.

7. Bhatia, M., Zhi, L., Zhang, H., Ng, S. W., and Moore, P. K. (2006) Role of substance P in hydrogen sulfide-induced pulmonary inflammation in mice, *Am J Physiol Lung Cell Mol Physiol 291*, L896-904.

8. Helyes, Z., Elekes, K., Nemeth, J., Pozsgai, G., Sandor, K., Kereskai, L., Borzsei, R., Pinter, E., Szabo, A., and Szolcsanyi, J. (2007) Role of transient receptor potential vanilloid 1 receptors in endotoxin-induced airway inflammation in the mouse, *Am J Physiol Lung Cell Mol Physiol 292*, L1173-1181.

9. Hwang, S. W., Cho, H., Kwak, J., Lee, S. Y., Kang, C. J., Jung, J., Cho, S., Min, K. H., Suh, Y. G., Kim, D., and Oh, U. (2000) Direct activation of capsaicin receptors by products of lipoxygenases: endogenous capsaicin-like substances, *Proc Natl Acad Sci U S A 97*, 6155-6160.

10. Li, L., Bhatia, M., Zhu, Y. Z., Zhu, Y. C., Ramnath, R. D., Wang, Z. J., Anuar, F. B., Whiteman, M., Salto-Tellez, M., and Moore, P. K. (2005) Hydrogen sulfide is a novel mediator of lipopolysaccharide-induced inflammation in the mouse, *Faseb J 19*, 1196-1198.

11. Liu, J., Batkai, S., Pacher, P., Harvey-White, J., Wagner, J. A., Cravatt, B. F., Gao, B., and Kunos, G. (2003) Lipopolysaccharide induces anandamide synthesis in macrophages via CD14/MAPK/phosphoinositide 3-kinase/NF-kappaB independently of platelet-activating factor, *J Biol Chem 278*, 45034-45039.

12. Maccarrone, M., De Petrocellis, L., Bari, M., Fezza, F., Salvati, S., Di Marzo, V., and Finazzi-Agro, A. (2001) Lipopolysaccharide downregulates fatty acid amide hydrolase expression and increases anandamide levels in human peripheral lymphocytes, *Arch Biochem Biophys 393*, 321-328.

13. Singh Tahim, A., Santha, P., and Nagy, I. (2005) Inflammatory mediators convert anandamide into a potent activator of the vanilloid type 1 transient receptor potential receptor in nociceptive primary sensory neurons, *Neuroscience 136*, 539-548.

14. Trevisani, M., Patacchini, R., Nicoletti, P., Gatti, R., Gazzieri, D., Lissi, N., Zagli, G., Creminon, C., Geppetti, P., and Harrison, S. (2005) Hydrogen sulfide causes vanilloid receptor 1-mediated neurogenic inflammation in the airways, *British journal of pharmacology 145*, 1123-1131.

15. Benham, C. D., Davis, J. B., and Randall, A. D. (2002) Vanilloid and TRP channels: a family of lipid-gated cation channels, *Neuropharmacology 42*, 873-888.

16. Caterina, M. J., and Julius, D. (2001) The vanilloid receptor: a molecular gateway to the pain pathway, *Annu Rev Neurosci 24*, 487-517.

17. Jordt, S. E., and Julius, D. (2002) Molecular basis for species-specific sensitivity to "hot" chili peppers, *Cell 108*, 421-430.

18. Szallasi, A., and Blumberg, P. M. (1999) Vanilloid (Capsaicin) receptors and mechanisms, *Pharmacol Rev 51*, 159-212.

19. Szallasi, A., Cortright, D. N., Blum, C. A., and Eid, S. R. (2007) The vanilloid receptor TRPV1: 10 years from channel cloning to antagonist proof-of-concept, *Nat Rev Drug Discov 6*, 357-372.

20. Bhatia, M., Slavin, J., Cao, Y., Basbaum, A. I., and Neoptolemos, J. P. (2003) Preprotachykinin-A gene deletion protects mice against acute pancreatitis and associated lung injury, *Am J Physiol Gastrointest Liver Physiol 284*, G830-836.

21. Elekes, K., Helyes, Z., Nemeth, J., Sandor, K., Pozsgai, G., Kereskai, L., Borzsei, R., Pinter, E., Szabo, A., and Szolcsanyi, J. (2007) Role of capsaicin-sensitive afferents and sensory neuropeptides in endotoxin-induced airway inflammation and consequent bronchial hyperreactivity in the mouse, *Regul Pept 141*, 44-54.

22. Groneberg, D. A., Quarcoo, D., Frossard, N., and Fischer, A. (2004) Neurogenic mechanisms in bronchial inflammatory diseases, *Allergy 59*, 1139-1152.

23. Ng, S. W., Zhang, H., Hegde, A., and Bhatia, M. (2008) Role of preprotachykinin-A gene products on multiple organ injury in LPS-induced endotoxemia, *J Leukoc Biol 83*, 288-295.

24. Puneet, P., Hegde, A., Ng, S. W., Lau, H. Y., Lu, J., Moochhala, S. M., and Bhatia, M. (2006) Preprotachykinin-A gene products are key mediators of lung injury in polymicrobial sepsis, *J Immunol 176*, 3813-3820.

25. Sio, S. W., Moochhala, S., Lu, J., and Bhatia, M. (2009) Early protection from burn-induced acute lung injury by deletion of preprotachykinin-A gene, *Am J Respir Crit Care Med 181*, 36-46.

26. Sio, S. W., Puthia, M. K., Lu, J., Moochhala, S., and Bhatia, M. (2008) The neuropeptide substance P is a critical mediator of burn-induced acute lung injury, *J Immunol 180*, 8333-8341.

27. Johansen, M. E., Reilly, C. A., and Yost, G. S. (2006) TRPV1 antagonists elevate cell surface populations of receptor protein and exacerbate TRPV1-mediated toxicities in human lung epithelial cells, *Toxicol Sci 89*, 278-286.

28. Karai, L. J., Russell, J. T., Iadarola, M. J., and Olah, Z. (2004) Vanilloid receptor 1 regulates multiple calcium compartments and contributes to Ca2+-induced Ca2+ release in sensory neurons, *J Biol Chem 279*, 16377-16387.

29. Olah, Z., Szabo, T., Karai, L., Hough, C., Fields, R. D., Caudle, R. M., Blumberg, P. M., and Iadarola, M. J. (2001) Ligand-induced dynamic membrane changes and cell deletion conferred by vanilloid receptor 1, *J Biol Chem 276*, 11021-11030.

30. Toth, A., Blumberg, P. M., Chen, Z., and Kozikowski, A. P. (2004) Design of a high-affinity competitive antagonist of the vanilloid receptor selective for the calcium entry-linked receptor population, *Mol Pharmacol 65*, 282-291.

31. Reilly, C. A., Taylor, J. L., Lanza, D. L., Carr, B. A., Crouch, D. J., and Yost, G. S. (2003) Capsaicinoids cause inflammation and epithelial cell death through activation of vanilloid receptors, *Toxicol Sci 73*, 170-181.

32. Thomas, K. C., Sabnis, A. S., Johansen, M. E., Lanza, D. L., Moos, P. J., Yost, G. S., and Reilly, C. A. (2007) Transient receptor potential vanilloid 1 agonists cause endoplasmic reticulum stress and cell death in human lung cells, *J Pharmacol Exp Ther 321*, 830-838.

33. Endo, M., Mori, M., Akira, S., and Gotoh, T. (2006) C/EBP homologous protein (CHOP) is crucial for the induction of caspase-11 and the pathogenesis of lipopolysaccharide-induced inflammation, *J Immunol 176*, 6245-6253.

34. Endo, M., Oyadomari, S., Suga, M., Mori, M., and Gotoh, T. (2005) The ER stress pathway involving CHOP is activated in the lungs of LPS-treated mice, *Journal of biochemistry 138*, 501-507.

35. Hiramatsu, N., Kasai, A., Hayakawa, K., Yao, J., and Kitamura, M. (2006) Real-time detection and continuous monitoring of ER stress in vitro and in vivo by ES-TRAP: evidence for systemic, transient ER stress during endotoxemia, *Nucleic Acids Res 34*, e93.

36. Reilly, C. A., Johansen, M. E., Lanza, D. L., Lee, J., Lim, J. O., and Yost, G. S. (2005) Calcium-dependent and independent mechanisms of capsaicin receptor (TRPV1)-mediated cytokine production and cell death in human bronchial epithelial cells, *J Biochem Mol Toxicol 19*, 266-275.

37. Roche, M., Kelly, J. P., O'Driscoll, M., and Finn, D. P. (2008) Augmentation of endogenous cannabinoid tone modulates lipopolysaccharide-induced alterations in circulating cytokine levels in rats, *Immunology 125*, 263-271.

CHAPTER 5

CONCLUSIONS

Everyday experiences are enriched by sensations of touch, taste, sight, smell and sound. The ability to differentiate between beneficial and dangerous experiences is important to be able to minimize harm as discussed in Chapter 1. TRP receptors are critical sensors of harmful environmental conditions, and TRPV1 is no exception. TRPV1 receptors do not function like light switches with simple on/off functionality; rather they are sensitive to changes in nearby conditions including intracellular TRPV1 distribution, cellular pH, extracellular ion concentrations, and posttranslational modification including phosphorylation state, nitrosylation, and glycosylation (*1-5*). As previously discussed, TRPV1 receptors are activated by many chemical irritants, exogenous substances, and endogenous inflammatory mediators. Varied activation states and numerous agonists make TRPV1 characterization difficult; nevertheless this receptor presents a challenge to scientists to elucidate the functional traits of TRPV1. Although it is the topic of much research, TRPV1 characterization is limited and many features of this receptor are not yet completely understood.

The goal for this work was to better understand how TRPV1 agonists cause damage to the lung epithelium through characterization of: 1) the mechanism of TRPV1

mediated cell death, 2) structure activity relationships of capsaicin analogues in different lung cell types, and 3) the role of TRPV1 in lung injury resulting from severe systemic inflammation, which increases select endovanilloids. We sought to answer the following questions with this research: why do TRPV1 agonists kill human lung epithelial cells? Which structural features of capsaicin and nonivamide are key for TRPV1 activation, and what are the consequences? Can we use chemical variants of nonivamide to better understand TRPV1 activation in *in vitro* models exhibiting different responses? Does TRPV1 play a role in lung injury after systemic inflammatory events, such as sepsis or trauma, where endovanilloids are known to be upregulated? We were able to answer each of these questions, although for each question answered many additional questions presented themselves. Indepth conclusions were presented at the end of each chapter. This chapter presents an integrated summary of the three main chapters, suggestions for additional experiments, and a proposed mechanism of TRPV1 activation in human lung epithelial cells (Figure 5.1).

5.1 Chapter 2

Chapter 2 described the results of our investigation into the mechanism of TRPV1 mediated lung cell death. In several different cell types it was determined that TRPV1 activation leads to calcium release from the ER, causing ER stress and cell death. TRPV1 agonist treatment caused ER stress responses in a manner consistent with known ER stress-inducing agents, and induced cytotoxicity through the PERK pathway. TRPV1 agonists did not induce ER stress with LJO-328 (TRPV1 antagonist) cotreatment, or in cells that do not express functional TRPV1 (*6*). Future studies for this portion of the

project include determining the ability of other TRPV1 agonists and antagonists to induce or prevent ER stress. Studies to determine whether or not ER stress is induced after neuronal TRPV1 activation and to what extent sensory neuron activation contributes to ER stress in nonneuronal cells would shed light on the cell/tissue specificity and fundamentals of this response in the lung. Consider also that TRPV1 activation may possibly induce ER stress through other pathways. In addition to EIF2αK3, other proximal sensors of ER stress are ATF6 and IRE1 (*7*). Downstream effects of these other pathways may be compensatory and, depending on the circumstances, may enhance or attenuate the deleterious effects of TRPV1 in different lung cells and in the intact lung. TRPV1 induced ER stress is presumably mediated by the intracellular pool of TRPV1 in nonneuronal cells, and shifting the majority of TRPV1 to the cell surface by unknown conditions similar to what occurs with LJO-328 pretreatment of TRPV1-OE cells may change the magnitude of ER stress induction or abrogate the response (*8*). Additionally, GADD153 is pro-apoptotic, but cell death due to capsaicin is generally oncotic. It would be interesting to evaluate the temporal relationship between ER stress and markers of apoptosis, necrosis, and/or autophagy to determine the exact mechanisms of cell death.

5.2 Chapter 3

Chapter 3 identified requisite structural features of nonivamide for TRPV1 activation through the examination of structure activity relationships for capsaicin analogues and TRPV1. Calcium flux, ER stress/GADD153 induction, and cell death were used to quantify TRPV1 activation. Modifying the core structure of nonivamide altered the ability of the analogues to interact with TRPV1, and molecular modeling confirmed

the essential structural features for TRPV1 activation, ER stress and cell death as previously identified in the literature (*9-17*). Future experiments to expand on these results include measurement of TRPV1 protein expression for confirmation of TRPV1 mRNA quantification. Metabolism studies of analogues may identify metabolites with the ability to activate TRPV1, since cytochrome P450 enzymes metabolize capsaicin (*18*). Investigation of *n*-(3,4-dihydroxybenzyl)nonanamide and whether it is inducing ER stress through alternate pathways (e.g., Nrf2/Keap1) instead of TRPV1 would enhance our understanding of its toxicity and would help extrapolate responses observed *in vitro* to responses of cells in the intact lung. Additional molecular modeling of analogues with variations in other portions of the nonivamide structure would also improve knowledge of the TRPV1 vanilloid binding site. Refinement of modeling parameters would strengthen the validity of these results – for example, a larger portion of TRPV1 could be modeled in a lipid environment to reproduce more physiologically relevant interactions.

5.3 Chapter 4

Chapter 4 described a potential role of TRPV1 as a mediator of endovanilloid-related lung injury. Endovanilloids have been implicated in lung inflammation and injury during experimental sepsis and following burn injury (*19-35*). This study tested the hypothesis that LPS-induced systemic inflammation could cause lung injury via the formation of pneumotoxic endovanilloids that migrate via systemic circulation and activate TRPV1 in the lung. TRPV1 activity was examined in primary human lung cells and in mice with and without TRPV1 antagonist cotreatment, and without TRPV1 expression (TRPV1-/-). These studies showed that TRPV1 genetic knockout or receptor

inhibition conferred protection from LPS-induced lung injury. Protective effects are presumably due to a reduction in endovanilloid dependent TRPV1 activation, and reduced lung cell production of cytokines that enhance lung injury, and leading to decreased cytotoxicity and GADD153 induction. Results with anandamide, a potential endovanilloid involved in LPS-induced lung injury, were less straightforward. Anandamide caused GADD153 induction and cytotoxicity, but its effects appeared to be primarily TRPV1-independent. Attenuation of lung injury by TRPV1 knockout and LJO-328 indicates a role for TRPV1 and endovanilloids in lung injury, although the mechanism is still ambiguous. Additional work with different endovanilloids may present a clearer picture of TRPV1 activation. Additional animal experiments with a more relevant model of septic lung injury (such as cecal ligation and puncture), in other animals (e.g., rats) or different lung cell or perfused lung models would add to this body of work. Immunohistochemical evaluation of TRPV1 and GADD153 co-localization and lung microdissection would also better identify specific cellular/regional effects of endovanilloids in the lung.

5.4 Summary

Based on the research presented in this dissertation, key determinants of TRPV1 activation in human lung epithelial cells include, but are not limited to:

- Quantity of TRPV1 in the cell
- Expression of functional TRPV1
- Subcellular distribution of TRPV1
- Cell permeability of agonists
- Agonist concentration

- Agonist potency
- Agonist ability to interact at key TRPV1 binding sites
- Duration of exposure

Additional determinants will be identified as TRPV1 is better characterized. Figure 1 summarizes the proposed mechanism by which TRPV1 and its agonists affect cellular homeostasis, lung physiology, and respiratory function. Briefly, there are two separate populations of TRPV1 in parenchymal lung cells and these sub-populations mediate immunomodulatory cytokine gene expression (inflammation), GADD153 induction, ER stress and cell death. *In vitro*, proinflammatory effects are altered with the addition of nonselective, cell impermeable antagonists of TRPV1 such as EGTA or ruthenium red, and cell death is not significantly decreased. Use of receptor specific, cell permeable TRPV1 antagonists such as LJO-328 attenuates GADD153 induction, ER stress, cell death, and cytokine responses. Overall, TRPV1 activation has the potential to cause several deleterious outcomes in lung cells that appear to ultimately translate into increased recruitment of inflammatory cells to the lung and lung cell damage involving apoptosis of lung parenchymal cells.

Overall, this work defines ER stress as the mechanism of TRPV1 mediated lung epithelial cell death, identifies key structural features of nonivamide for TRPV1 interactions, presents capsaicin analogues as molecular tools to probe TRPV1 function in different models, and indicates a potential role for TRPV1 in lung injury.

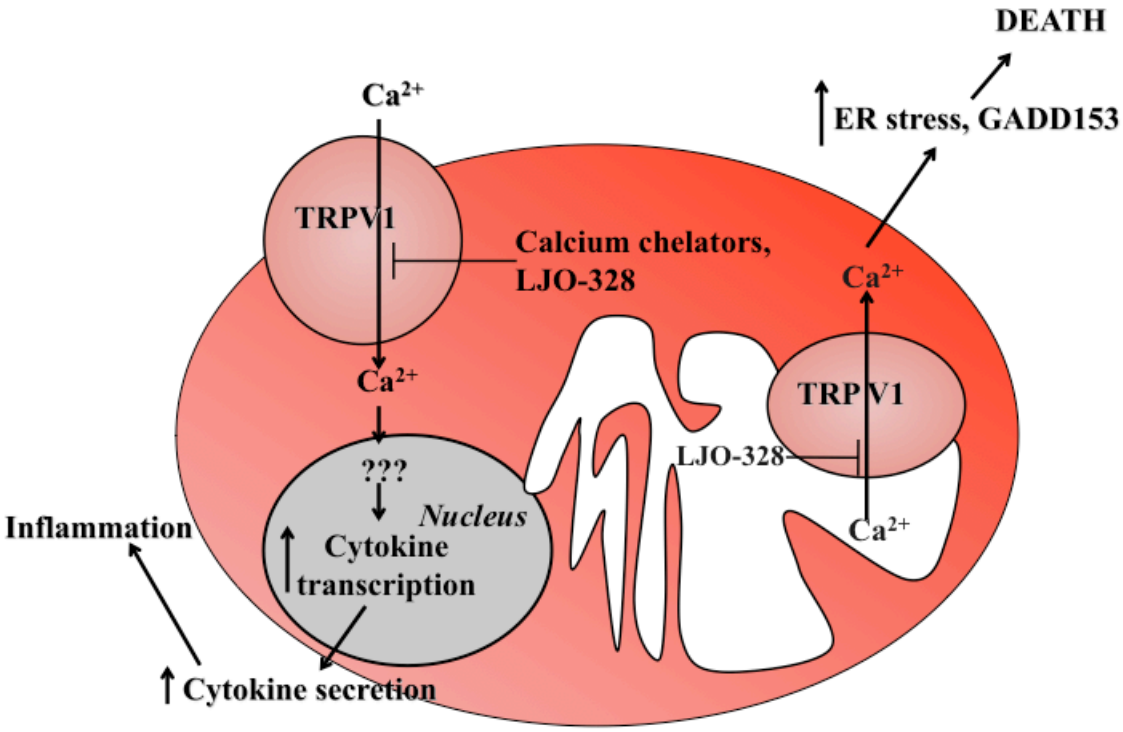

Figure 5.1. Summary diagram highlighting proinflammatory cytotoxic and proapoptotic ER stress pathway activation in lung cells exposed to TRPV1 agonists.

5.5 References

1. Caterina, M. J., and Julius, D. (2001) The vanilloid receptor: a molecular gateway to the pain pathway, *Annu Rev Neurosci 24*, 487-517.

2. Caterina, M. J., Schumacher, M. A., Tominaga, M., Rosen, T. A., Levine, J. D., and Julius, D. (1997) The capsaicin receptor: a heat-activated ion channel in the pain pathway, *Nature 389*, 816-824.

3. Szallasi, A., and Blumberg, P. M. (1999) Vanilloid (Capsaicin) receptors and mechanisms, *Pharmacol Rev 51*, 159-212.

4. Szallasi, A., Cortright, D. N., Blum, C. A., and Eid, S. R. (2007) The vanilloid receptor TRPV1: 10 years from channel cloning to antagonist proof-of-concept, *Nat Rev Drug Discov 6*, 357-372.

5. Vriens, J., Appendino, G., and Nilius, B. (2009) Pharmacology of vanilloid transient receptor potential cation channels, *Mol Pharmacol 75*, 1262-1279.

6. Thomas, K. C., Sabnis, A. S., Johansen, M. E., Lanza, D. L., Moos, P. J., Yost, G. S., and Reilly, C. A. (2007) Transient receptor potential vanilloid 1 agonists cause endoplasmic reticulum stress and cell death in human lung cells, *J Pharmacol Exp Ther 321*, 830-838.

7. Schroder, M., and Kaufman, R. J. (2005) ER stress and the unfolded protein response, *Mutat Res 569*, 29-63.

8. Johansen, M. E., Reilly, C. A., and Yost, G. S. (2006) TRPV1 antagonists elevate cell surface populations of receptor protein and exacerbate TRPV1-mediated toxicities in human lung epithelial cells, *Toxicol Sci 89*, 278-286.

9. Fernandez-Ballester, G., and Ferrer-Montiel, A. (2008) Molecular modeling of the full-length human TRPV1 channel in closed and desensitized states, *J Membr Biol 223*, 161-172.

10. Gavva, N. R., Klionsky, L., Qu, Y., Shi, L., Tamir, R., Edenson, S., Zhang, T. J., Viswanadhan, V. N., Toth, A., Pearce, L. V., Vanderah, T. W., Porreca, F., Blumberg, P. M., Lile, J., Sun, Y., Wild, K., Louis, J. C., and Treanor, J. J. (2004) Molecular determinants of vanilloid sensitivity in TRPV1, *J Biol Chem 279*, 20283-20295.

11. Johnson, D. M., Garrett, E. M., Rutter, R., Bonnert, T. P., Gao, Y. D., Middleton, R. E., and Sutton, K. G. (2006) Functional mapping of the transient receptor potential vanilloid 1 intracellular binding site, *Mol Pharmacol 70*, 1005-1012.

12. Jordt, S. E., and Julius, D. (2002) Molecular basis for species-specific sensitivity to "hot" chili peppers, *Cell 108*, 421-430.

13. Salazar, H., Jara-Oseguera, A., Hernandez-Garcia, E., Llorente, I., Arias, O., II, Soriano-Garcia, M., Islas, L. D., and Rosenbaum, T. (2009) Structural determinants of gating in the TRPV1 channel, *Nat Struct Mol Biol 16*, 704-710.

14. Sutton, K. G., Garrett, E. M., Rutter, A. R., Bonnert, T. P., Jarolimek, W., and Seabrook, G. R. (2005) Functional characterisation of the S512Y mutant vanilloid human TRPV1 receptor, *British journal of pharmacology 146*, 702-711.

15. Walpole, C. S., Wrigglesworth, R., Bevan, S., Campbell, E. A., Dray, A., James, I. F., Masdin, K. J., Perkins, M. N., and Winter, J. (1993) Analogues of capsaicin with agonist activity as novel analgesic agents; structure-activity studies. 3. The hydrophobic side-chain "C-region", *J Med Chem 36*, 2381-2389.

16. Walpole, C. S., Wrigglesworth, R., Bevan, S., Campbell, E. A., Dray, A., James, I. F., Masdin, K. J., Perkins, M. N., and Winter, J. (1993) Analogues of capsaicin with agonist activity as novel analgesic agents; structure-activity studies. 2. The amide bond "B-region", *J Med Chem 36*, 2373-2380.

17. Walpole, C. S., Wrigglesworth, R., Bevan, S., Campbell, E. A., Dray, A., James, I. F., Perkins, M. N., Reid, D. J., and Winter, J. (1993) Analogues of capsaicin with agonist activity as novel analgesic agents; structure-activity studies. 1. The aromatic "A-region", *J Med Chem 36*, 2362-2372.

18. Reilly, C. A., and Yost, G. S. (2006) Metabolism of capsaicinoids by P450 enzymes: a review of recent findings on reaction mechanisms, bio-activation, and detoxification processes, *Drug Metab Rev 38*, 685-706.

19. Ang, S. F., Moochhala, S. M., and Bhatia, M. (2010) Hydrogen sulfide promotes transient receptor potential vanilloid 1-mediated neurogenic inflammation in polymicrobial sepsis, *Crit Care Med 38*, 619-628.

20. Bhatia, M., Slavin, J., Cao, Y., Basbaum, A. I., and Neoptolemos, J. P. (2003) Preprotachykinin-A gene deletion protects mice against acute pancreatitis and associated lung injury, *Am J Physiol Gastrointest Liver Physiol 284*, G830-836.

21. Bhatia, M., Wong, F. L., Fu, D., Lau, H. Y., Moochhala, S. M., and Moore, P. K. (2005) Role of hydrogen sulfide in acute pancreatitis and associated lung injury, *Faseb J 19*, 623-625.

22. Bhatia, M., Zhi, L., Zhang, H., Ng, S. W., and Moore, P. K. (2006) Role of substance P in hydrogen sulfide-induced pulmonary inflammation in mice, *Am J Physiol Lung Cell Mol Physiol 291*, L896-904.

23. Helyes, Z., Elekes, K., Nemeth, J., Pozsgai, G., Sandor, K., Kereskai, L., Borzsei, R., Pinter, E., Szabo, A., and Szolcsanyi, J. (2007) Role of transient receptor potential vanilloid 1 receptors in endotoxin-induced airway inflammation in the mouse, *Am J Physiol Lung Cell Mol Physiol 292*, L1173-1181.

24. Hwang, S. W., Cho, H., Kwak, J., Lee, S. Y., Kang, C. J., Jung, J., Cho, S., Min, K. H., Suh, Y. G., Kim, D., and Oh, U. (2000) Direct activation of capsaicin receptors by products of lipoxygenases: endogenous capsaicin-like substances, *Proc Natl Acad Sci U S A 97*, 6155-6160.

25. Li, L., Bhatia, M., Zhu, Y. Z., Zhu, Y. C., Ramnath, R. D., Wang, Z. J., Anuar, F. B., Whiteman, M., Salto-Tellez, M., and Moore, P. K. (2005) Hydrogen sulfide is a novel mediator of lipopolysaccharide-induced inflammation in the mouse, *Faseb J 19*, 1196-1198.

26. Liu, J., Batkai, S., Pacher, P., Harvey-White, J., Wagner, J. A., Cravatt, B. F., Gao, B., and Kunos, G. (2003) Lipopolysaccharide induces anandamide synthesis in macrophages via CD14/MAPK/phosphoinositide 3-kinase/NF-kappaB independently of platelet-activating factor, *J Biol Chem 278*, 45034-45039.

27. Maccarrone, M., De Petrocellis, L., Bari, M., Fezza, F., Salvati, S., Di Marzo, V., and Finazzi-Agro, A. (2001) Lipopolysaccharide downregulates fatty acid amide hydrolase expression and increases anandamide levels in human peripheral lymphocytes, *Arch Biochem Biophys 393*, 321-328.

28. Ng, S. W., Zhang, H., Hegde, A., and Bhatia, M. (2008) Role of preprotachykinin-A gene products on multiple organ injury in LPS-induced endotoxemia, *J Leukoc Biol 83*, 288-295.

29. Orliac, M. L., Peroni, R., Celuch, S. M., and Adler-Graschinsky, E. (2003) Potentiation of anandamide effects in mesenteric beds isolated from endotoxemic rats, *J Pharmacol Exp Ther 304*, 179-184.

30. Puneet, P., Hegde, A., Ng, S. W., Lau, H. Y., Lu, J., Moochhala, S. M., and Bhatia, M. (2006) Preprotachykinin-A gene products are key mediators of lung injury in polymicrobial sepsis, *J Immunol 176*, 3813-3820.

31. Singh Tahim, A., Santha, P., and Nagy, I. (2005) Inflammatory mediators convert anandamide into a potent activator of the vanilloid type 1 transient receptor potential receptor in nociceptive primary sensory neurons, *Neuroscience 136*, 539-548.

32. Sio, S. W., Moochhala, S., Lu, J., and Bhatia, M. (2009) Early protection from burn-induced acute lung injury by deletion of preprotachykinin-A gene, *Am J Respir Crit Care Med 181*, 36-46.

33. Sio, S. W., Puthia, M. K., Lu, J., Moochhala, S., and Bhatia, M. (2008) The neuropeptide substance P is a critical mediator of burn-induced acute lung injury, *J Immunol 180*, 8333-8341.

34. Trevisani, M., Patacchini, R., Nicoletti, P., Gatti, R., Gazzieri, D., Lissi, N., Zagli, G., Creminon, C., Geppetti, P., and Harrison, S. (2005) Hydrogen sulfide causes vanilloid receptor 1-mediated neurogenic inflammation in the airways, *British journal of pharmacology 145*, 1123-1131.

35. Zhang, H., Zhi, L., Moore, P. K., and Bhatia, M. (2006) Role of hydrogen sulfide in cecal ligation and puncture-induced sepsis in the mouse, *Am J Physiol Lung Cell Mol Physiol 290*, L1193-1201.